Texas A&M University

Department of
OCEANOGRAPHY

N71-20422
NASA CR-117316

CASE FILE
COPY

OCEANOGRAPHIC EXPERIMENT SUPPORT

(Remote Sensing of Coastal Oceans)

ANNUAL REPORT

May 1969 through May 1970

U.S. Naval Oceanographic Office
Contract N62306-69-C-0263

A&M Project 658
Ref. No. 70-20-A

Funded by

National Aeronautics and Space Administration

through the

U.S. Naval Oceanographic Office

Research Conducted Through the
Texas A&M Research Foundation
College Station, Texas

Texas A & M University
Department of Oceanography
College Station, Texas 77843

Research Conducted Through the
Texas A & M Research Foundation

A & M Project 658

ANNUAL REPORT

Dr. Luis R. A. Capurro
Project Supervisor

May 1969 through May 1970

Project 658 is operated through funding provided by the Spacecraft Oceanography Project of the U. S. Naval Oceanographic Office (Contract N62306-69-C-0263) and is part of the National Aeronautics and Space Administration's Earth Resources Survey Program. The work reported herein is of a preliminary nature and the results are not necessarily in final form. Reproduction in whole or in part is permitted for any purpose of the United States Government.

10 May 1970

TABLE OF CONTENTS

Chapter		Page
I.	Introduction and Background	1
II.	Objectives and Approach	3
III.	Progress	5
	A. General	5
	B. The Present Status of the Uses of Microwave Radiometry in Making Meaningful Oceanographic Observations	7
	C. International Program - General	62
	D. International Program - Mexico	64
	E. International Program - Brazil	90
	F. Analysis of Apollo IX Photography	101
	G. Newsletter	122
	H. Upwelling Detection from Space Photography	124
	I. Staff Travels - June, 1969 through March, 1970	132
IV.	Contributions	137
V.	Reports	138
VI.	Office Facilities and Personnel	139
VII.	Film Data Acquired from May, 1969 - March, 1970	140

CHAPTER I

INTRODUCTION AND BACKGROUND

Initial work at Texas A&M University on the uses of remote sensing methods in oceanography started with a project previously known as the Space Oceanography Project and was part of the National Aeronautics and Space Administration's Earth Resources Survey Program. Its primary goal was to coordinate oceanographic activities of the Department of Oceanography with remote sensor flights of NASA aircraft. The main experimental site was the outflow region of the Mississippi River and, in some cases, some of the neighboring islands. Three types of aircraft were used in this study: the NASA 926 (Convair 240A); the NASA 927 (P3A); and the NASA T-38. Multispectral data were collected from these aircraft through the use of passive sensors. Ground truth was acquired from surface ships, oil platforms, river stations, and meteorological stations in the test areas.

This work was part of a general study of the Gulf of Mexico sponsored by the Office of Naval Research under Contract 2119(04) and included (1) the distribution outflow of the Mississippi River, (2) the relationship between low cloud development and ocean circulation, (3) the location of the Gulf Loop Current, and (4) the use of remote sensors in surveying these phenomena.

These studies have been instrumental in determining the nature of the current project at Texas A&M University. Funding for the current project was obtained in May, 1969, through the U. S. Naval Oceanographic

Office and is being administered by the Texas A&M Research Foundation under Contract N62306-69-C-0263.

CHAPTER II

OBJECTIVES AND APPROACH

In the course of our research in spacecraft oceanography at Texas A&M University, it has become obvious that many research programs could become more productive with improved communication and coordination with their counterparts in government and industry. Many airborne experiments have been made without proper planning. This was particularly true with respect to many of the earlier aircraft flights. This is, of course, to be expected in the early stages of a new science and method of operation. With the coming flights of NASA aircraft and planned satellites, such as the Earth Resources Survey Satellites and the future Apollo Applications Vehicles, it becomes necessary to coordinate to a greater degree than ever before the aircraft and spacecraft support effort.

Our experience has shown that, although it is not often done, proper use of oceanographic research vessels, buoys, offshore platforms, instrumented aircraft, commercial ships, and coastal oceanographic and meteorological stations must be made to derive maximum benefit from the aircraft and satellite sensor systems. Our overall spacecraft oceanography research programs should be studied in detail and, with better coordination, we can all benefit from increased quantity and quality of usable data.

The objective of this study is to determine the system necessary to support spacecraft operations for oceanography to be flown in the mid-1970's. The present and future resources of research vessels, buoys,

and scientific personnel will be determined and related to these spacecraft activities.

During this fiscal year, we proposed to continue to broaden our base of knowledge concerning the present state of remote sensing applications in oceanography. Members of our staff have had conferences with investigators in this program and ascertained the state of their investigations, the nature of the problems in conducting coordinated missions, and the relation of their studies to spacecraft operations. Using this information, we proposed to define specific objectives and procedures whereby these problems might be faced. We would continue to participate in the oceanographic evaluation of photography to be obtained during Apollo spacecraft flights.

CHAPTER III

PROGRESS

A. General

In order to be responsive to the objectives of this contract, we have broadened our outlook and contacts with the several similar activities. Several visits were made to other investigators operating under the Naval Oceanographic Office. A listing of these trips is shown under "Staff Travels" of this report. The purpose of these conferences was to gain an insight into the activities and problem areas of others in similar projects. It is our feeling that the time was well spent in that it gave us a greater appreciation of the methods being employed by the current investigators.

Early in the program, considerable time was spent gathering reports and other information pertinent to the project work statement. Along with this activity, much effort was put forth in increasing the holdings of the project library which now consists of approximately 1800 reports, reprints, and pertinent periodicals.

Recently, each of these items was keyworded and filed in a system using the IBM "Port-a-Punch" cards for the rapid retrieval of information. The system has been put to very good use by not only the project but by staff members of other projects. In addition to this, we have had requests for copies of some of our holdings; and, thus far, we have been able to fill those without too much difficulty.

In order to better define the progress in each area, we have prepared a subsection for each. This, we feel, will allow better appraisal.

CHAPTER III - PROGRESS (cont.)

B. The Present Status of the Uses of Microwave Radiometry in Making Meaningful Oceanographic Observations

Introduction

Beginning in the 1960's, environmental scientists have been considering the problems and prospects involved with the applications of microwave radiometry to their observational problems. There have been relatively few oceanographers involved in these studies; and, consequently, oceanographic applications have been slow in their development. Even worse, the claims that have been made about the applications of microwave radiometers have far exceeded the performances witnessed thus far. This report summarizes the current state-of-the-science of applied microwave radiometry and suggests certain courses of action. These conclusions and recommendations are based on our collective experience since 1966 and on informal discussions with various scientists and engineers who are involved in microwave theory and measurements.

General Scientific Background

The microwave properties of atmospheric gases, water, and solid materials have been under study for many years; however, it was not until the time of World War II that serious, analytical studies were made. The main impetus for these studies was involved with the uses of radar for detection and tracking of aircraft and ships. Before this time, however, there were many scientific achievements which have a

bearing on our investigations today.

The many empirical laws of electromagnetics were consolidated in the equations of Maxwell (1892) at the turn of the century. These led to many classical treatments of the interactions between certain configurations of electromagnetic waves and various simple material structures. Included in these are the laws of reflection for a flat, infinite, homogeneous dielectric given by Fresnel and the solution to the problem of scattering and absorption by homogeneous dielectric spheres first consolidated by Mie (1908).

The importance of these developments lay in the fact that natural surfaces, such as water or land, may be considered as flat, homogeneous materials as a first approximation. Also, individual droplets in water clouds may be considered as homogeneous spheres as a first approximation.

In 1931, Jansky (1932) first detected thermal radiation from extra-terrestrial sources at 20.5 MHz using a crude radio receiver. In 1946, Dicke (1946) proposed a method for minimizing the errors in microwave-frequency measurements of naturally-occurring thermal radiation. This method, which is in use today, enables one to measure the field of microwave radiation to an absolute accuracy of about 1-3 percent and with a relative sensitivity of less than one percent.

Developments in the 1940's

The reflective, scattering, absorptive, and emissive properties of water depend on its dielectric constant, its configuration and the frequency of radiation. The first accurate measurements of the dielectric constant of pure water were made by Lane and Saxton and have been reported

in a series of exemplary papers, e.g., see Saxton (1946a, 1946b, 1949, 1952), Saxton and Lane (1946, 1952a, 1952b, 1952c), and Lane and Saxton (1952a, 1952b). The dielectric constant for solutions of sodium chloride and water were measured also in the above. It should be noted that as of this date, no extensive measurements of the dielectric constant of sea water have been made. Thus, scientists are forced into assuming that the dielectric properties of aqueous sodium chloride and that of sea water are the same. This remains to be shown. The differences are likely to be greatest for frequencies below about 5 GHz if the measurements on aqueous sodium chloride are any indication. In addition, Hasted (1961), Hasted and El-Sabell (1953), Hasted, Ritson and Collie (1948), Hasted and Roderick (1958), and Collie, Ritson and Hasted (1946) have measured the dielectric constant of water and aqueous sodium chloride. Their measurements agree in general with those of Lane and Saxton.

The results of these measurements show that the dielectric constant of water and aqueous sodium chloride is complex and has large real and imaginary parts. The main effect of salts in the solution is to greatly increase the ohmic conductivity of the solution. This increase is effective only for frequencies less than about 5 GHz. In addition, these investigators found that the measurements could be fitted to a simple model proposed by Debye (1929). Thus, the dielectric constant for water and aqueous sodium chloride may be predicted for any microwave frequency as a function of three variables--the static relative permittivity (ε_s), the relaxation time (τ_o, sec), and the ionic conductivity (σ_i mhos, m^{-1}). These three variables are only a function of the water temperature and

the water salinity or normality. In general, ε_s and τ_o are only slightly affected by the salinity of the solution. Of course, σ_i is strongly dependent on the salinity.

The complex dielectric constant of ice was measured by Dunsmuir and Lamb (1945) and was found to be close to 3.165 for all frequencies and temperature and to have a small imaginary part that depends on the ice temperature.

Based on these measurements of the dielectric constant of water and ice, Ryde (1946) computed the extinction of microwaves by fog, cloud, rain, snow, and hail at specific radar frequencies by applying the Mie theory to model clouds having exponential drop-size distributions. Goldstein (1951) elaborated on Ryde's work.

Measurements of the reflectivity and absorptivity of a level layer of water, salt water, turf-covered ground, dry sand, and wet sand were made by Ford and Oliver (1946) at 9 cm (3.33 GHz) for zenith angles of 44.5, 55, and 70 deg. They found that turf-covered ground was not a specular reflector; however, bare soil (sandy loam) and water were specular reflectors. The reflectivities of soil were about 0.03 for dry soil and about 0.45 for wet soil. Tap water had a reflectivity of about 0.617 and salt water (salinity of 40 o/oo) had a reflectivity of 0.656.

In the late 1940's, Van Vleck successfully applied the quantum theory to the molecules of oxygen (O_2) and water vapor (H_2O). Using accurate measurements of the absorption of microwaves by water vapor made by Becker and Autter (1946), Van Vleck was able to obtain a practical

formula that could be used to predict the volume absorption coefficient for water vapor (α_w, km^{-1}). This formula used an empirical correction for the contribution due to pressure-broadened infrared lines. Many subsequent investigators have failed to use this correction in their calculations.

The 1950's

The early 1950's saw a continuing expansion of theoretical studies of the electromagnetic properties of rain and other clouds of water droplets. Engineers were interested in knowing the probability of severe microwave absorption due to heavy rains, i.e., see Bussey (1950). Also, the Mie theory was expanded to include multi-shell dielectrics such as liquid-water on hail (Aden, 1952; Aden and Kerker, 1951). Similar work was proceeding in the Soviet Union (Shifrin, 1951). The classic paper in this field of study was produced by Gunn and East (1954). In this comprehensive paper, they predicted the total extinction coefficients and back-scattering cross sections for a multitude of model clouds, both ice and liquid water, at a number of microwave frequencies. Many regression expressions were developed relating the total attenuation and radar reflectivity to either the rate fall rate of a precipitating cloud or to the liquid-water content of a non-raining cloud. A similar contribution was made by Imai (1957) some years later. It is a tribute to these early investigators that their work still remains the bases of many applied studies. One very serious drawback of their work as applied to microwave radiometry is the fact that extinction by true absorption (conversion to heat) and extinction by scattering (redistribution) were combined into a

single volume extinction coefficient. Precise radiometric calculations for microwave radiometry require that these phenomena be separated and dealt with separately. For example, the thermal emission properties of a medium depend only on its absorptive properties. A medium that only scatters will not emit thermal radiation. On the other hand, extinction by scattering implies that some apparent emission will arise due to the scattering of energy from other pencils of radiant energy along the pencil of concern. The problem has not been properly considered.

Near the end of the decade, many investigators began to direct their attention to problems of communications between land stations and between land and aerial stations. These studies were centered around the 4-11 GHz band [Hathaway and Evans, 1959; Hogg (1959)].

In 1959 also, two important papers were published. The first dealt with a general method of inference of the vertical distribution of atmospheric temperature from remote radiation measurements (Kaplan, 1959). This general method suggested for use in the 15μ CO_2 band opened the way for similar investigation in the microwave spectrum notably the series of O_2 absorption lines near 60 GHz. The second paper is a classical treatment of the problem of the interaction of electromagnetic waves with rough surfaces given by Peake (1959).

The 1960's

The vast majority of papers dealing with the microwave properties of the environments and their exploitation were given in this period. In this section, we will review only the most notable papers. These may be broken down to four categories: (1) the effects of atmospheric gases,

(2) the effects of atmospheric liquid-water, (3) the effects of oceanographic variables (temperature, salinity, roughness, foam), and (4) general review papers.

The atmosphere has a large effect on the intensity of microwave radiation coming from the ocean-atmosphere system. This effect is stronger over water surfaces than it is over land surfaces due to the high reflectivity of water. Thus, the absorption, emission, and scattering properties of the atmosphere need to be fully understood and predictable if one is to derive information about the ocean's surface from aircraft or spacecraft measurements of microwave radiational intensities.

In general, the Van Vleck theory has been used and is sufficiently accurate when certain empirical corrections are used to predict the volume absorption coefficients due to water vapor (α_w, km^{-1}) or due to molecular oxygen (α_{ox}, km^{-1}). One may find many expressions in the literature that give explicit expressions for α_w and α_{ox}. Many of these are useless since the units of the independent variables are not prescribed. In fact, in all the literature sources surveyed, there did not appear to be any expression that was completely free of error or that matched some other expression. In many cases, careful attention to the effect of change of variable was not maintained. In others, they were obvious typographical errors. An expression that gives reasonably accurate values for α_w and α_{ox} and which incorporates most of the functional forms given in the literature is given in a subsequent section. The basic investigators in this area are Meeks and Lilley (1963), Westwater (1965a, 1965b, 1967), and recently, Liebe (1969a, 1969b, 1969c).

Several investigators have used the above theory to predict the

intensity of microwave radiation at the surface due to atmospheric gases only for several microwave frequencies and for several atmospheric conditions [e.g., see Hogg and Mumford (1960), Weger (1960), Wulfsberg (1964), and Hogg and Semplak (1961, 1963)]. In addition, these and other investigators have measured the intensity of microwave radiation coming from the sky [Cummings and Hull (1966) and Haroules and Brown (1968, 1969)].

The emission of clouds of hydrometeors has been poorly treated. Most investigators have used the volume extinction coefficients predicted by Ryde or Goldstein as a basis for predictions of the emission of clouds. This is an improper procedure as indicated before. Measurements of the emission of rainclouds reveals that clouds may absorb significantly even for fairly low frequencies. Thus, the "all weather" capability of microwave radiometers is to be questioned.

The theoretical emission and reflection of microwaves from a calm or slightly disturbed sea surface has been fully investigated. In general, investigators have found that the emission of the sea surface is fairly constant with respect to temperature, salinity and roughness for small incidence angles and for frequencies greater than about 8 GHz. Measurements have confirmed these predictions. Theory also indicates that the emission is weakly dependent on temperature at frequencies near 6 GHz and is strongly dependent on salinity in areas where large changes of salinity occur when the frequency is less than about 5 GHz (Sirounian, 1968; Paris, 1969).

Using an 8.5 cm (3.53 GHz), Gurvich and Egorov (1966) of the Soviet Union successfully determined the distribution of sea surface temperature from aircraft over the Caspian Sea. The choice of this frequency was based

on extensive theoretical work reported by Pereslegin (1967) published some years later.

It is apparent that the emissivity of sea foam or sea water impregnated with a large number of air bubbles is much higher than that of sea water that is relatively undisturbed (Williams, 1969). The emission of sea foam is an intractable theoretical problem and its precise characteristics will be discovered only through extensive and well-controlled measurements. It is not known whether or not sea foam is an important factor for all frequencies and for all viewing angles. The effect of foam was confirmed by airborne measurements from the NASA/GSFC Convair 990 (Nordberg, Conaway, and Thaddeus, 1969). Their measurements did not support the predictions of Stogryn (1967); however, his theory did not intend to account for sea foam or air bubbles and dealt only with the effects of a statistically rough sea surface. The effect of this type of surface roughness apparently is small compared to the effect of bubbles and foam.

Several papers have been written with the purpose of reviewing the literature on microwave radiometry and its applications to oceanography, e.g. Porter and Florance (1969), Paris (1969), and Haroules and Brown (1969). A comprehensive review of the efforts in this area is being conducted in the Soviet Union and is given in the publication by Shifrin (1969). Two other excellent publications that deal mainly with the effects of the atmosphere are the papers by Thompson (1969) and Lukes (1968).

Current Status

The Dielectric Constant of Sea Water--The dielectric constant of sea water, $\varepsilon' - j\varepsilon''$, is complex and may be given as shown in the following

equations:

$$\varepsilon' = \varepsilon_o + \frac{\varepsilon_s - \varepsilon_o}{1 + \omega^2 \tau_o^2} \qquad (1)$$

and

$$\varepsilon'' = \frac{\omega \tau_o (\varepsilon_s - \varepsilon_o)}{1 + \omega^2 \tau_o^2} + \frac{36\pi\sigma_i \times 10^9}{\omega} \qquad (2)$$

where τ_o, ε_s, and σ_i are functions of salinity and temperature only. The best values for these quantities are those given by Saxton and Lane (1952b) where ε_o is assumed to be 4.9 and where the salinities of a 0.5, 1.0, and 1.5 normal solution are taken to be 28.3, 55.5, and 81.6 o/oo, respectively.

The effects of salinity, temperature and frequency on ε' and ε'' are clearly shown in two figures in Lane and Saxton (1952b) which are given here in Figs. 1 and 2. The salinity of "sea water" is 36 o/oo, and the salinity of fresh water is such that σ_i is about 0.01 mho m^{-1}. The absorption is closely associated with ε''. Thus, the results of Sirounian (1968) and Paris (1969) were indirectly anticipated by Lane and Saxton though they were not aware of the possibility of using these effects to measure sea surface salinity or temperature.

Of course, the dielectric constant of sea water (not aqueous sodium chloride) has yet to be measured for a wide range of frequencies, temperatures, and salinities. Certainly, this is one area that needs immediate attention.

The Dielectric Constant of Ice--The results of the measurements of the dielectric constant of ice show that it is essentially constant with

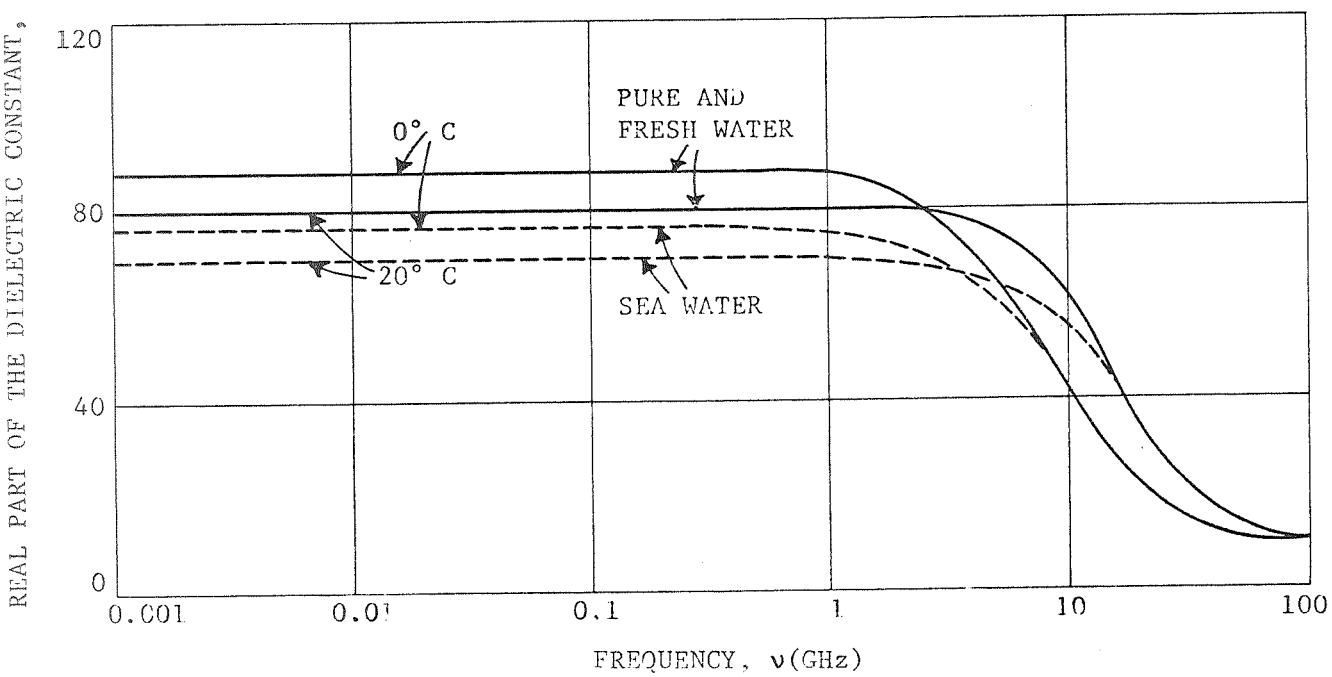

Figure 1. Real part of the complex dielectric constant of pure, fresh and sea water versus frequency for 0° C and 20° C.

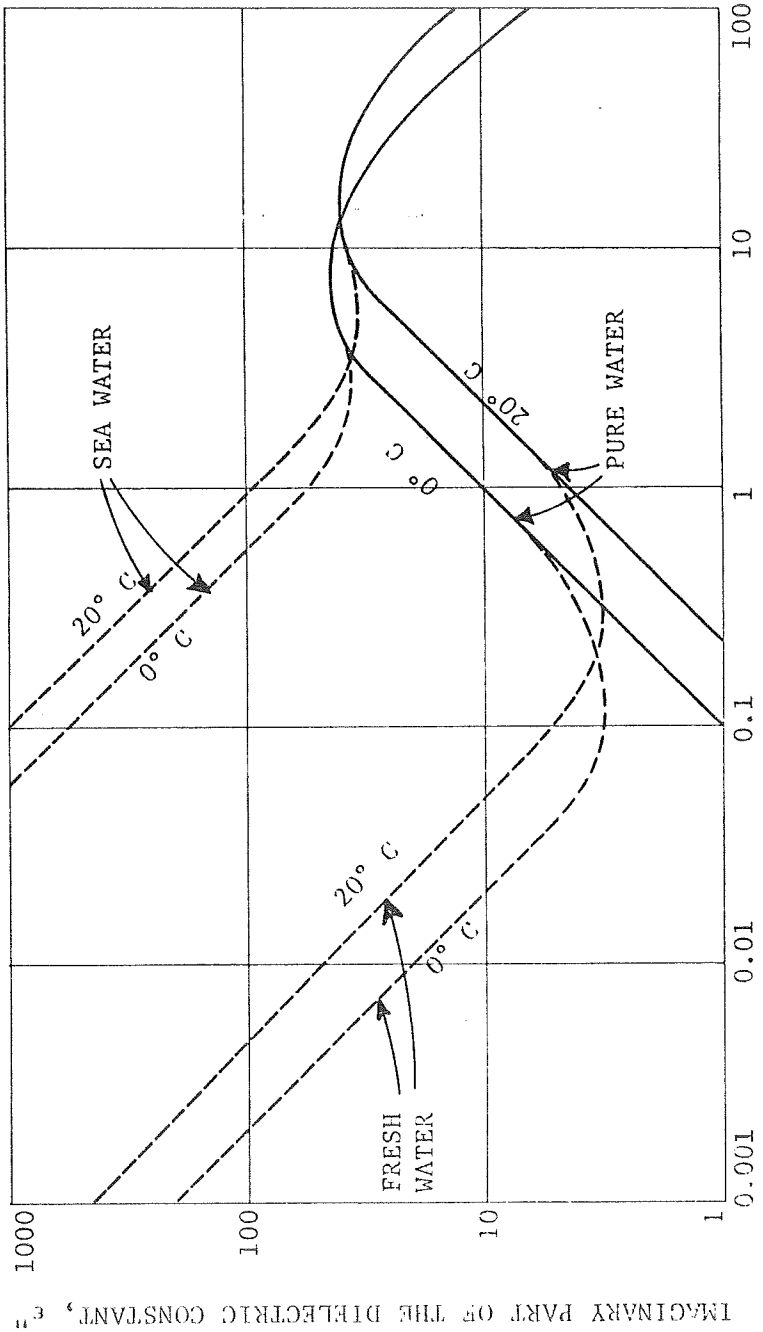

Figure 2. Imaginary part of the complex dielectric constant of pure, fresh and sea water versus frequency for a water temperature of 0° C and 20° C.

frequency and has values shown in Table I.

TABLE I. Dielectric Constant of Ice (after Gunn and East, 1954).

Temperature, T (°C)	ε'	ε''
0	3.165	0.00855
-10	3.165	0.00281
-20	3.165	0.00196

The Volume Absorption Coefficient of Water Vapor

The absorption of microwaves by water vapor is due to (1) absorption by a single rotational line at 22.235 GHz and (2) absorption by a host of pressure-broadened infrared lines. The following equations should be used to give the volume absorption coefficient for water vapor (α_w, km^{-1}) as a function of frequency (ν, Hz), temperature (T,K), pressure (P, mb) and density of water vapor (ρ_w, gm m^{-3}).

$$\alpha_w = 3.615 \times 10^{-7} \frac{\rho_w \nu^2}{T^{3/2}} \left[\frac{\exp(-642/T)}{T} f_w + 7.07 \times 10^{-24} \Delta_w \right] \quad (km^{-1})$$

where

$$\Delta_w = 2.62 \times 10^{9} \left(\frac{P}{1013.3} \right) \left(\frac{318}{T} \right)^{0.625} \left[1 + \frac{0.0147 \rho_w T}{P} \right] \quad (Hz)$$

$$f_w = \frac{\Delta_w}{(\nu_w - \nu)^2 + \Delta_w^2} + \frac{\Delta_w}{(\nu_w + \nu)^2 + \Delta_w^2}$$

$$\nu_w = 22.235 \times 10^{9} \text{ Hz}$$

The absorption coefficient of water vapor is greater than that of molecular oxygen for frequencies of about 15 GHz to 30 GHz. Since the amount of water vapor in the atmosphere is highly variable, one would best avoid this frequency band if the effect of the atmosphere is to be predictable.

The Volume Absorption Coefficient of Molecular Oxygen

Molecular oxygen is a strong absorber of microwave radiation. The volume absorption coefficient for molecular oxygen (α_{ox}, km^{-1}) is mostly dependent on the absorption of 44 closely spaced resonance lines near 60 GHz plus one line at 118 GHz and is given by

$$\alpha_{ox}(km^{-1}) = 4.6182 \times 10^{-10} \frac{P\nu^2}{T^3} \sum_{\substack{N \text{ odd} \\ N = 1}}^{45} S_n \exp\left[-2.06844\, N(N+1)/T\right] (km^{-1})$$

where

$$S_n = g_n^+ f_{n+} + g_n^- f_{n-} + g_n^o f_o$$

$$g_n^+ = \frac{N(2N + 3)}{N + 1}$$

$$g_n^- = \frac{(N + 1)(2N - 1)}{N}$$

$$g_n^o = \frac{2(N^2 + N + 1)(2N + 1)}{N(N + 1)}$$

$$f_{n+} = \frac{\Delta_{ox}}{(\nu_{n+} - \nu)^2 + \Delta_{ox}^2} + \frac{\Delta_{ox}}{(\nu_{n+} + \nu)^2 + \Delta_{ox}^2}$$

$$f_{n-} = \frac{\Delta_{ox}}{(\nu_{n-} - \nu)^2 + \Delta_{ox}^2} + \frac{\Delta_{ox}}{(\nu_{n-} + \nu)^2 + \Delta_{ox}^2}$$

$$f_o = \frac{\Delta_o}{\nu^2 + \Delta_o^2}$$

$$\Delta_o = 1.463 \times 10^6 \, P \left(\frac{300}{T}\right)^{0.85} (0.21 + 0.78 \, \beta)$$

$$\beta = \begin{cases} 0.25 : & P > 356 \text{ mb} \\ 0.25 + 0.435 \, (2.551 - \log_{10} P) : & 25.3 < P < 356 \text{ mb} \\ 0.75 : & P < 25.3 \text{ mb} \end{cases}$$

P = total pressure (mb)

T = air temperature (K)

ν = frequency (Hz)

ν_{n+}'s and ν_{n-}'s are given in Table I of Meeks and Lilley (1963)

The Apparent Sky Temperature for a Cloudy Sky

The best way to get a feel for the range of values to be expected for the apparent sky temperature is to consider the various values that have been either observed or calculated from simple models. These values are plotted in Fig. 3.

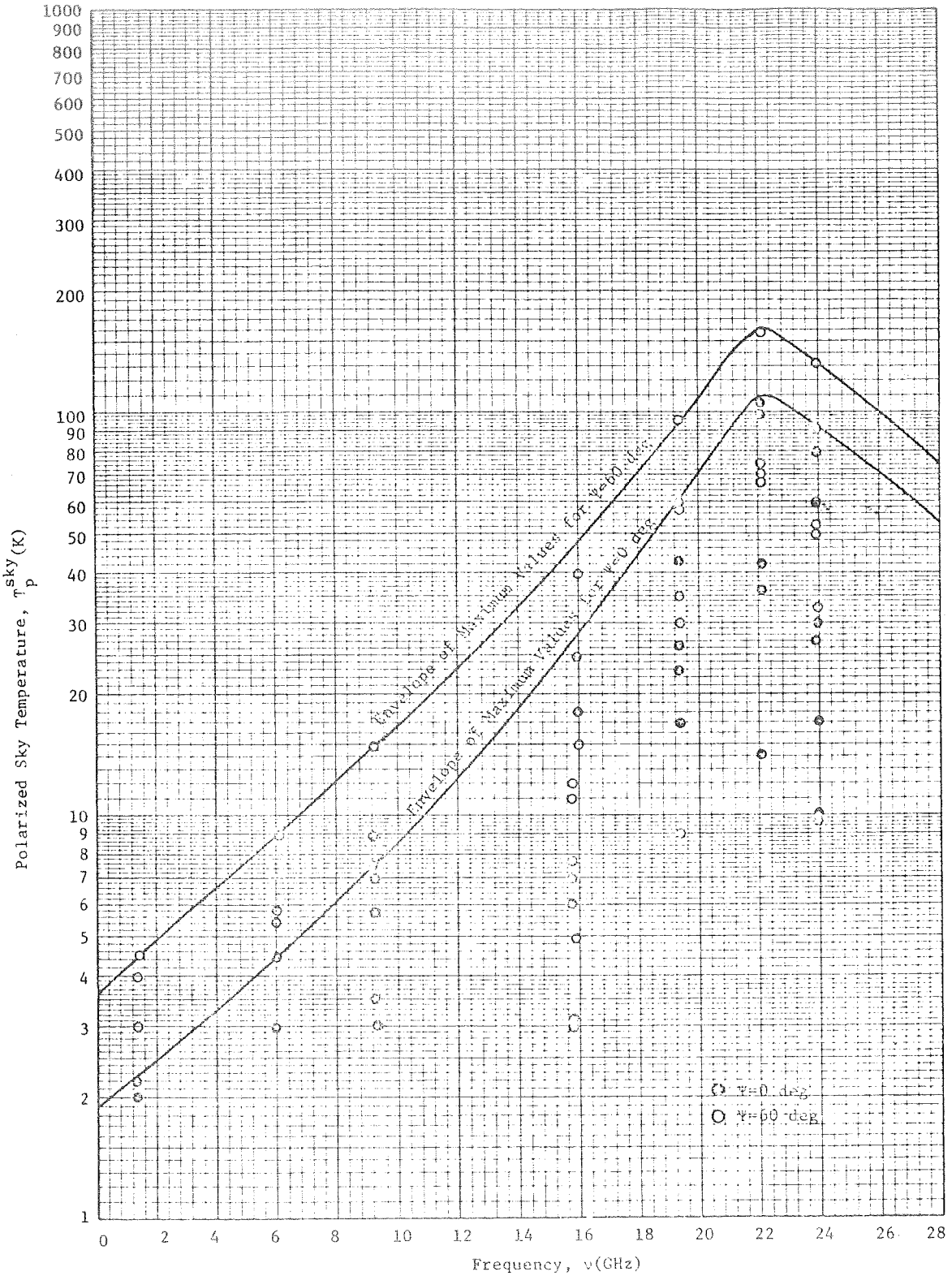

Figure 3. Observed and calculated values of polarized sky temperature from the literature.

The scatter of values is especially large near 22.235 GHz amounting to up to 90 K. This scatter is due primarily to differences in the distribution and total amount of water vapor. Thus, to avoid this unwanted effect, oceanographers must use frequencies outside the range from 15 GHz to 30 GHz.

The Volume Absorption Coefficient of Liquid-Water Clouds

Recent research has been conducted by Paris (1970) into the radiative properties of raining and non-raining clouds. The volume absorption coefficient for a model liquid water cloud having a distribution of drop-sizes given by Marshall and Palmer (1948) was calculated from a knowledge of the absorption cross sections (Q_A) and scattering cross sections (Q_s) of individual water droplets. The formulation of these cross sections from the Mie theory is shown below:

Computational Procedure for Mie Parameters (Adapted from Diermendjian [1969])

Given: m complex index of refraction ($n - i\kappa$)

ν frequency (Hz)

d drop diameter (m)

c speed of light (2.99791×10^8 m sec^{-1})

π 3.1415927

Scheme: $x = \pi\nu d/c$

$y = mx$

$A_o = \cot(y)$

$A_n = -(n/y) + [(n/y) - A_{n-1}]^{-1}$

$w_{-1} = \cos(x) - i \sin(x)$

$w_o = \sin(x) + i \cos(x)$ [Deirmendjian made a sign error in his expression for w_o using $\sin x - i \cos x$]

$$a_n = \frac{\left(\frac{A_n}{m} + \frac{n}{x}\right) \mathrm{Re}\{w_n\} - \mathrm{Re}\{w_{n-1}\}}{\left(\frac{A_n}{m} + \frac{n}{x}\right) w_n - w_{n-1}}$$

$$b_n = \frac{\left(mA_n + \frac{n}{x}\right) \mathrm{Re}\{w_n\} - \mathrm{Re}\{w_{n-1}\}}{\left(mA_n + \frac{n}{x}\right) w_n - w_{n-1}}$$

$\mu = \cos\theta$ where θ is the angle between the forward direction and the direction of scattering

$\pi_o = 0$ $\qquad$ $\tau_o = 0$

$\pi_1 = 1$ $\qquad$ $\tau_1 = \mu$

$\pi_2 = 3\mu$ $\qquad$ $\tau_2 = 6\mu^2 - 3$

$$\pi_n = \mu\left(\frac{2n-1}{n-1}\right)\pi_{n-1} - \left(\frac{n}{n-1}\right)\pi_{n-2}$$

[There is an error in this expression as given by Deirmendjian in that n is omitted in numerator of the second term]

$$\tau_n = \mu(\pi_n - \pi_{n-2}) - (2n-1)(1-\mu^2)\pi_{n-1} + \tau_{n-2}$$

[Note: Van de Hulst (1957, p. 124) has an error in a corresponding expression for τ_n in that sin θ should read $\sin^2\theta$]

$$Q_t = \frac{\pi d^2}{2x^2} \sum_{n=1}^{\infty} (2n+1)\,\mathrm{Re}\{a_n + b_n\}$$

$$Q_s = \frac{\pi d^2}{2x^2} \sum_{n=1}^{\infty} (2n+1)\,\{|a_n|^2 + |b_n^2|\}$$

$$S_1 = \sum_{n=1}^{\infty} \frac{2n+1}{n(n+1)} \{a_n \pi_n + b_n \tau_n\}$$

$$S_2 = \sum_{n=1}^{\infty} \frac{2n+1}{n(n+1)} \{a_n \tau_n + b_n \pi_n\}$$

$$i_1 = S_1 S_1^*$$

$$i_2 = S_2 S_2^*$$

$$i_3 = \mathrm{Re}\{S_1 S_2^*\}$$

$$i_4 = -\mathrm{Im}\{S_1 S_2^*\}$$

where Q_t is the total extinction cross section (m^2)

Q_s is the scattering cross section (m^2)

Q_a is the absorption cross section, $Q_a = Q_t - Q_s$ (m^2)

S_1 and S_2 are the dimensionless, complex amplitude functions related to components perpendicular and parallel, respectively, to the scattering plane.

i_1, i_2, i_3, i_4 are the scattering intensities.

These expressions were programmed and the resulting values of volume absorption coefficient (ALPHA, m^{-3}) and volume scattering coefficient (BETA, m^{-3}) were plotted versus the liquid-water content (M, gm m^{-3}). The plots of ALPHA versus M are shown in the following series of graphs for twenty-seven frequencies in the range from 0.5 GHz to 60 GHz.

In summary, these graphs show that a dense, raining cloud [2 gm m^{-3}, 5 km thick] will have significant absorption and emission [brightness temperature for emission of 10 K or greater] for frequencies greater than about 3 GHz; for a non-raining cloud, the absorption is significant for frequencies above about 6 GHz. For frequencies of 30 GHz or greater, a light raining cloud would have a transmissivity of only about 50 percent.

The Emission of Sea Water

Using the French Law of Reflection and complex dielectric constants given by Lane and Saxton (1952b), the microwave emission of "sea water" was calculated for several frequencies. These calculations are shown in Fig. 4.

It is clearly seen that temperature is not a significant independent variable for frequencies greater than about 9 GHz.

Conclusions and Recommendations

Due to the unpredictability of the effect of water vapor in the region from 15 GHz to 30 GHz, the severity of liquid-water absorption for frequencies above 30 GHz and the homogeneity of microwave emission for frequencies above 9 GHz, one must conclude that the usefulness of the microwave spectrum above 9 GHz is quite limited as far as direct

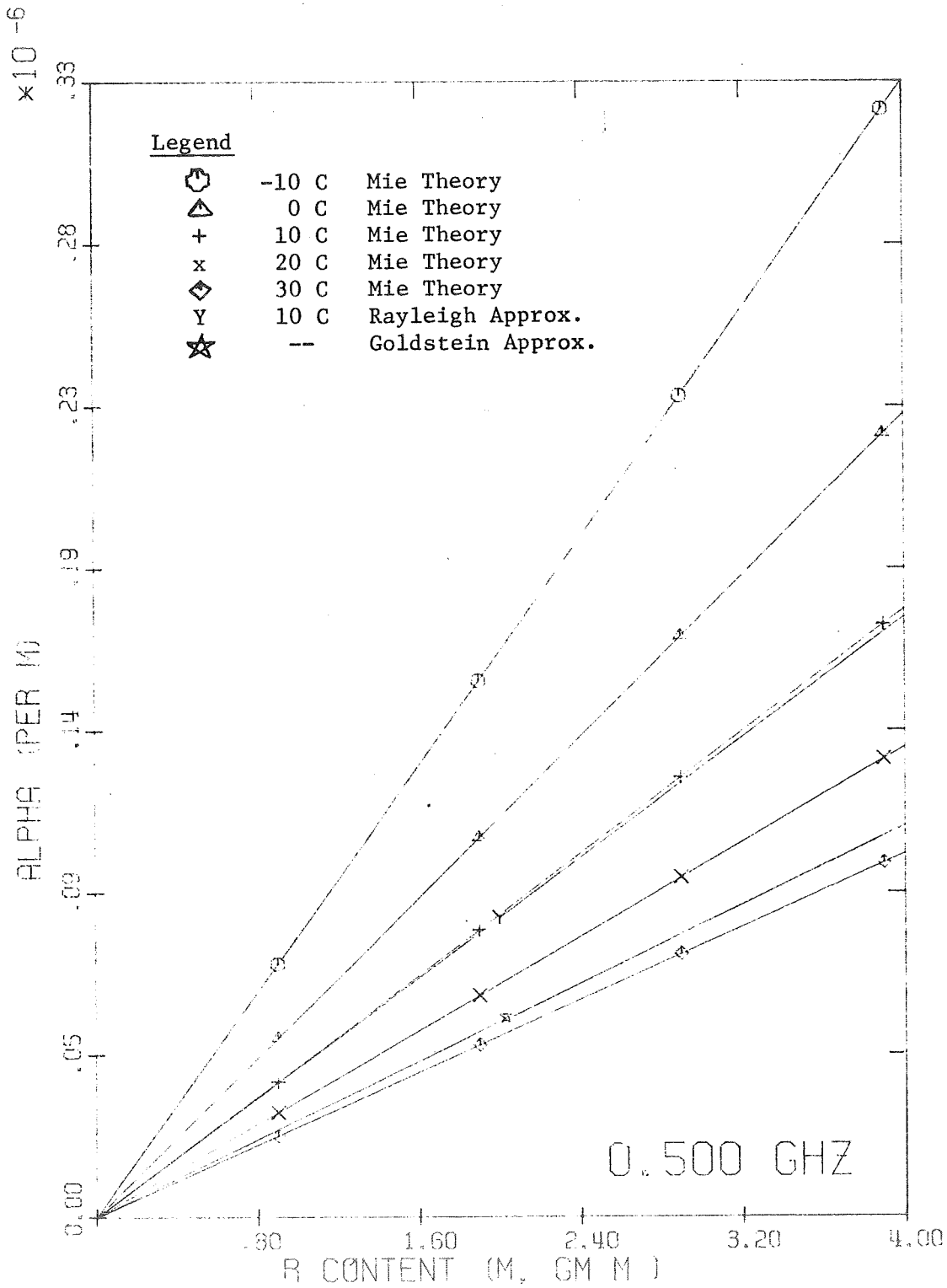
Legend
-10 C Mie Theory
0 C Mie Theory
10 C Mie Theory
20 C Mie Theory
30 C Mie Theory
10 C Rayleigh Approx.
-- Goldstein Approx.
0.500 GHZ
ALPHA (PER M)
x10 -6
0.00
.05
.09
.14
.19
.23
.28
.33
.80
1.60
2.40
3.20
4.00
R CONTENT (M, GM M)

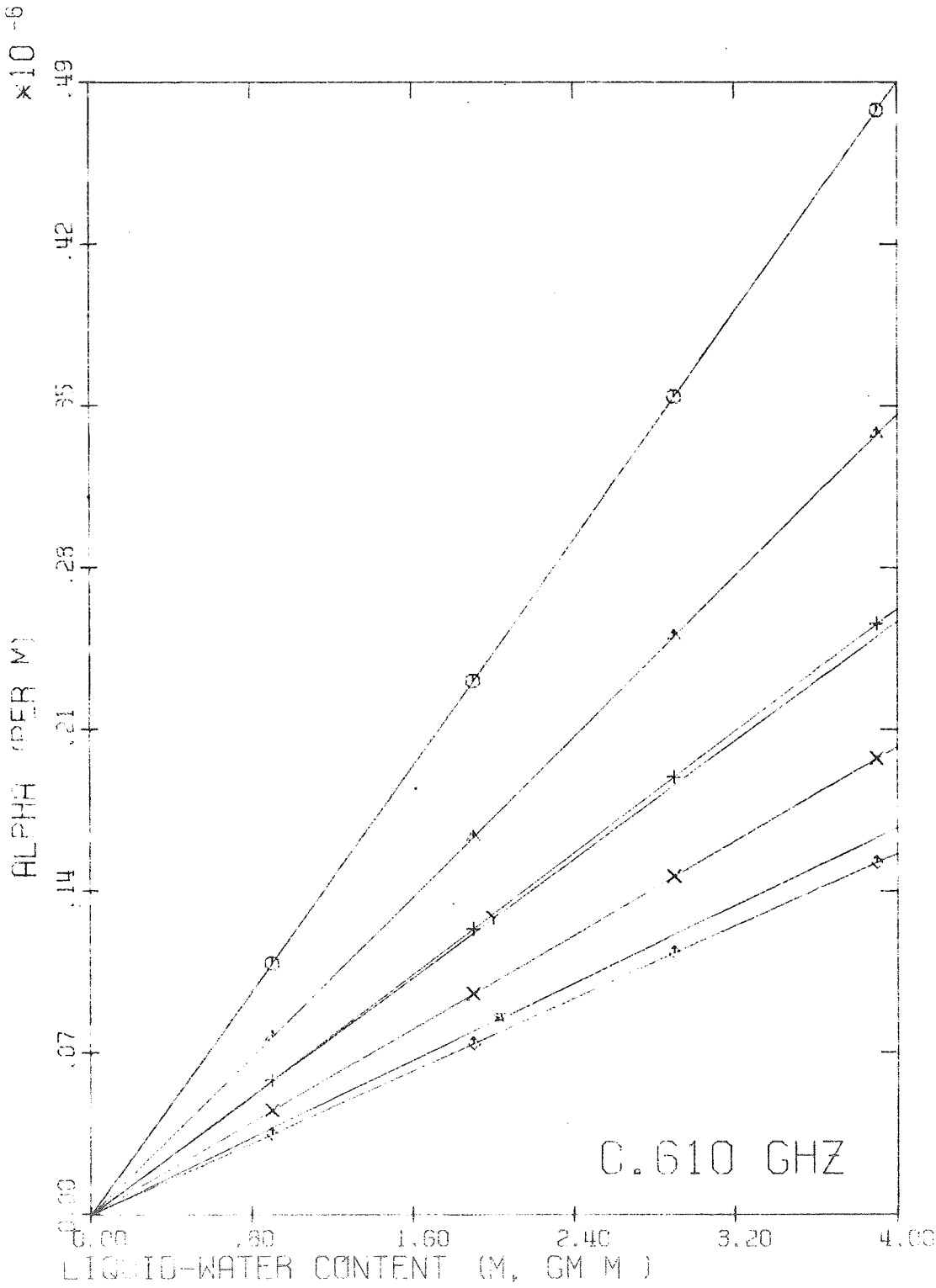
ALPHA (PER M)
*10-6
.49
.42
.35
.28
.21
.14
.07
0.00
0.00
.80
1.60
2.40
3.20
4.00
LIQUID-WATER CONTENT (M, GM M)
0.610 GHZ

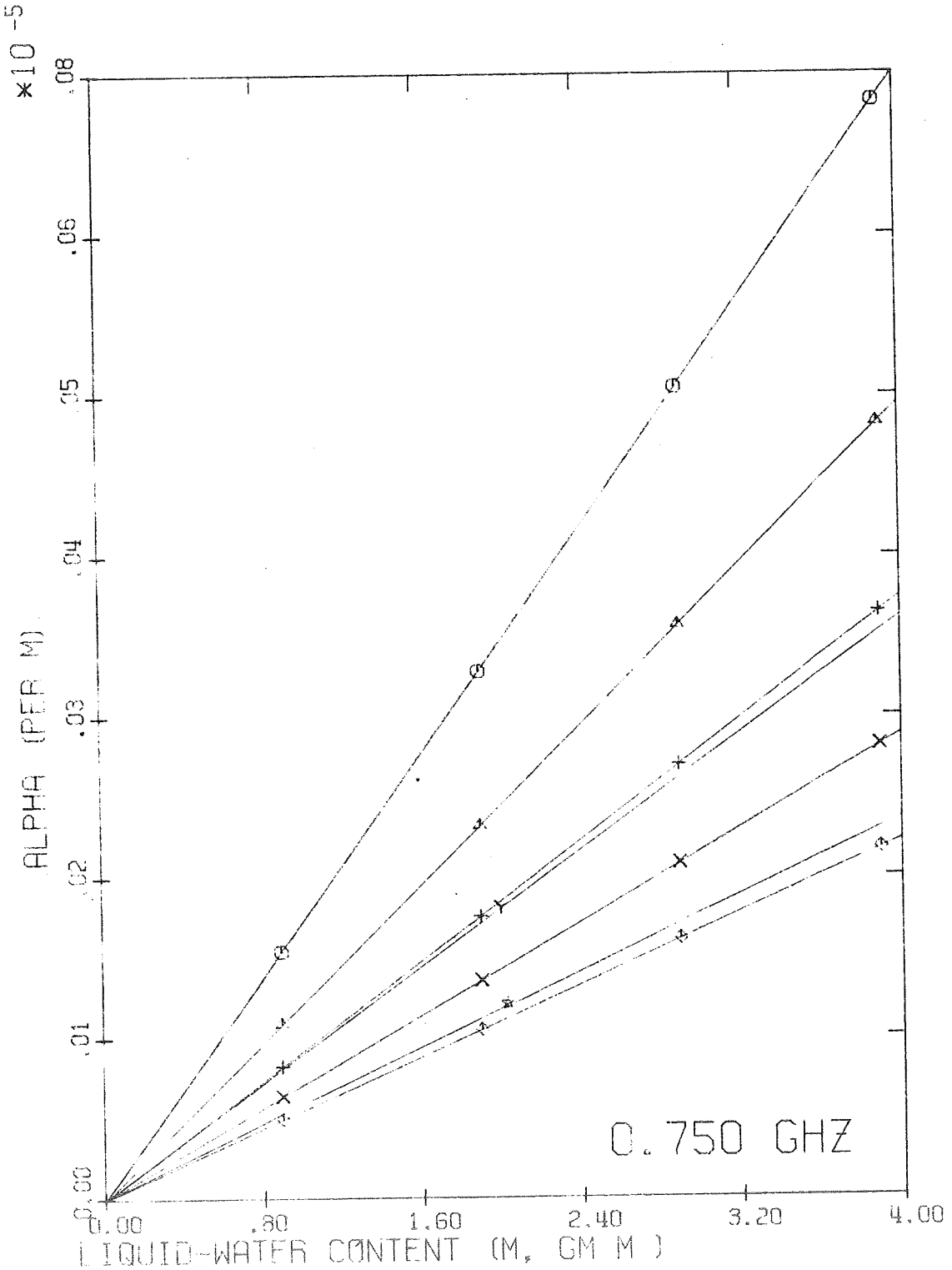
*10 -5
.08
.06
.05
.04
.03
.02
.01
0.00
ALPHA (PER M)
0.750 GHZ
0.00
.80
1.60
2.40
3.20
4.00
LIQUID-WATER CONTENT (M, GM M)

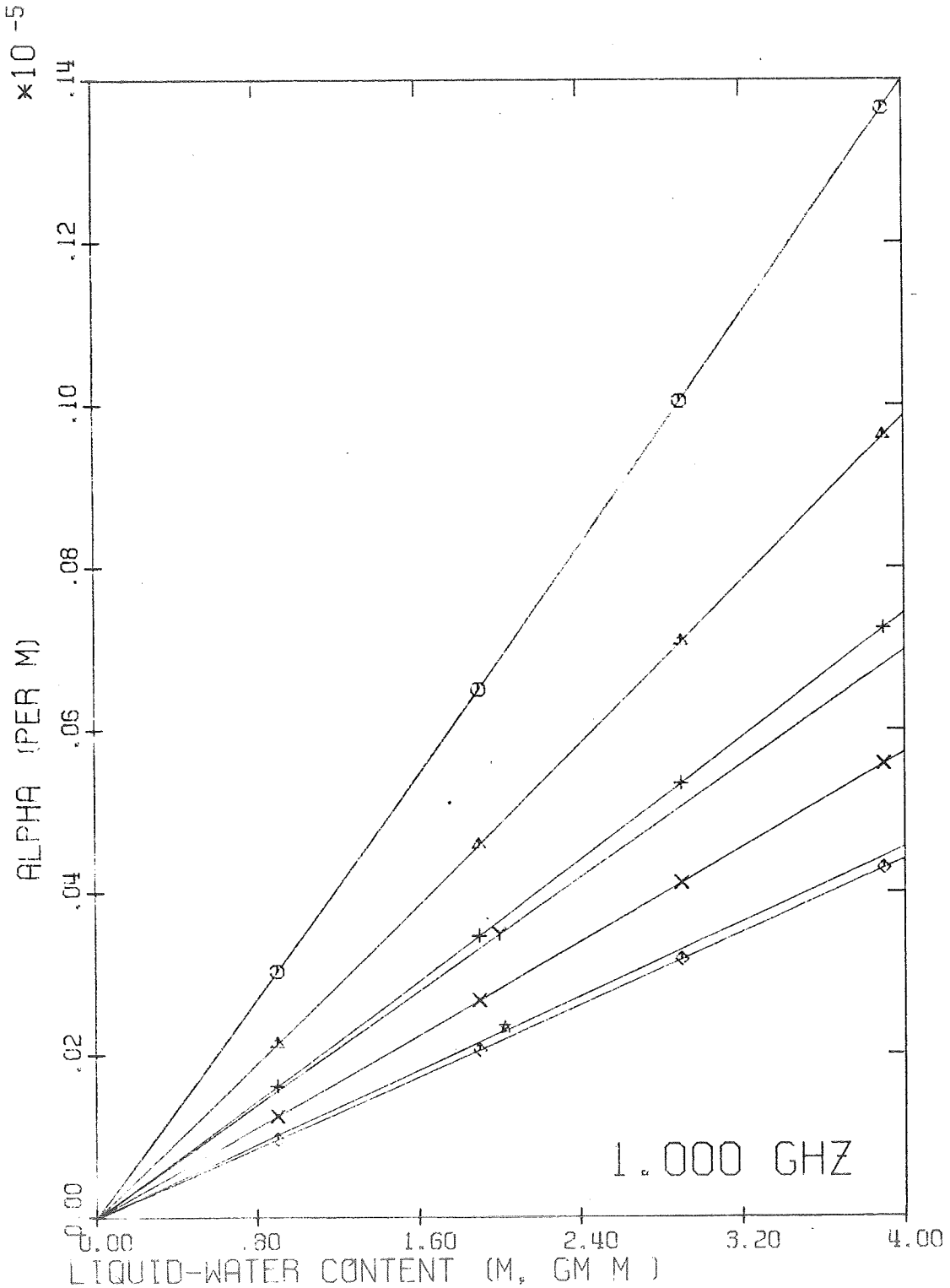
ALPHA (PER M)
×10⁻⁵
.14
.12
.10
.08
.06
.04
.02
0.00
0.00
.80
1.60
2.40
3.20
4.00
LIQUID-WATER CONTENT (M, GM M)
1.000 GHZ

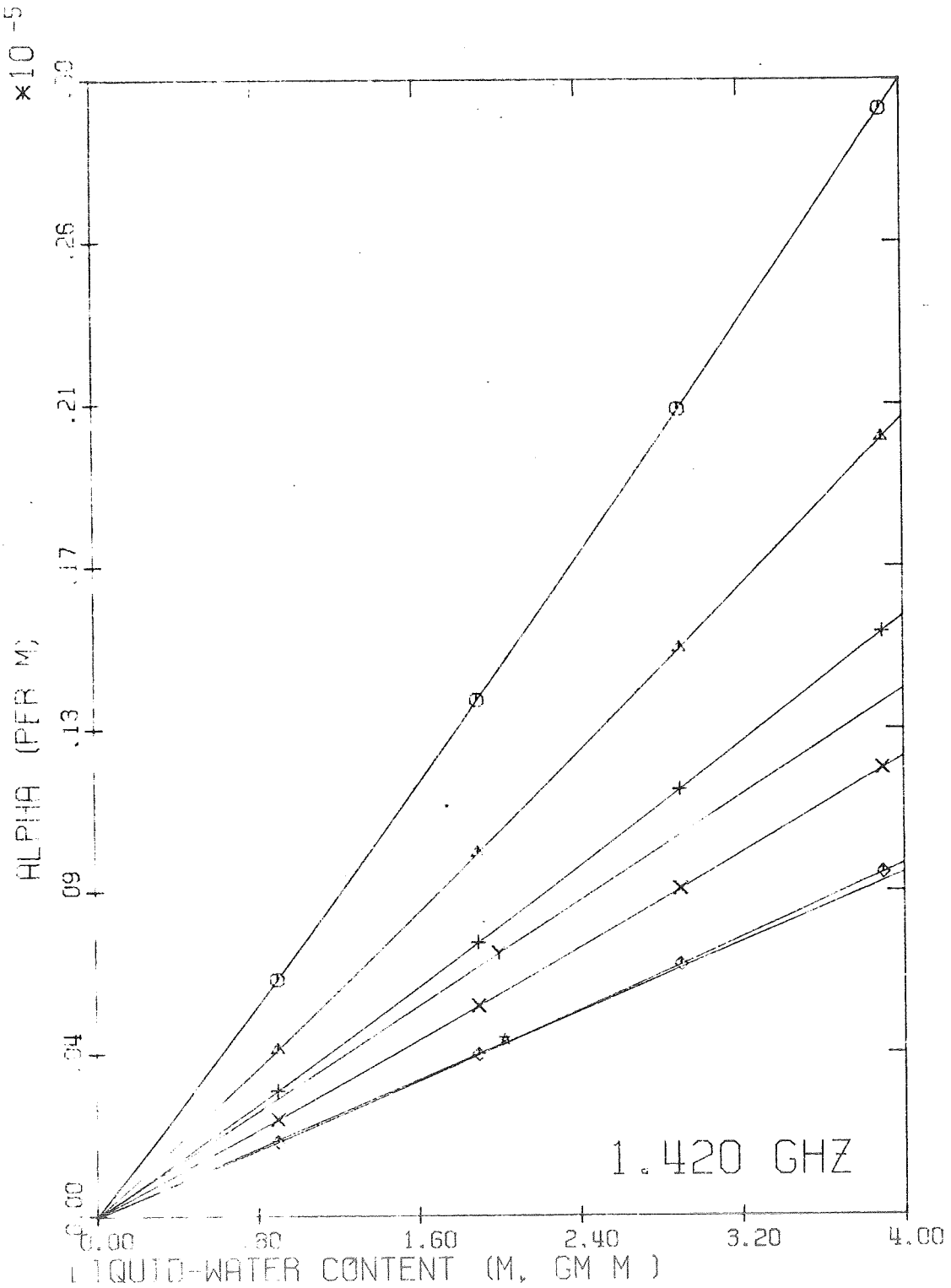
*10 -5
.30
.26
.21
.17
.13
.09
.04
0.00
ALPHA (PER M)
1.420 GHZ
0.00
.80
1.60
2.40
3.20
4.00
LIQUID-WATER CONTENT (M, GM M)

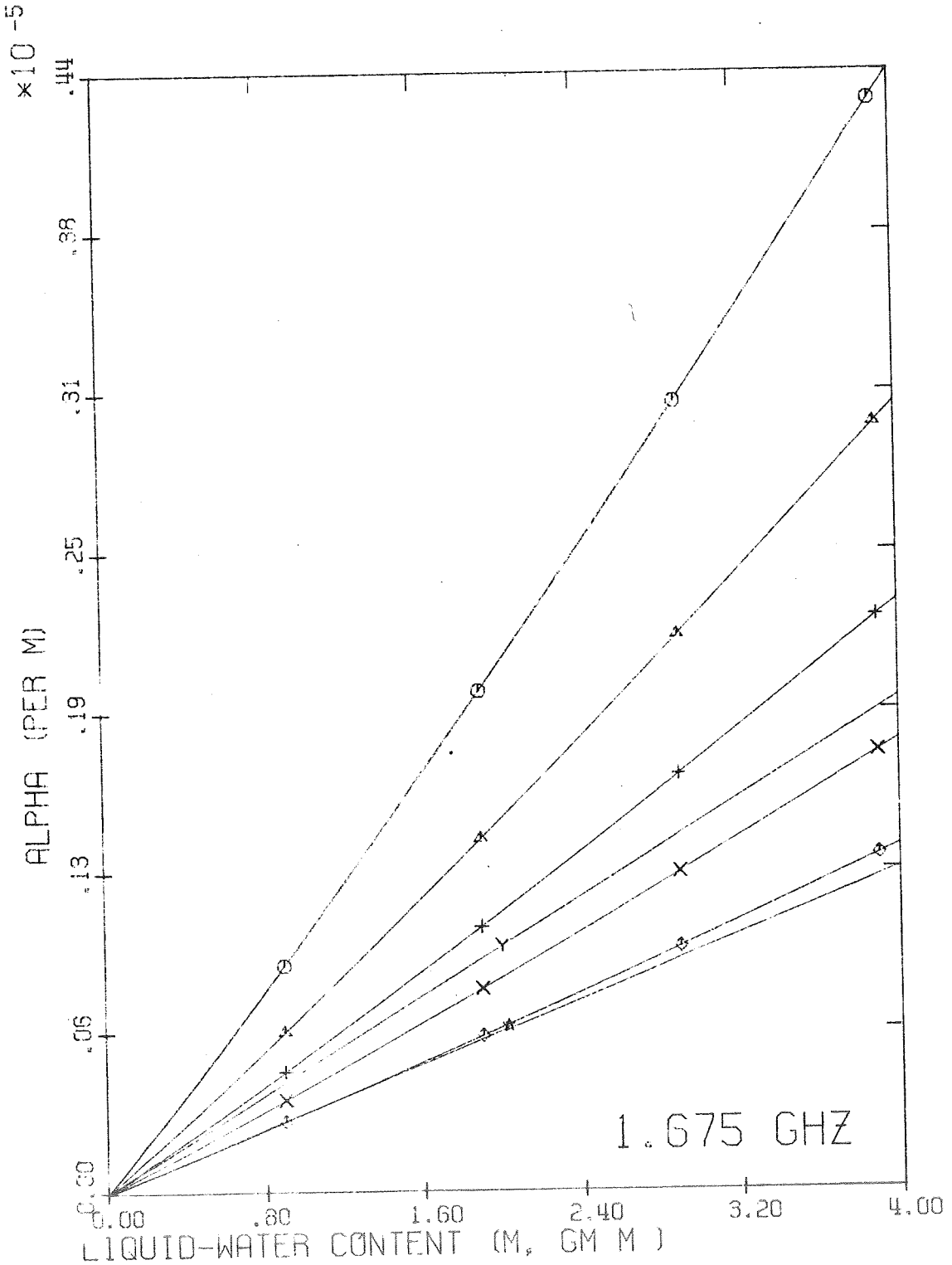
×10 -5
.44
.38
.31
.25
.19
.13
.06
.00
ALPHA (PER M)
1.675 GHZ
0.00
.80
1.60
2.40
3.20
4.00
LIQUID-WATER CONTENT (M, GM M)

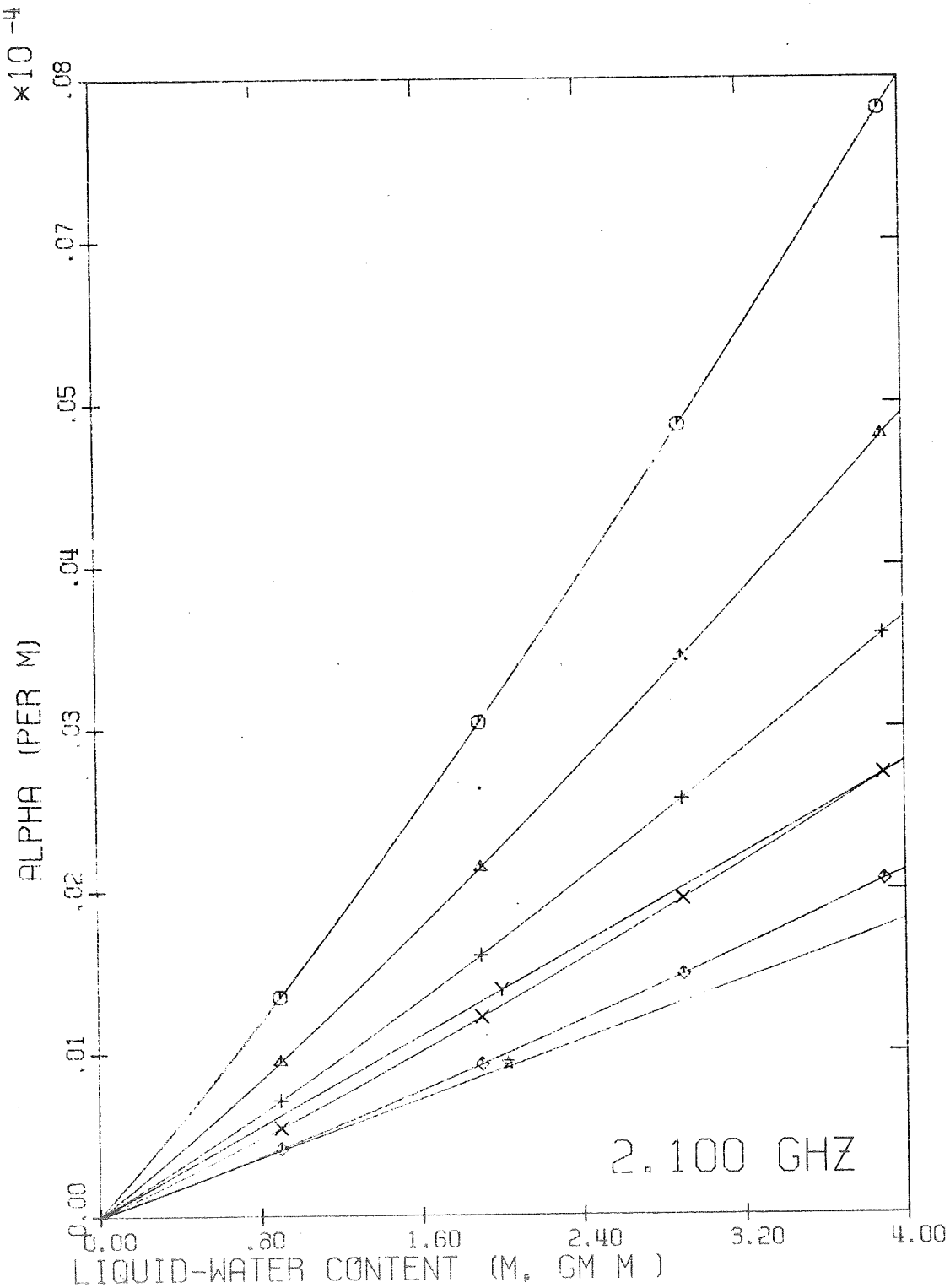
*10 -4
.08
.07
.05
.04
.03
.02
.01
.00
ALPHA (PER M)
2.100 GHZ
0.00
.80
1.60
2.40
3.20
4.00
LIQUID-WATER CONTENT (M. GM M)

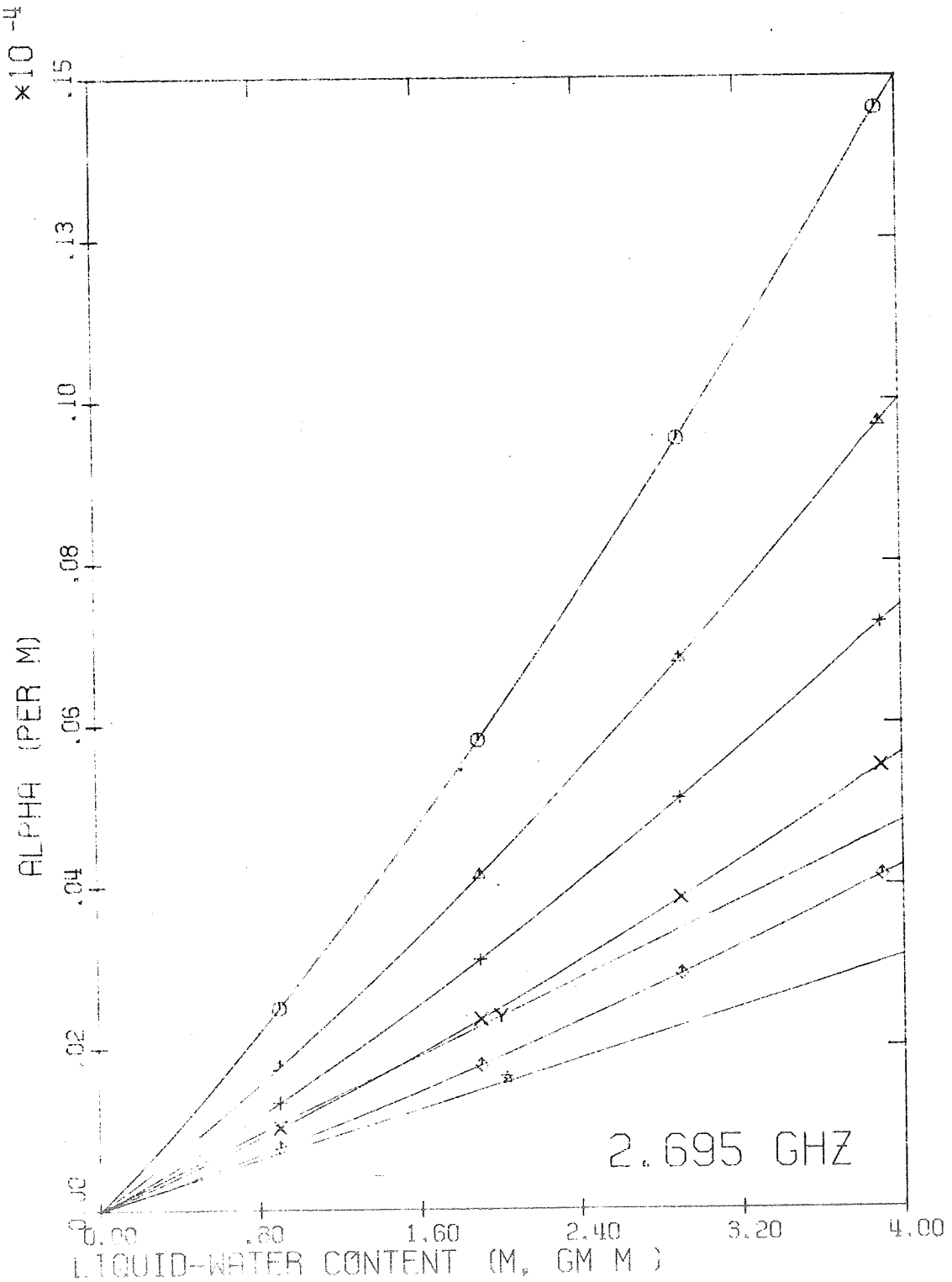
*10 -4
.15
.13
.10
.08
.06
.04
.02
.00
ALPHA (PER M)
2.695 GHZ
0.00
.80
1.60
2.40
3.20
4.00
LIQUID-WATER CONTENT (M. GM M)

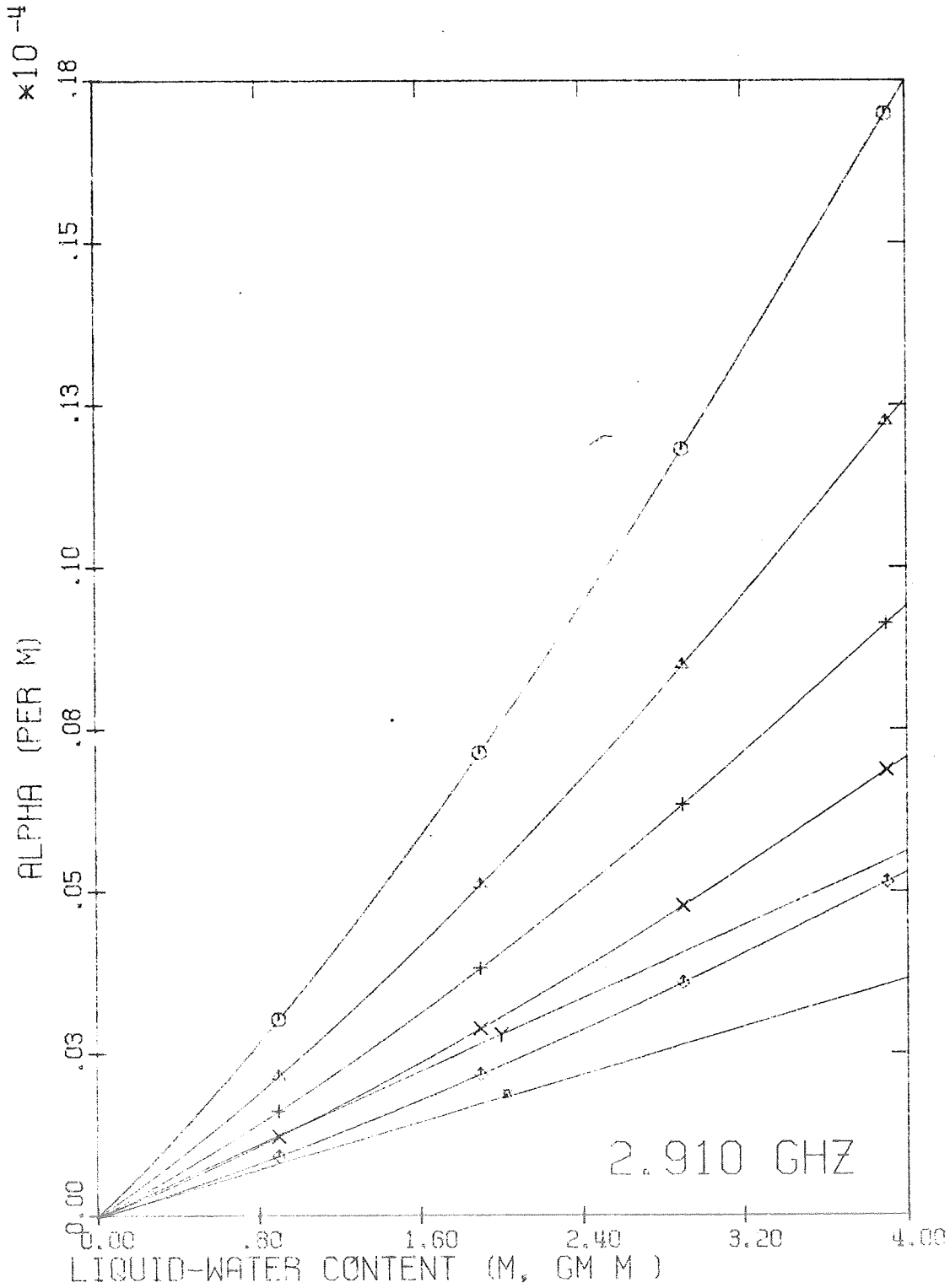
*10 -4
.18
.15
.13
.10
.08
.05
.03
0.00
ALPHA (PER M)
0.00
.80
1.60
2.40
3.20
4.00
LIQUID-WATER CONTENT (M, GM M)
2.910 GHZ

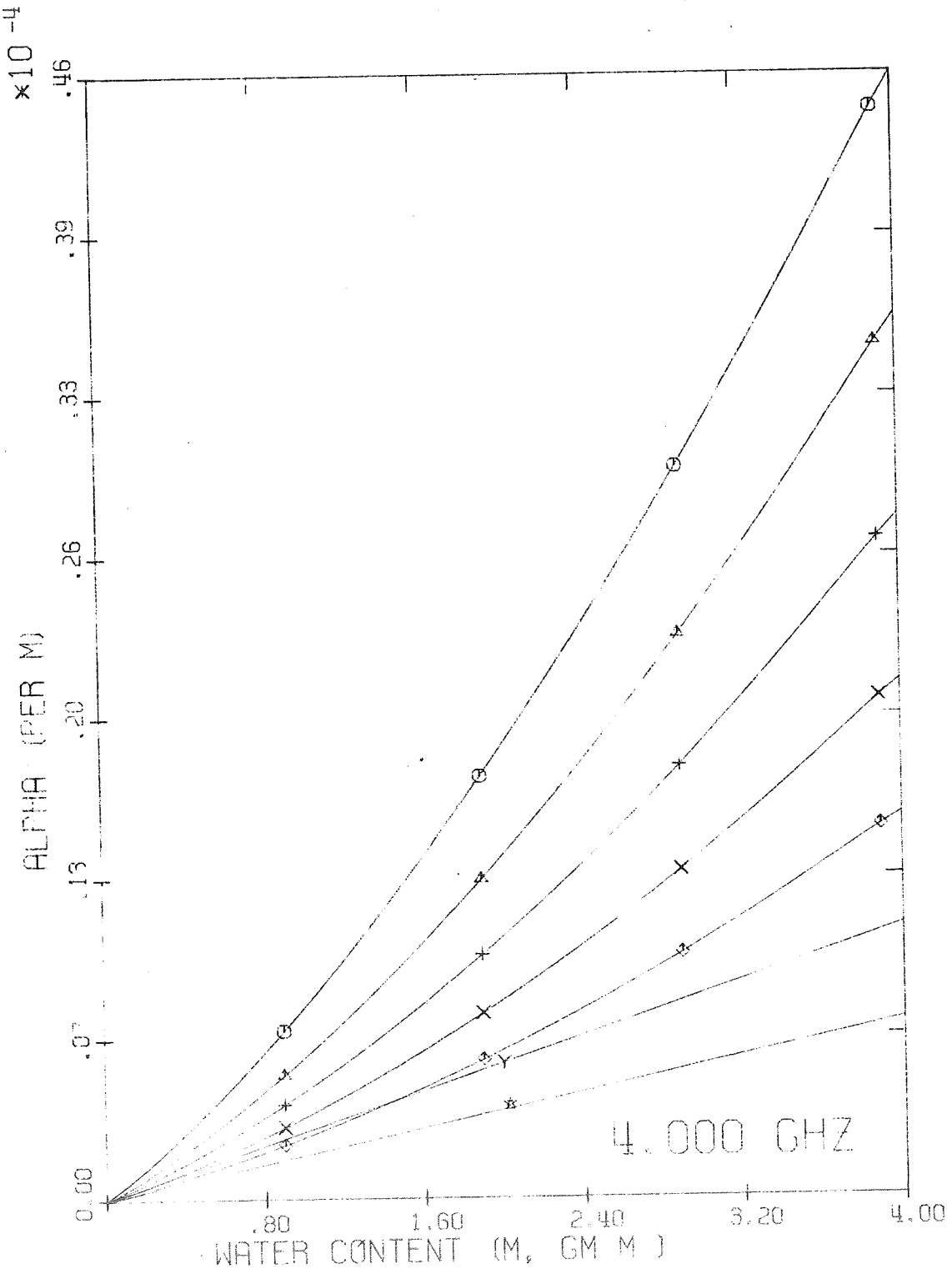
*10-4
.46
.39
.33
.26
.20
.13
.07
0.00
ALPHA (PER M)
.80
1.60
2.40
3.20
4.00
WATER CONTENT (M, GM M)
4.000 GHZ

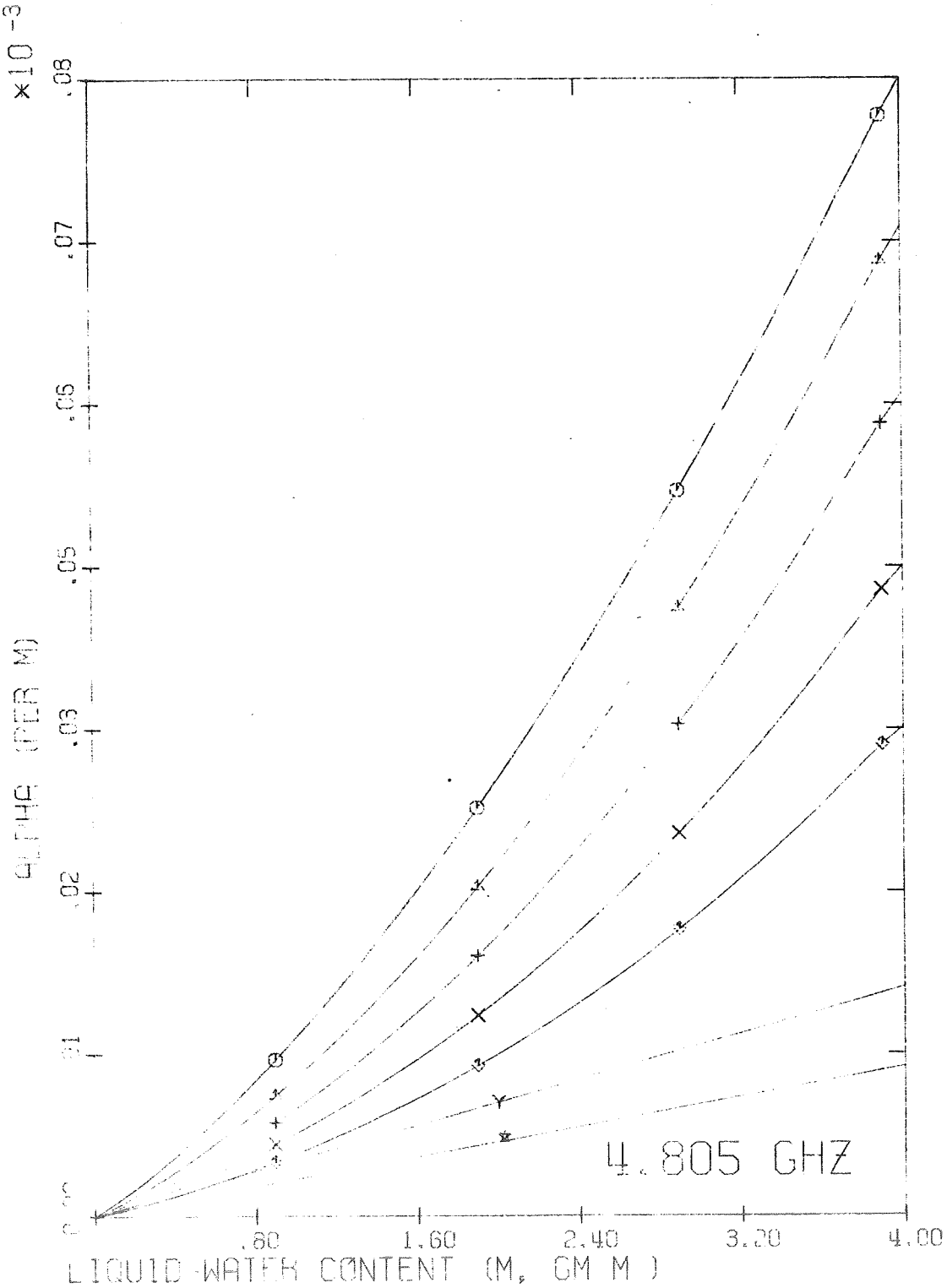
×10⁻³
.08
.07
.06
.05
.03
.02
.01
4.805 GHZ
.80
1.60
2.40
3.20
4.00
LIQUID WATER CONTENT (M, GM M)

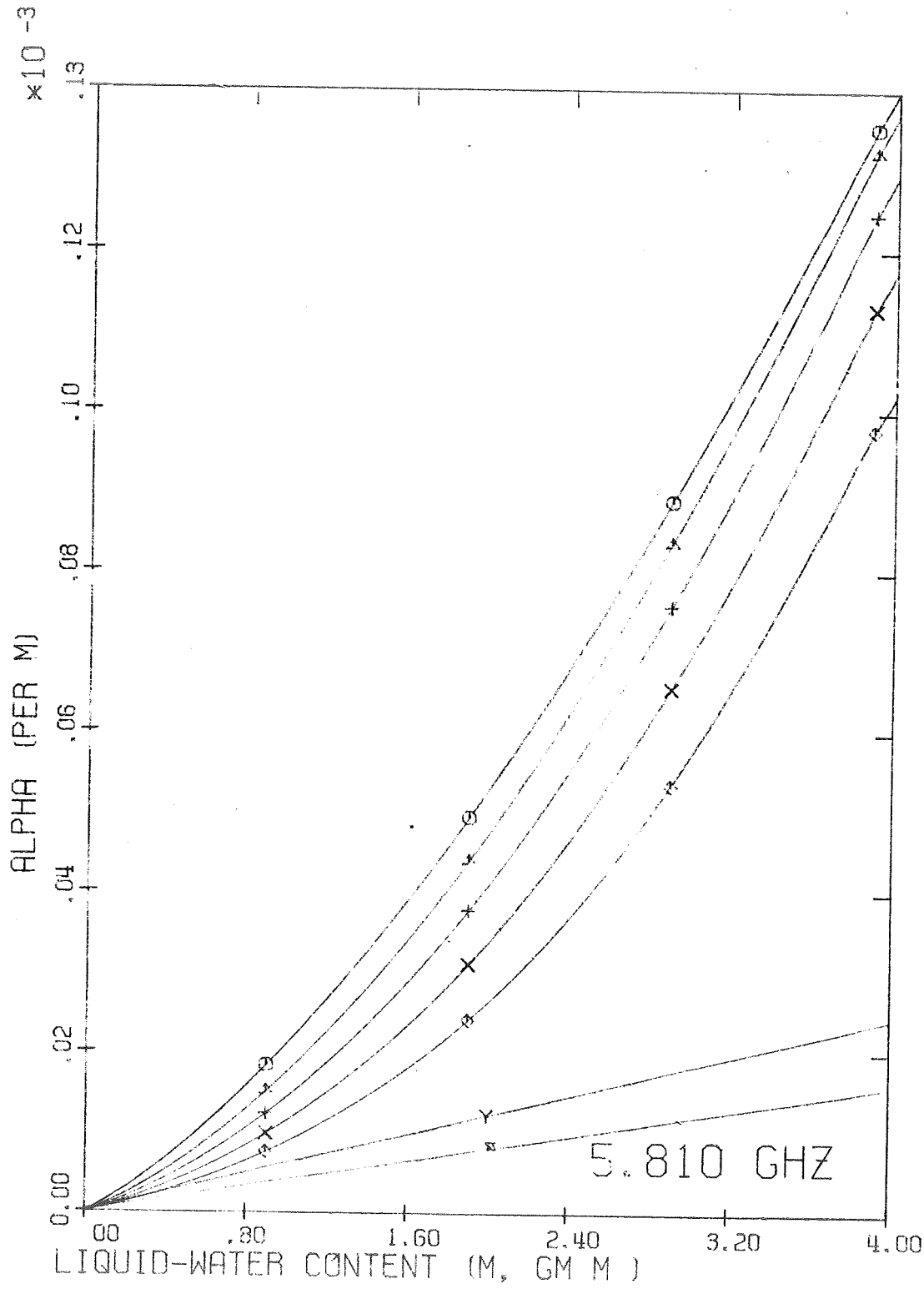
ALPHA (PER M)
*10 -3
.13
.12
.10
.08
.06
.04
.02
0.00
.00
.80
1.60
2.40
3.20
4.00
LIQUID-WATER CONTENT (M, GM M)
5.810 GHZ

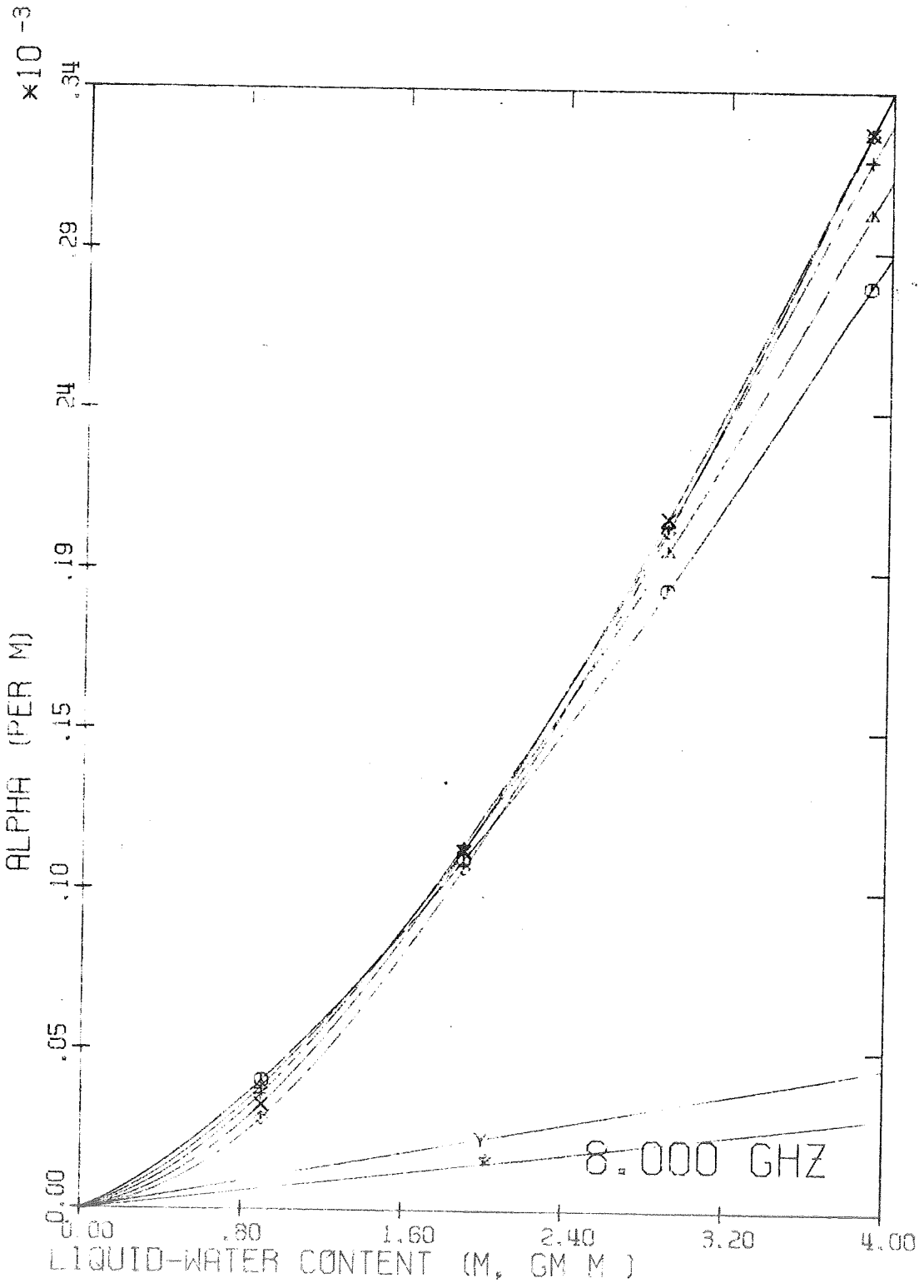
*10 -3
.34
.29
.24
.19
.15
.10
.05
0.00
ALPHA (PER M)
0.00
.80
1.60
2.40
3.20
4.00
LIQUID-WATER CONTENT (M, GM M)
8.000 GHZ

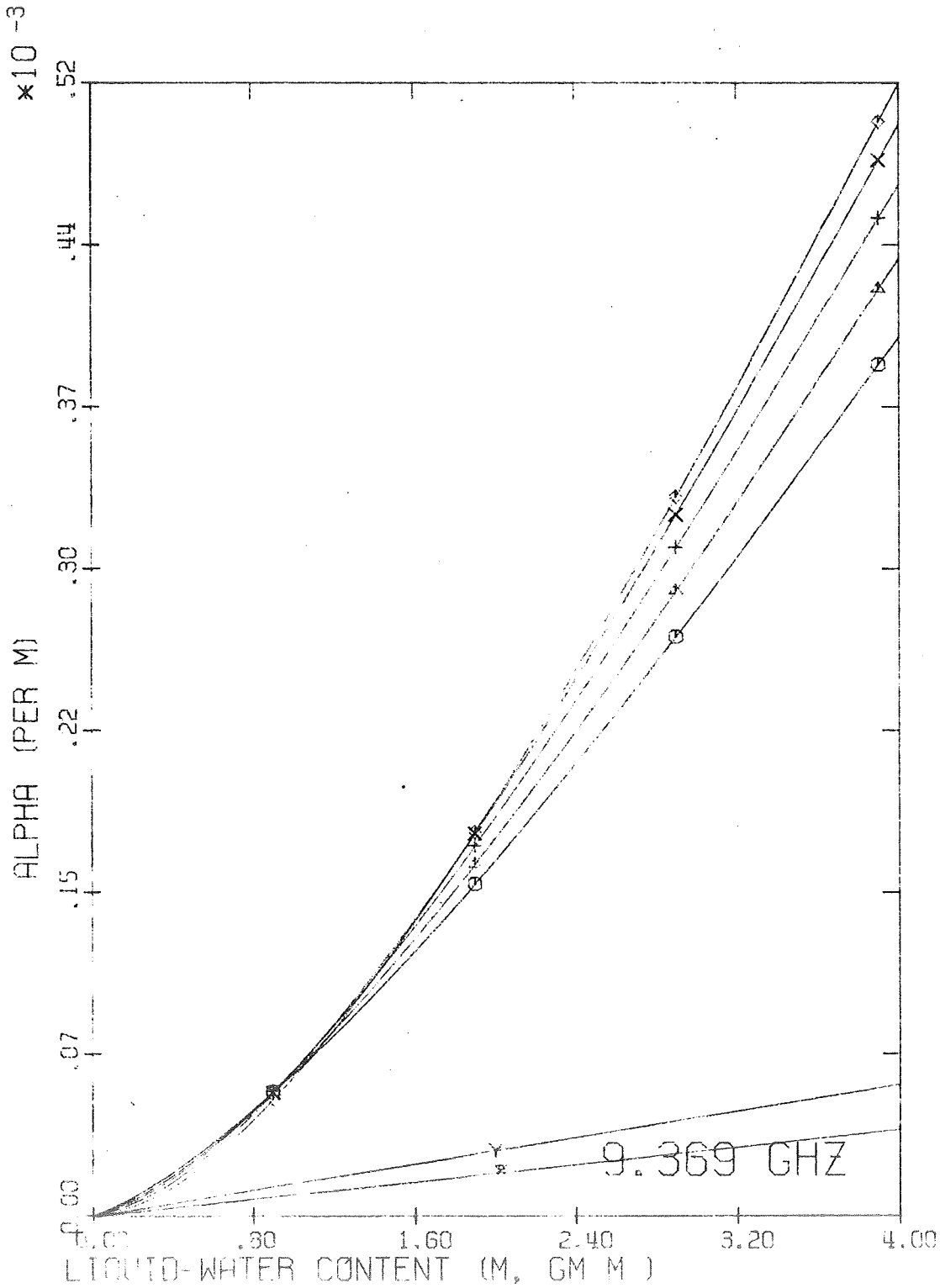
*10 -3
.52
.44
.37
.30
.22
.15
.07
0.00
ALPHA (PER M)
9.369 GHZ
.30
1.60
2.40
3.20
4.00
LIQUID-WATER CONTENT (M, GM M)

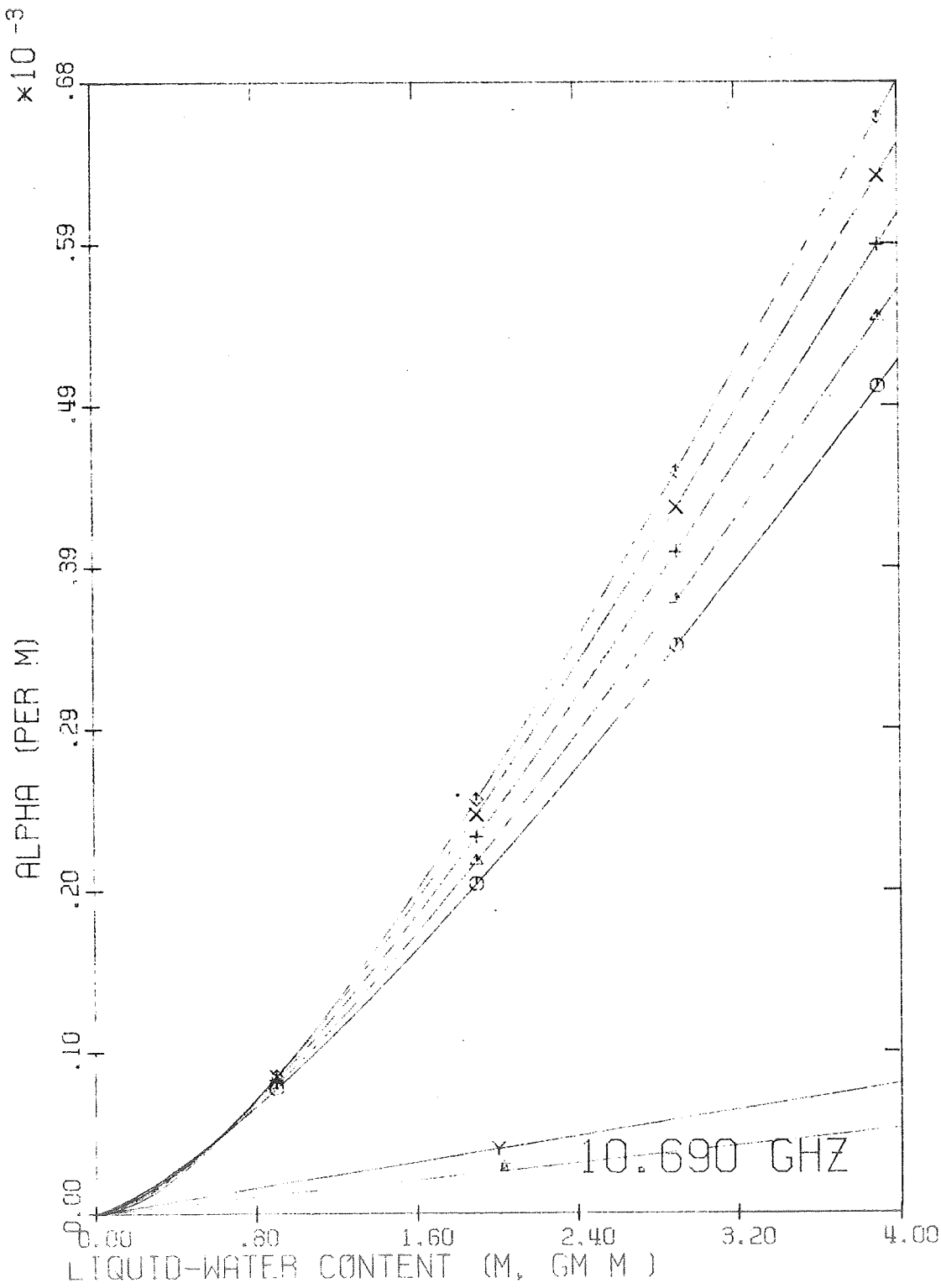
ALPHA (PER M)
*10 -3
.68
.59
.49
.39
.29
.20
.10
.00
0.00
.80
1.60
2.40
3.20
4.00
LIQUID-WATER CONTENT (M, GM M)
10.690 GHZ

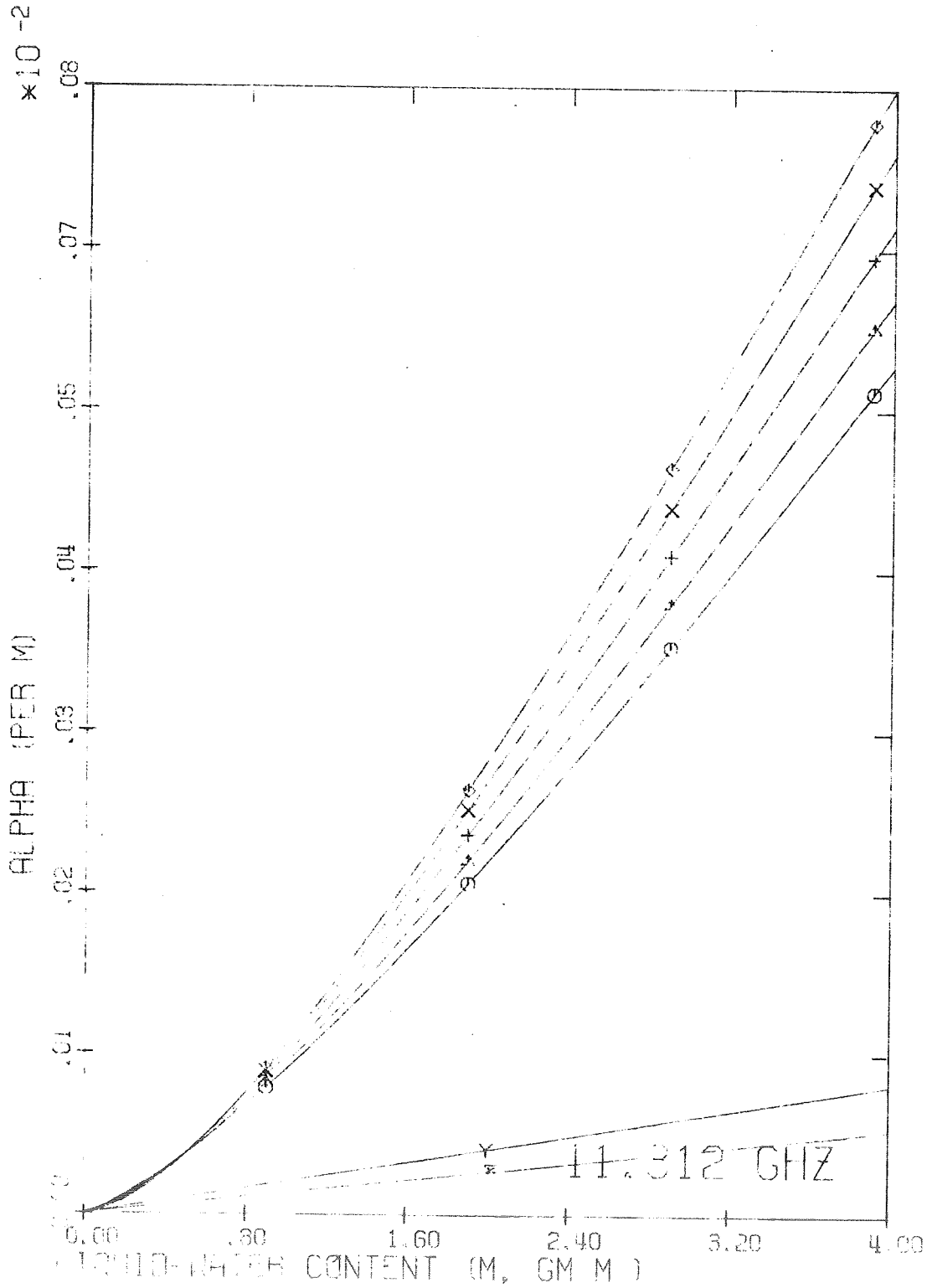
*10 -2
.08
.07
.05
.04
.03
.02
.01
ALPHA (PER M)
11.312 GHZ
0.00
.80
1.60
2.40
3.20
4.00
LIQUID-WATER CONTENT (M, GM M)

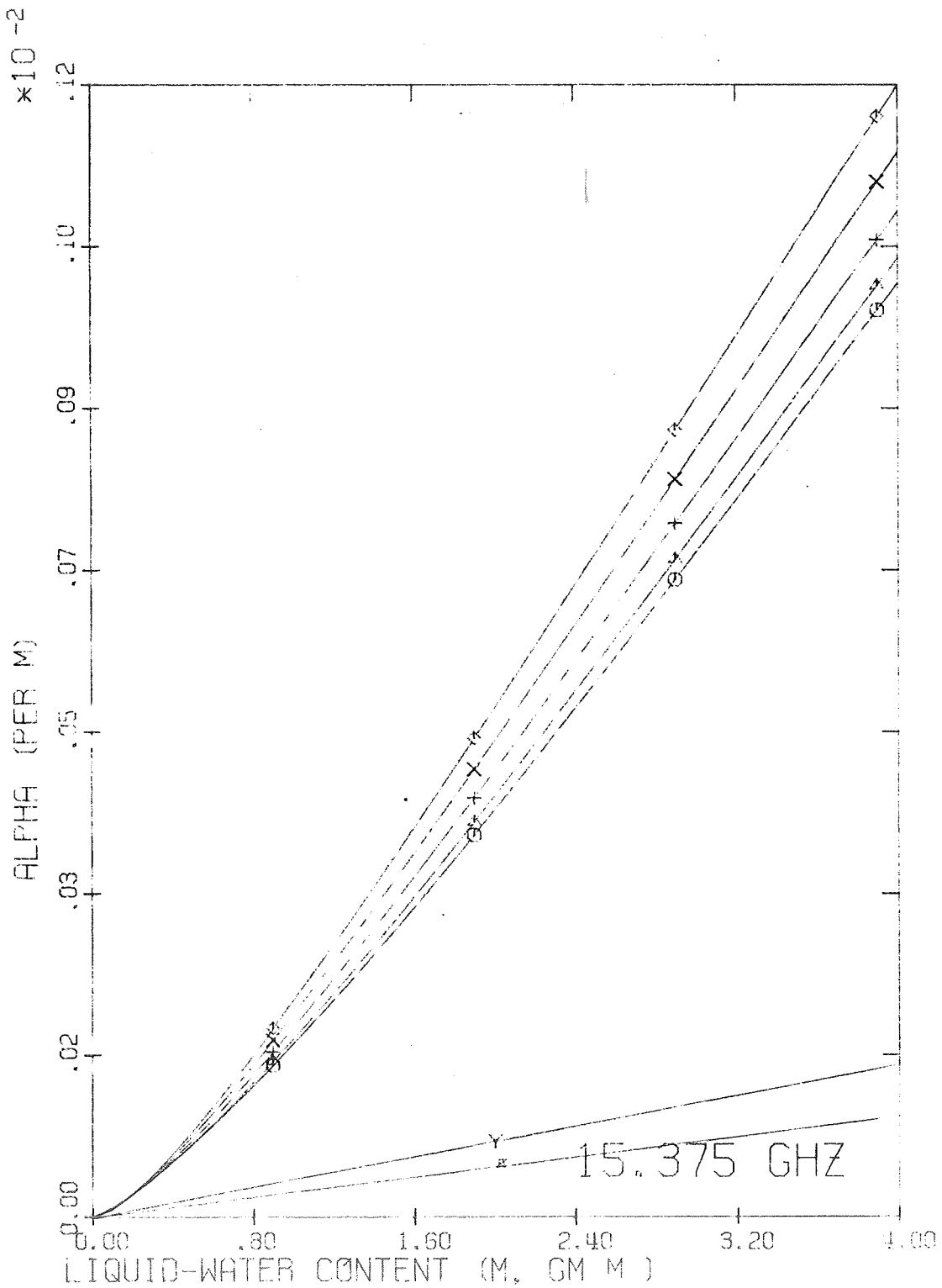
*10 -2
.12
.10
.09
.07
.05
.03
.02
0.00
ALPHA (PER M)
15.375 GHZ
0.00
.80
1.60
2.40
3.20
4.00
LIQUID-WATER CONTENT (M. GM M)

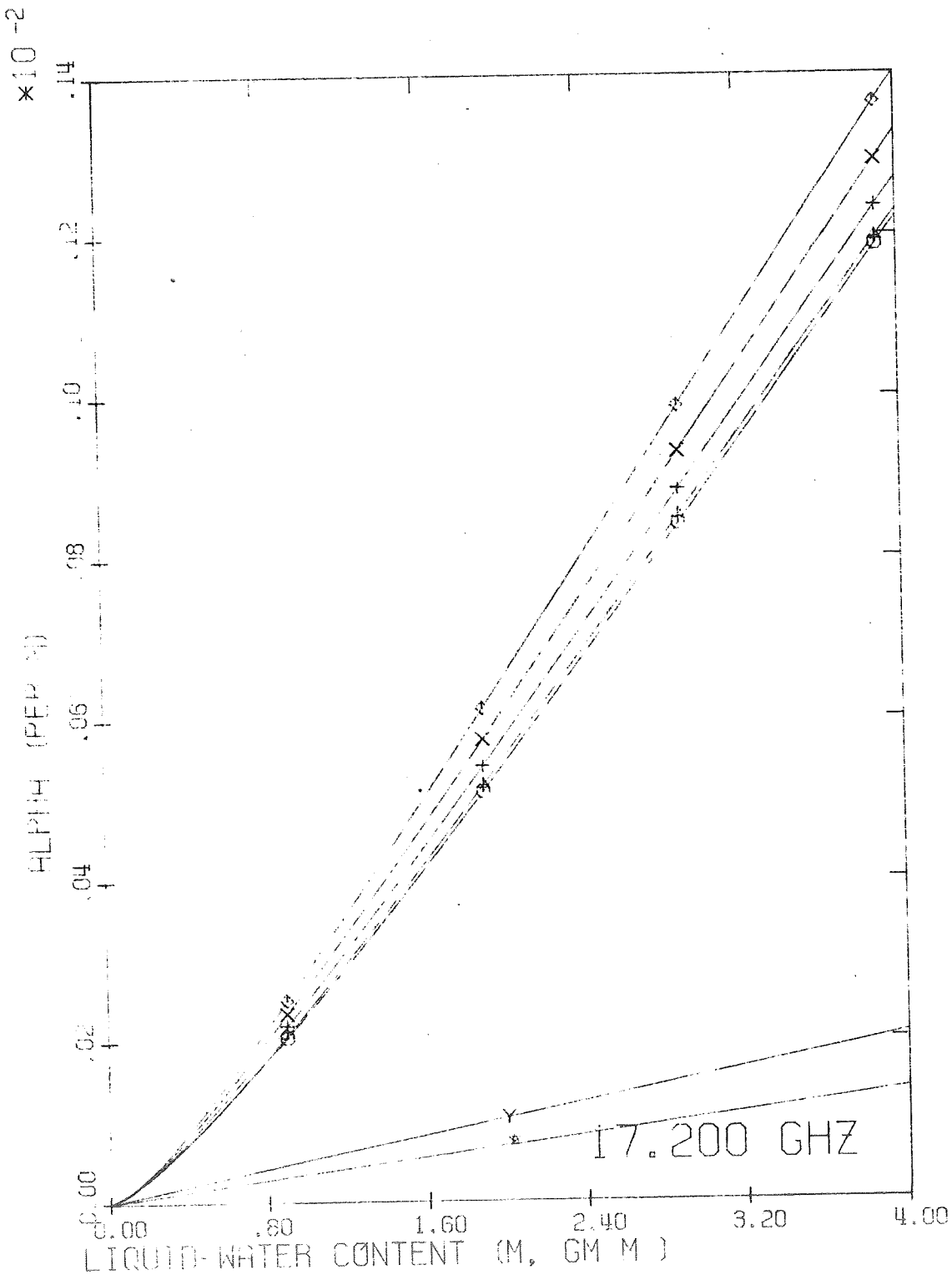
ALPHA (PER M)
*10-2
.14
.12
.10
.08
.06
.04
.02
.00
0.00
.80
1.60
2.40
3.20
4.00
LIQUID-WATER CONTENT (M, GM M)
17.200 GHZ

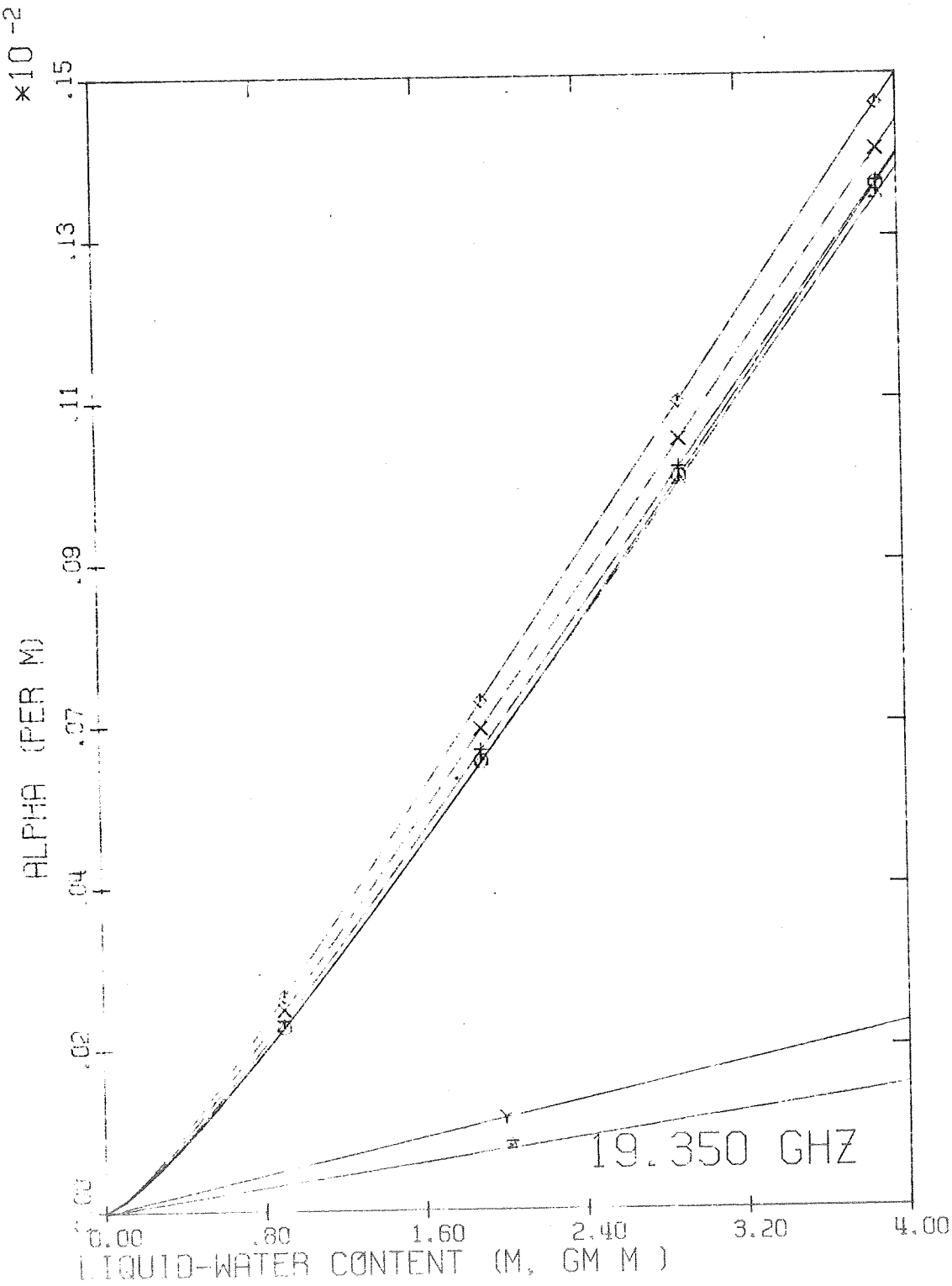
*10 -2
.15
.13
.11
.09
.07
.04
.02
.00
ALPHA (PER M)
19.350 GHZ
0.00
.80
1.60
2.40
3.20
4.00
LIQUID-WATER CONTENT (M. GM M)

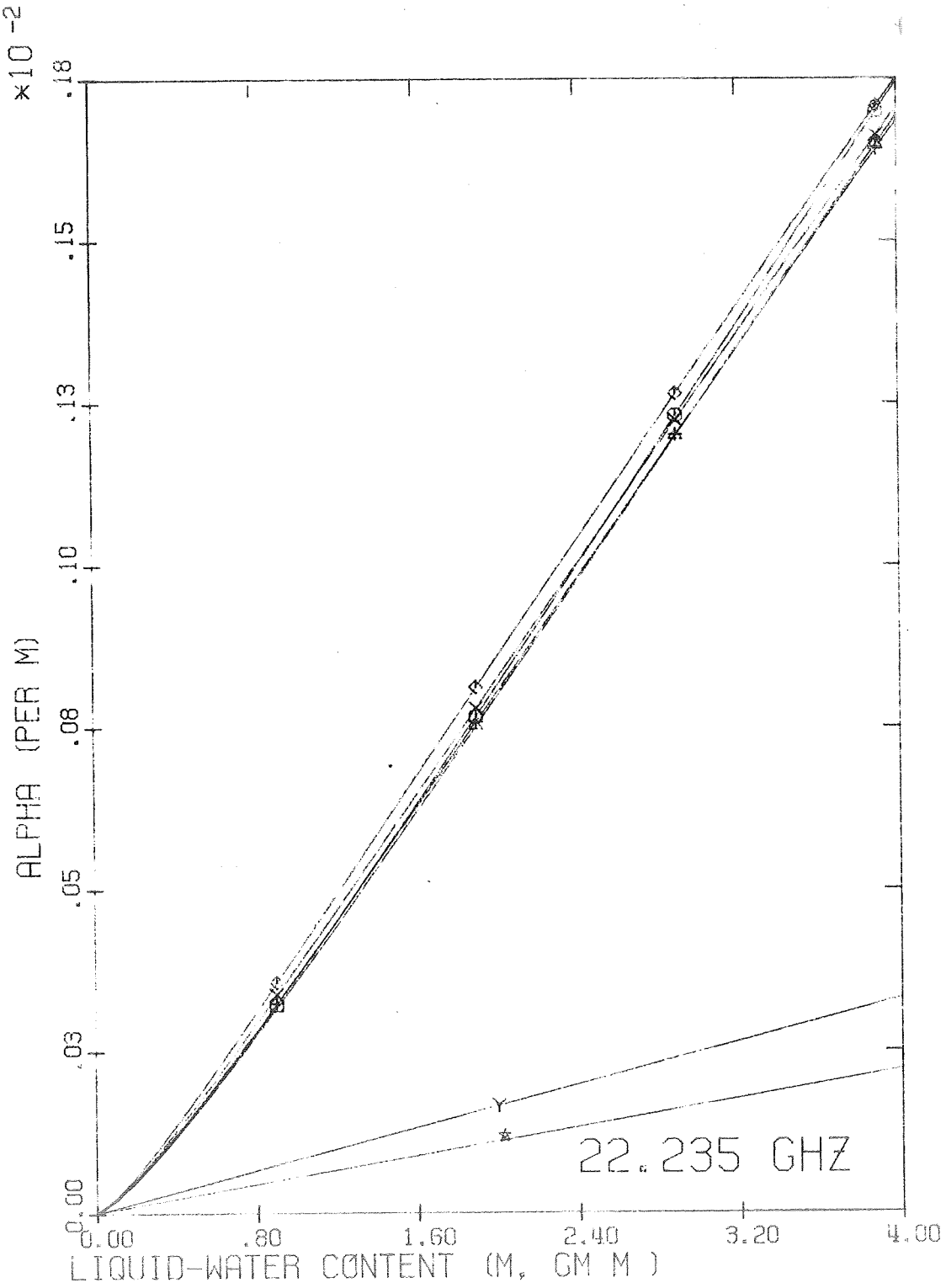
*10 -2
.18
.15
.13
.10
.08
.05
.03
0.00
ALPHA (PER M)
22.235 GHZ
0.00
.80
1.60
2.40
3.20
4.00
LIQUID-WATER CONTENT (M, GM M)

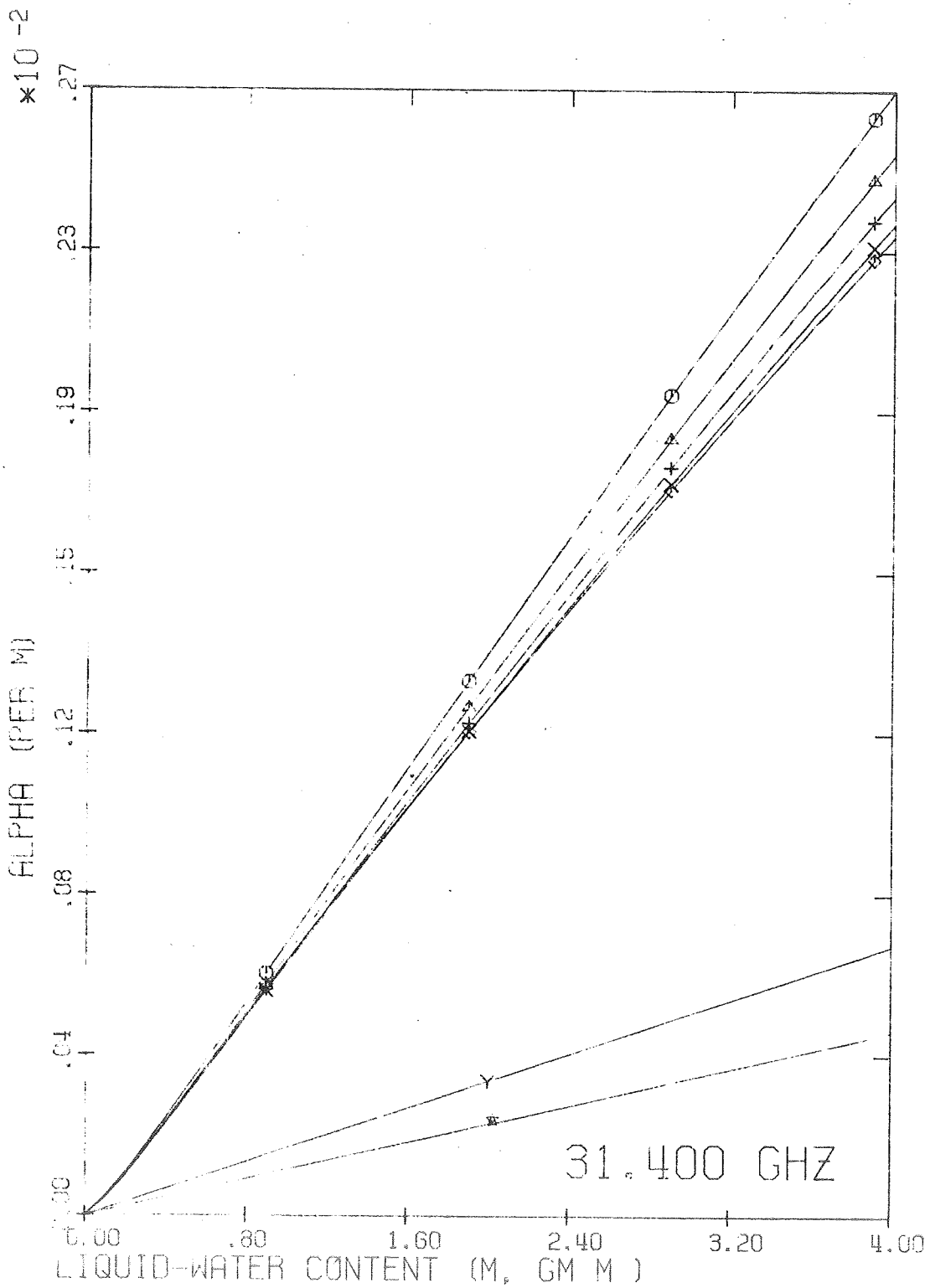
*10 -2
.27
.23
.19
.15
.12
.08
.04
ALPHA (PER M)
31.400 GHZ
0.00
.80
1.60
2.40
3.20
4.00
LIQUID-WATER CONTENT (M, GM M)

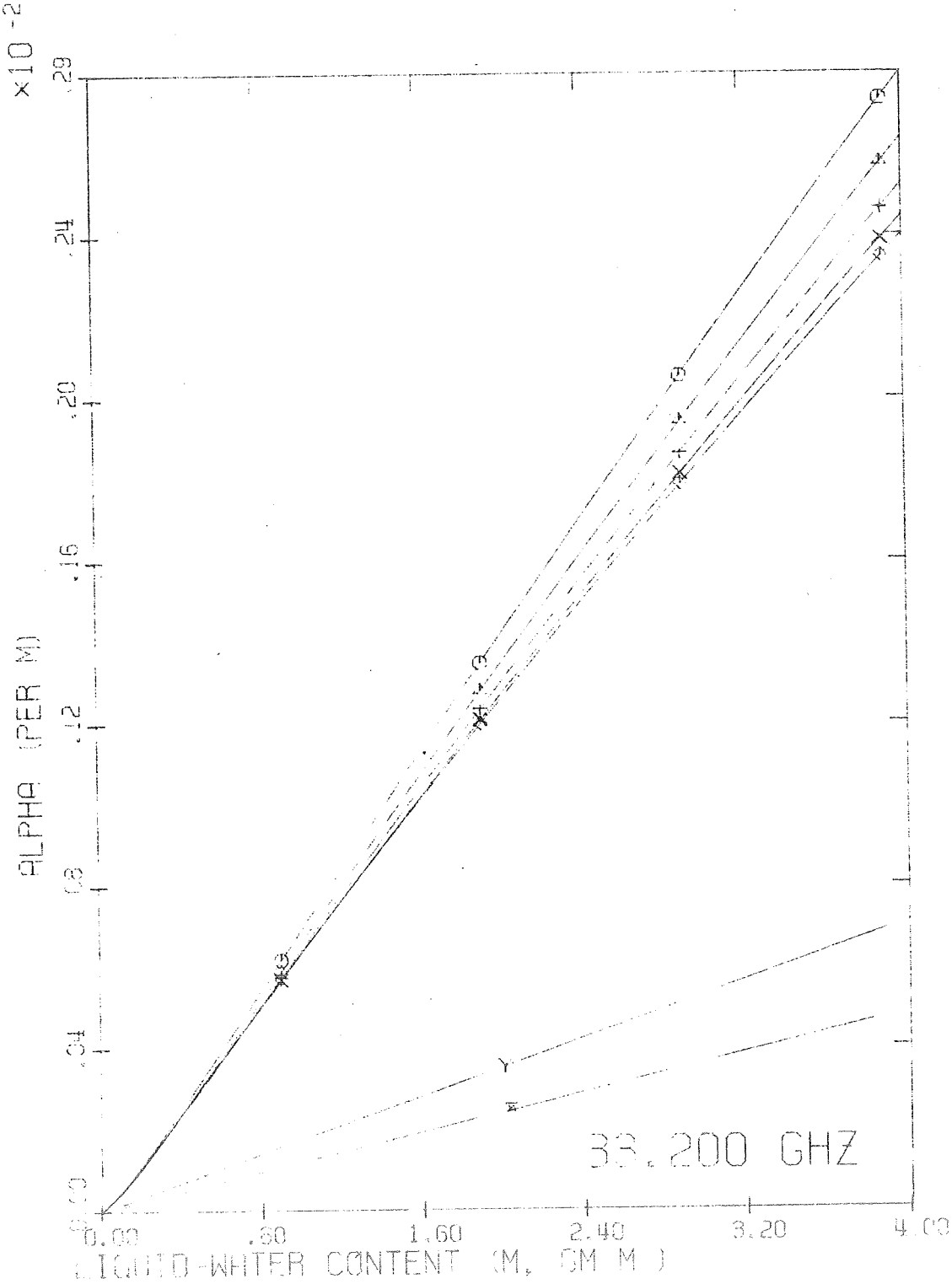
x10 -2
ALPHA (PER M)
.28
.24
.20
.16
.12
.08
.04
0.00
.80
1.60
2.40
3.20
4.00
LIQUID-WATER CONTENT (M. GM M)
33.200 GHZ

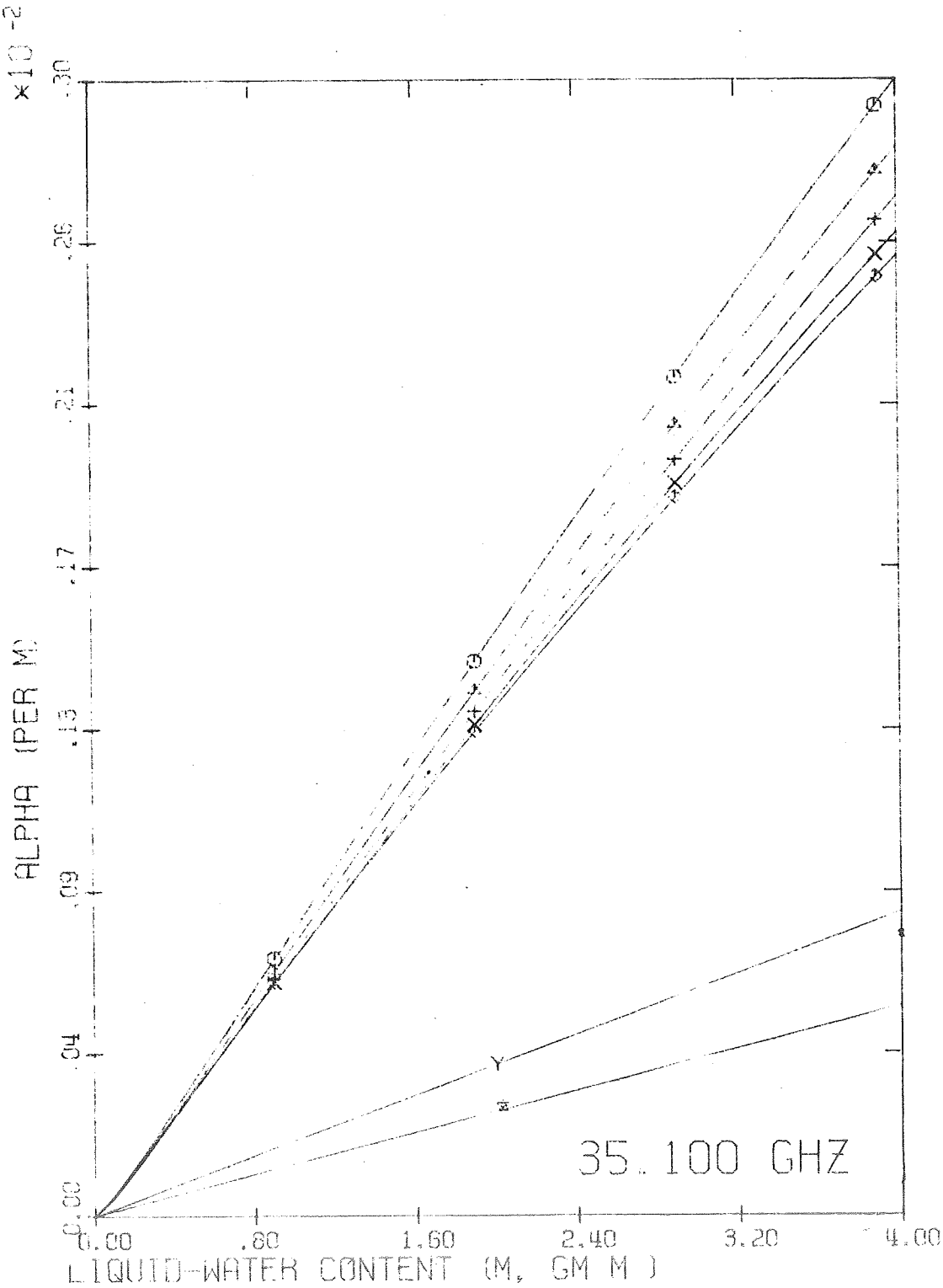
*10 -2
.30
.26
.21
.17
.13
.09
.04
0.00
ALPHA (PER M)
35.100 GHZ
0.00
.80
1.60
2.40
3.20
4.00
LIQUID-WATER CONTENT (M, GM M)

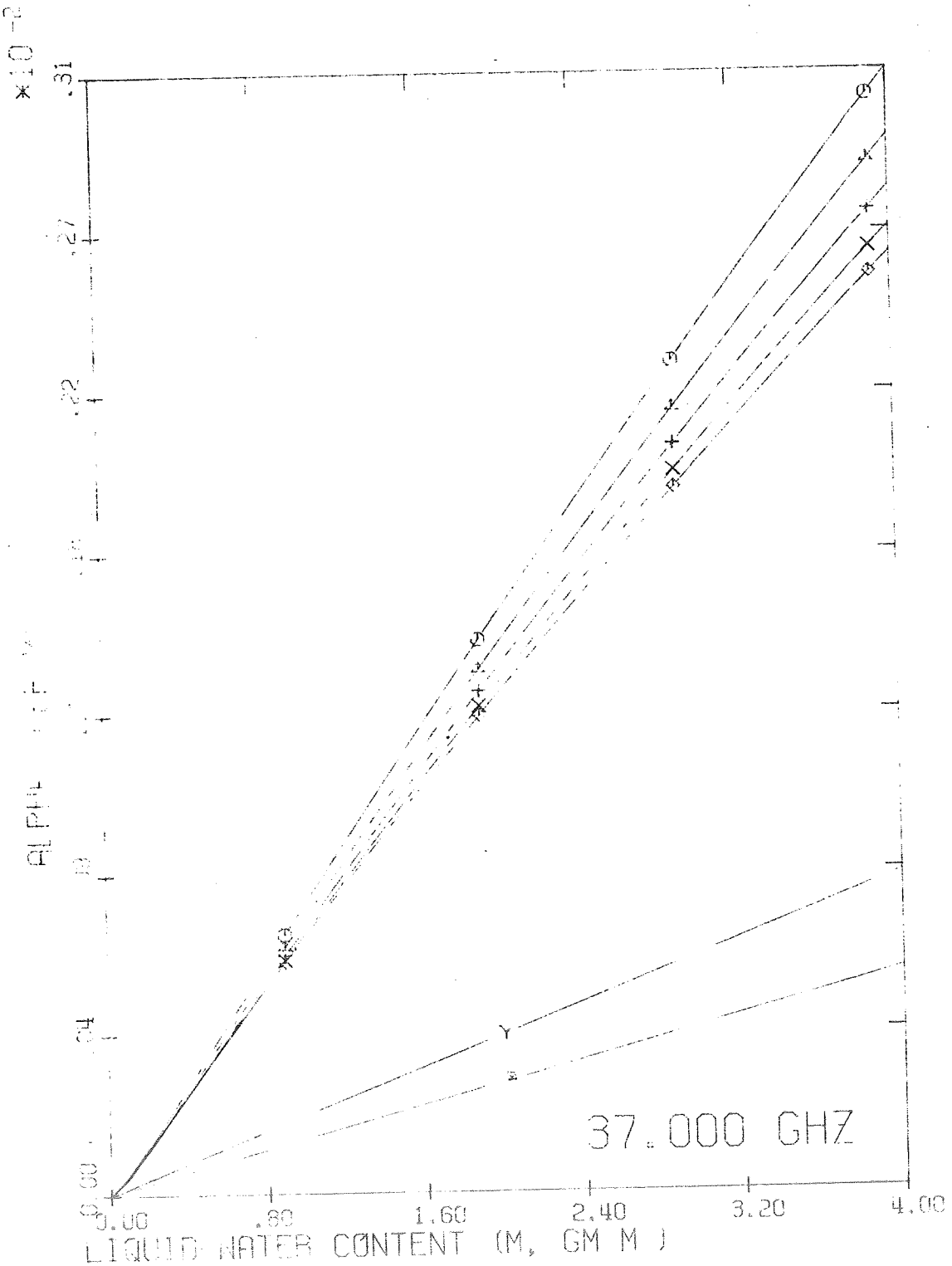
*10-2
.31
.27
.22
.18
.14
.10
.06
37.000 GHZ
0.00
.80
1.60
2.40
3.20
4.00
LIQUID WATER CONTENT (M, GM M)

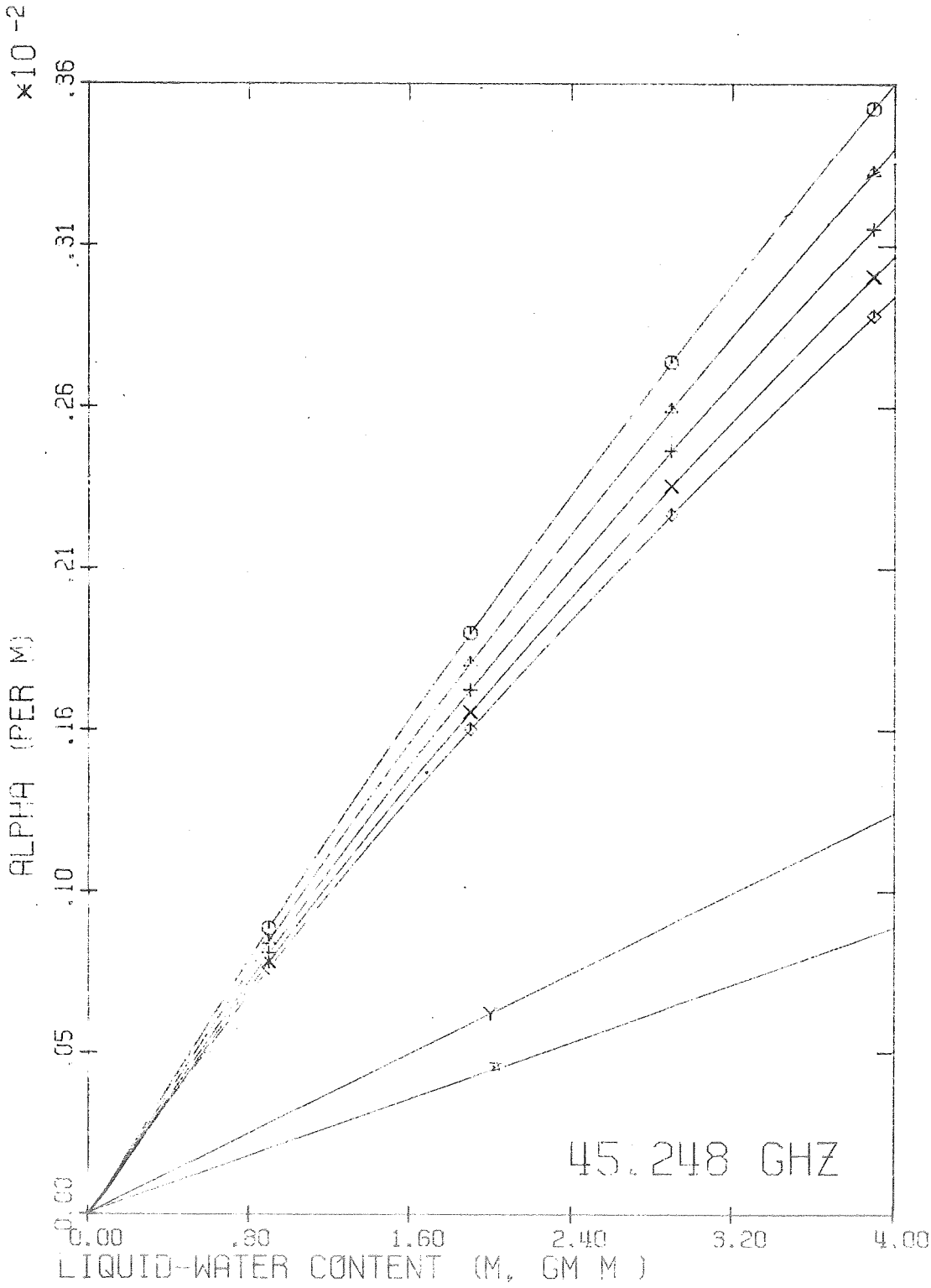
*10 -2
.36
.31
.26
.21
.16
.10
.05
0.00
ALPHA (PER M)
45.248 GHZ
0.00
.80
1.60
2.40
3.20
4.00
LIQUID-WATER CONTENT (M, GM M)

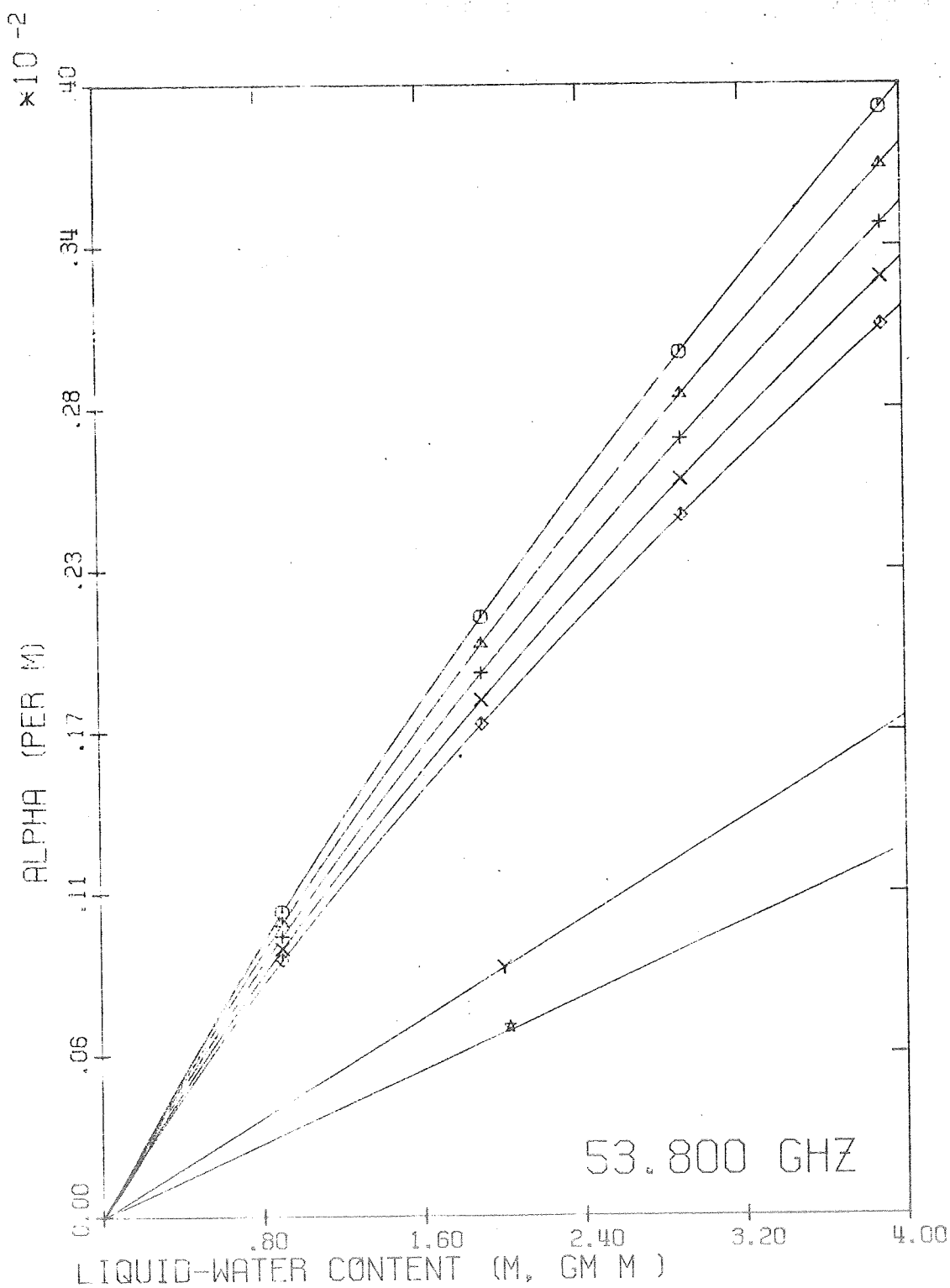
*10 -2
.40
.34
.28
.23
.17
.11
.06
0.00
ALPHA (PER M)
.80
1.60
2.40
3.20
4.00
LIQUID-WATER CONTENT (M, GM M)
53.800 GHZ

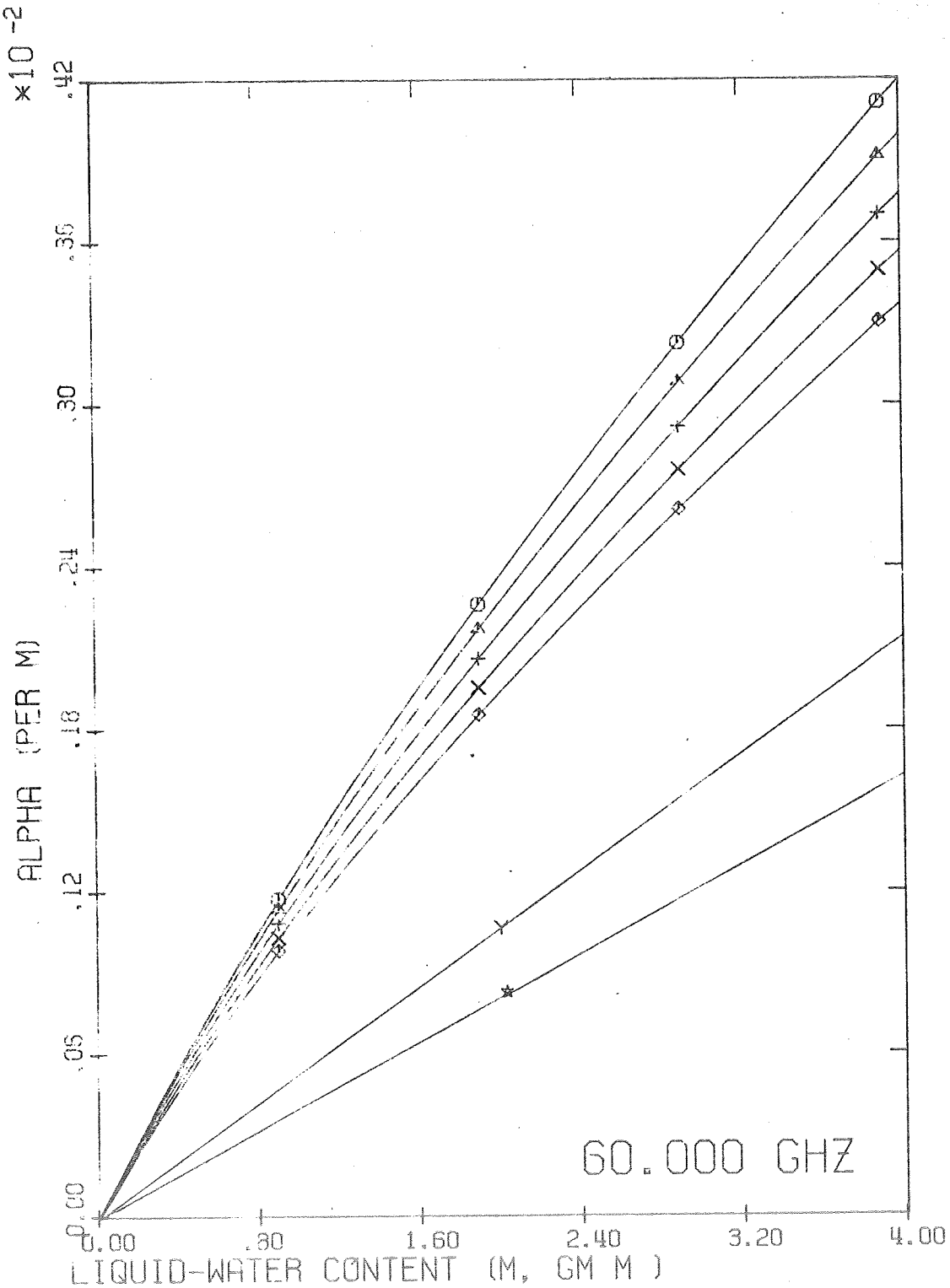
ALPHA (PER M)
×10 -2
.00
.05
.12
.18
.24
.30
.35
.42
0.00
.80
1.60
2.40
3.20
4.00
LIQUID-WATER CONTENT (M, GM M)
60.000 GHZ

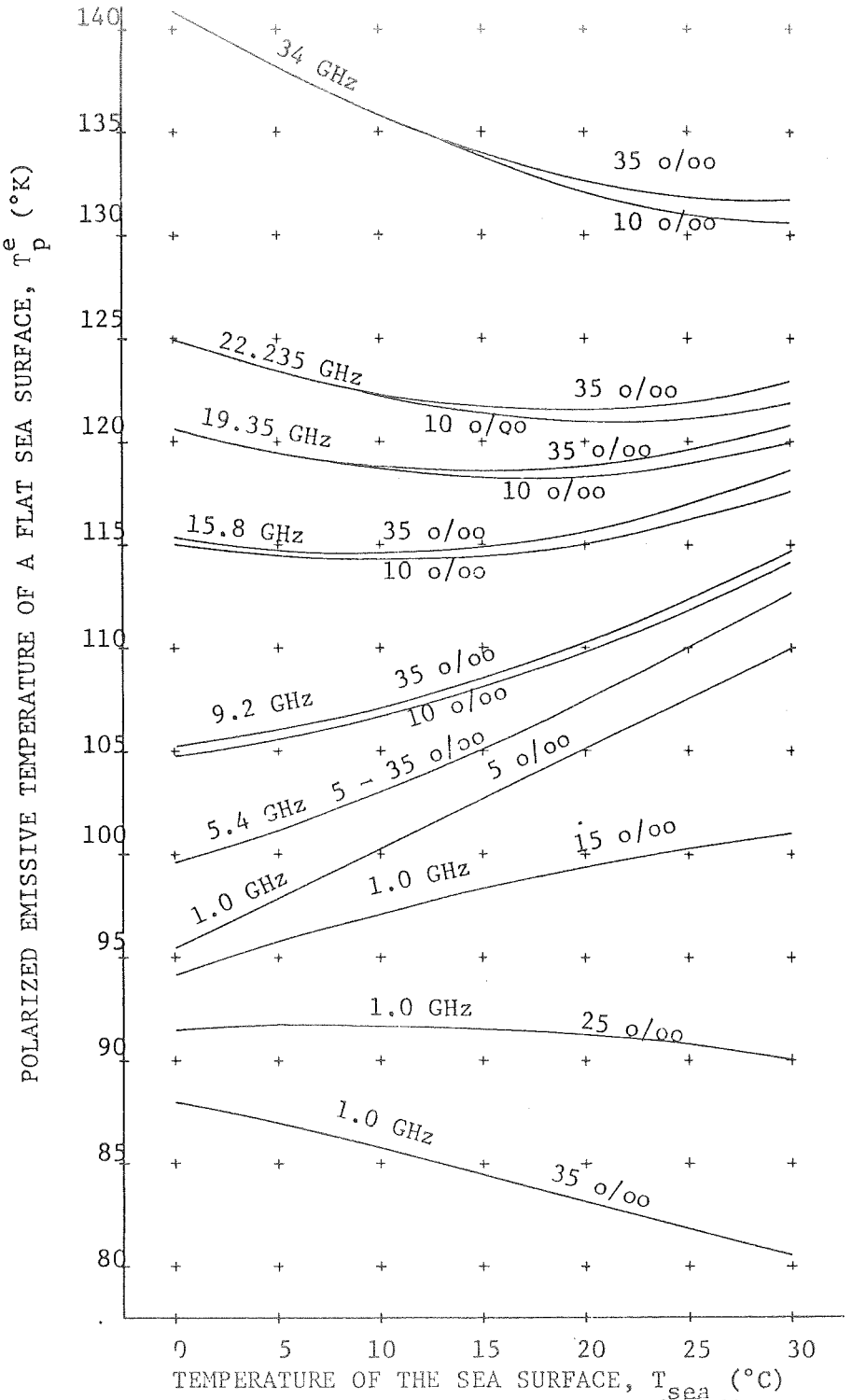

Figure 4. The polarized emissive temperature of a flat sea surface versus the thermometric temperature of the sea surface for frequencies of 1, 5.4, 9.2, 15.8, 19.35, 22.235, and 34 GHz and for various salinities.

oceanographic applications are concerned. At the present time, few measurements of the microwave radiance of the sea at frequencies below 9 GHz exist. One indirect oceanographic application, namely, rain detection at sea, is quite feasible at frequencies above 9 GHz.

It is recommended that:

(1) precise measurements of the dielectric constant of true sea water be made for a wide range of frequencies (0.5 GHz to 60 GHz), for a wide range of temperatures (0 C to 40 C) and for a wide range of salinities (0 o/oo to 40 o/oo).

(2) laboratory measurements on sea foam and sea bubbles should be made to determine the effects of bubble-size distribution and other factors.

(3) more measurements of the emission of the sea surface under varying conditions of sea temperature, salinity, roughness, and surface foam be made at frequencies less than 9 GHz.

References

Aden, A. L., 1952: Back-scattering of electromagnetic waves from spheres and spherical shells. Geophys. Res. Paper 15, Geophys. Res. Div., Air Force Cambridge Res. Center, Cambridge, Massachusetts, 42 pp.

Aden, A. L., and M. Kerker, 1951: Scattering of electromagnetic waves by two concentric spheres. J. Appl. Phys., 22, 1242-1246.

Becker, G. E., and S. H. Autler, 1946: Water vapor absorption of electromagnetic radiation in the centimeter wavelength range. Phys. Rev., 70, 300-307.

Bussey, H. E., 1950: Microwave attenuation statistics estimated from rainfall and water vapor statistics. Proc. IRE., 38, 781-785.

Collie, C. H., D. M. Ritson, and J. B. Hasted, 1946: Dielectric properties of water, Trans. Faraday Soc., 42A, 129-136.

Cummings, C. A., and J. W. Hull, 1966: Microwave radiometric meteorological observations. Proc. Fourth Symp. on Remote Sensing of Environment, Ann Arbor, Michigan, University of Michigan, 263-271.

Debye, P., 1929: Polar Molecules, New York, Dover Pub., Inc., 172 pp.

Deirmendjian, D., 1969: Electromagnetic scattering on spherical polydispersions. R-456-PR, Santa Monica, Calif., The RAND Corp., 290 pp. (Also available from Am. Elsevier Pub. Co., Inc., New York.)

Dicke, R. H., 1946: The measurement of thermal radiation at microwave frequencies. Rev. Sci. Instruments, 17, 268-275.

Dunsmuir, R., and J. Lamb, 1945: The dielectric properties of ice at wavelengths of 3 and 9 cm. Manchester Univ. Rept. No. 61.

Ford, L. H., and R. Oliver, 1946: An experimental investigation of the reflection and absorption of radiation of 9 cm wavelengths. Proc. Phys. Soc. London, 58, 265-280.

Goldstein, H., 1951: Attenuation by condensed water. Propagation of Short Radio Waves, D. E. Kerr, Ed., New York, McGraw-Hill Book Co., Inc., 671-692.

Gunn, K. L. S., and T. W. R. East, 1954: The microwave properties of precipitation particles. Quart. J. Roy. Meteoro. Soc., 80, 522-545.

Gurvich, A. S., and S. T. Egorov, 1966: Determination of the surface temperature of the sea from its thermal radio-emission. Izv. Atm. and Oceanic Phys. (English translation), 2, 305-307.

Haroules, G. G., and W. E. Brown, III, 1968: Radiometric measurement of attenuation and emission by the Earth's atmosphere at wavelengths from 4 cm to 8 mm. IEEE Trans. on Microwave Theory and Techniques, MTT-16, 611-620.

Haroules, G. G., and W. E. Brown, III, 1969: The simultaneous investigation of attenuation and emission by the Earth's atmosphere at wavelengths from 4 centimeters to 8 millimeters. Jour. Geophys. Res., 74, 4453-4471.

Hasted, J. B., 1961: The dielectric properties of water. Progress in Dielectrics, 3, 102-149.

Hasted, J. B., and S. M. El-Sabell, 1953: The dielectric properties of water in solutions. Trans. Faraday Soc., 49, 1003-1011.

Hasted, J. B., D. M. Ritson, and C. H. Collie, 1948: Dielectric properties of aqueous ionic solutions. J. Chem. Phys., 16, 1-21.

Hasted, J. B., and G. W. Roderick, 1958: Dielectric properties of aqueous and alcoholic electrolytic solutions. J. Chem. Phys., 29, 17-26.

Hathaway, S. D., and H. W. Evans, 1959: Radio attenuation at 11 kmc and implications affecting relay system engineering. Bell Sys. Tech. J., 38, 73-97.

Hogg, D. C., 1959: Effective antenna temperature due to oxygen and water vapor in the atmosphere. J. Appl. Phys., 30, 1417-1419.

Hogg, D. C., 1968: Millimeter-wave communication through the atmosphere. Sci., 159, 39-46.

Hogg, D. C., and W. W. Mumford, 1960: The effective noise temperature of the sky. Microwave J., 3(3), 80-84.

Hogg, D. C., and R. A. Semplak, 1961: The effect of rain and water vapor on sky noise at centimeter wavelengths. Bell Sys. Tech. J., 40, 1331-1348.

Hogg, D. C., and R. A. Semplak, 1963: Estimated sky temperatures due to rain for the microwave band. Proc. IEEE, 51, 499-500.

Hogg, D. C., R. A. Semplak, and D. A. Gray, 1963: Measurement of microwave interference at 4 Gc due to scatter by rain. Proc. IEEE, 51, 500.

Imai, I., 1957: Attenuation of microwaves through rain for various dropsize distributions. 75th Anniversary Volume of J. Meteor. Soc., Japan, 65-71.

Jansky, K. G., 1932: Directional studies of atmospherics at high frequencies. Proc. IRE, 20, 1920-1932.

Kaplan, L. D., 1959: Inference of atmospheric structure from remote radiation measurements. J. Opt. Soc. Am., 49, 1004-1007.

Lane, J. A., and J. A. Saxton, 1952(a): Dielectric dispersion in pure polar liquids at very high radio-frequencies. I. Measurements on water, methyl and ethyl alcohols. Proc. Roy. Soc. A., 213, 400-408.

Lane, J. A., and J. A. Saxton, 1952(b): Dielectric dispersion in pure polar liquids at very high radio frequencies. III. the effect of electrolytes in solution. Proc. Roy. Soc. A., 214, 531-545.

Liebe, H. J., 1969(a): Atmospheric propagation properties in the 10- to 75-GHz region: Summary and recommendations, Tech. Rep., Boulder, Colorado, ESSA Res. Labs, 24 pp, (in press).

Liebe, H. J., 1969(b): Calculated tropospheric dispersion and absorption due to the 22-GHz H_2O line. IEEE Trans. Ant. Prop.

Liebe, H. J., 1969(c): Laboratory studies of microwave dispersion caused by atmospheric gases. Proc. Symp. on the Application of Atmos. Studies to Satellite Transmissions, Boston, 3-5.

Lukes, G. D., 1968: Penetrability of haze, fog, clouds, and precipitations by radiant energy over the spectral range 0.1 micron to 10 cm. Study 61, Center for Naval Analysis, Univ. of Rochester, N. Y., 225 pp.

Marshall, J. S., and W. McK. Palmer, 1948: The distribution of raindrops with size. J. Meteor., 5, 165-166.

Maxwell, J. C., 1892: A Treatise on Electricity and Magnetism, Vol. II. Oxford, Clarendon Press, 96 pp.

Medhurst, R. G., 1965: Rainfall attenuation of centimeter waves: comparison of theory and measurement. IEEE Trans. on Antennas and Propagation, AP-13, 550-564.

Meeks, M. L., 1961: Atmospheric emission and opacity at millimeter wavelengths due to oxygen. J. Geophys. Res., 66, 3749-3757.

Meeks, M. L., and A. E. Lilley, 1963: The microwave spectrum of oxygen in the Earth's atmosphere. J. Geophys. Res., 68, 1683-1703.

Mie, G., 1908: Beiträge zur Optik trüber Medien, speziell kolloidaler Metallösungen. 25, 377-445, Annalen der Physik, (German).

Nordberg, W., J. Conaway and P. Thaddeus, 1969: Microwave observations of sea state from aircraft. Quart. J. Roy. Meteor. Soc., 95, 408-413.

Paris, J. F., 1969: Microwave radiometry and its application to marine meteorology and oceanography. Ref. No. 69-1I, Contract Nonr 2119(04), Dept. of Oceanography, Texas A & M University, College Station, Texas, 210 pp.

Paris, J. F., 1970: Microwave studies at Texas A & M University. Paper submitted to the NASA-Navy Microwave Review, Spacecraft Oceanography Project, Washington, D. C., 34 pp.

Peake, W. H., 1959: Interaction of electromagnetic waves with some natural surfaces. IRE Trans. on Antennas and Propagation, AP-7, S324-S329.

Peake, W. H., 1967: The microwave radiometer as a remote sensing instrument, with applications to geology. Notes for a Short Course on Geologic Remote Sensing, Palo Alto, Calif., Stanford Univ., 34 pp.

Peake, W. H., and S. N. C. Chen, 1961: Apparent temperature of smooth and rough terrain. IRE Trans. on Antennas and Propagation, AP-9, 567.

Pereslegin, S. V., 1967: On the relationship between the thermal and radio brightness contrasts of the sea surface. Izv. Atm. and Oceanic Phys., English Translation, 3, 47-57.

Porter, R. A., and E. T. Florance, 1969: Feasibility study of microwave radiometric remote sensing. NASA Contract No. NAS 12-629, Electronics Res. Center, Cambridge, Mass., 836 pp.

Ryde, J. W., 1946: The attenuation and radar echoes produced at centimeter wavelengths by various meteorological phenomena. Meteorological Factors in Radio-Wave Propagation, London, England, The Physical Society, 169-188.

Saxton, J. A., 1946(a): The anomalous dispersion of water at very high frequencies. Part IV: A note on the effect of salt in solution. Meteorological Factors in Radio-Wave Propagation, London, England, The Physical Society, 316-325.

Saxton, J. A., 1946(b): The dielectric properties of water vapour at very high radio frequencies. Meteorological Factors in Radio-Wave Propagation, London, England, The Physical Society, 215-238.

Saxton, J. A., 1949: Electrical properties of water. Wireless Engineer, 26, 288-292.

Saxton, J. A., 1952: Dielectric dispersion in pure polar liquids at very high radio-frequencies. II. relation of experimental results to theory. Proc. Roy. Soc. A., 213, 473-492.

Saxton, J. A., and J. A. Lane, 1946: The anomalous dispersion of water at very high radio frequencies. Part I: experimental determination of the dielectric properties of water in the temperature range 0°C to 40°C for wavelengths of 1.24 cm and 1.58 cm. Meteorological Factors in Radio-Wave Propagation, London, The Physical Society, 278-291.

Saxton, J. A., and J. A. Lane, 1952(a): Dielectric dispersion in pure polar liquids at very high frequencies. Part I: measurements on water, methyl and ethyl alcohols. Proc. Roy. Soc. London, A213, 400.

Saxton, J. A., and J. A. Lane, 1952(b): Dielectric dispersion in pure polar liquids at very high frequencies. Part III: the effect of electrolytes in solution. Proc. Roy. Soc. London.

Saxton, J. A., and J. A. Lane, 1952(c): Electrical properties of sea water: reflection and attenuation characteristics at v. h. f. Wireless Engineer, 29, 269-275.

Shifrin, K. S., 1951: Rasseyaniya sveta v mutnoy srede. (Scattering of light in a cloudy atmosphere), Gostekhizdat, Moscow-Leningrad, 287 pp. (available in English as Scattering of light in a cloudy atmosphere, 1968, NASA TT F-477, Washington, D. C., The Natl. Aeronautics and Space Admin., 212 pp., from the CFSTI, Springfield, Virginia, price $3.00)

Sirounian, V., 1968: The effect of temperature, angle of observation, salinity, and thin ice on the microwave emission of water. J. Geophys. Res., 73, 4481-4486.

Stogryn, A., 1967: The apparent temperature of the sea at microwave frequencies. IEEE Trans. Ant. Prop., AP-15, 278-286.

Thompson, W. I., III, 1969: Atmospheric transmission handbook. Electronics Res. Center, NASA, Cambridge, Mass. (in press).

van de Hulst, H. C., 1957: Light Scattering by Small Particles. New York, John Wiley and Sons, 470 pp.

Van Vleck, J. N., 1947(a): The abosrption of microwaves by oxygen. Phys. Rev., 71, 413-424.

Van Vleck, J. N., 1947(b): The absorption of microwaves by uncondensed water vapor, Phys. Rev., 71, 425-433.

Van Vleck, J. H., 1951: Theory of absorption by uncondensed gases. Propagation of Short Radio Waves, D. E. Kerr, Ed., New York, McGraw-Hill Book Co., Inc., 646-664.

Van Vleck, J. H., and V. F. Weisskopf, 1945: On the shape of collision broadened lines. Rev. Mod. Phys., 17, 227-236.

Weger, E., 1960: Apparent sky temperature in the microwave region. J. Meteor., 17, 159-165.

Westwater, E. R., 1965(a): A method for determination of the tropospheric temperature structure from ground-based measurement of oxygen emission. Proc. Third Symp. on Remote Sensing of Environment, Ann Arbor, Mich., Univ. of Mich., 245-256.

Westwater, E. R., 1965(b): Ground-based passive probing using the microwave spectrum of oxygen. Radio Sci. J. of Res. Nat. Bu. of Standards, 69D, 1201-1211.

Westwater, E. R., 1967: An analysis of the correction of range errors due to atmospheric refraction by microwave radiometric techniques. ESSA Institute for Telecommunication Sciences and Aeronomy, IER 30-ITSA 30, Boulder, Colorado, 68 pp.

Williams, G. F., Jr., 1969: Microwave radiometry of the ocean and the possibility of marine wind velocity determination from satellite observation. J. Geophys. Res., 74, 4591-4594.

Wulfsberg, K. N., 1964: Sky noise measurements at millimeter wavelengths. Proc. IEEE, 52, 321-322.

Wulfsberg, K. N., 1967: Atmospheric attenuation at millimeter wavelengths. Radio Sci., 2, 319-324.

CHAPTER III - PROGRESS (cont.)

C. International Program - General

International cooperative oceanographic expeditions aimed to measure the fertility of the sea in known productive regions of the oceans are being planned by the Intergovernmental Oceanographic Commission (IOC), International Council for the Exploration of the Sea (ICES), Food and Agriculture Organization of the United States (FAO), Scientific Committee on Oceanic Research (SCOR), and other organizations. Their programs include the measurement of biomass production and the associated phenomena in the marine environment (upwelling, currents, etc.). Cruises dealing with intercalibration and standardization of techniques have also been planned. Discussions have been held in order to determine the feasibility and convenience of having the NASA aircraft fly over such a region when the ship's operation is underway.

Arrangements were made through this project for Mexican Engineers and Scientists to tour the R/V ALAMINOS in Veracruz, Mexico, on October 27-28.

Dr. Luis Capurro is serving as Chariman of the Panel on General Circulation of the Gulf of Mexico for GSY/CICAR. This position enables him to better coordinate the activities of the well-instrumented vessels and platforms of the U. S. Coast Guard, as well as the utilization of the instrumented monster buoys.

Mrs. Rosemary Boykin just recently completed a bibliography dealing with marine-biology, geology, and geophysics of the Gulf of Mexico and Caribbean Sea specifically for CICAR and GSY. Containing over 14,000 references, many of which will be annotated or will include abstracts,

this bibliography will be issued in two volumes by the National Oceanographic Data Center and the Gulf Universities Research Corporation. Although this work was not done on project time, it is felt that personal contacts made by Mrs. Boykin within those countries within these areas of investigation will be helpful in furthering the efforts of this project and in the planning of possible upwelling experiments.

On October 8, three specialists in space engineering from France visited our facilities and were briefed by members of the staff regarding our project activities and were given copies of some of our reports which were of interest to them. The group was hosted by the International Affairs Office of NASA Headquarters, and toured various NASA facilities in the U. S. Their interests are in the location and observation of earth resources through remote sensing.

CHAPTER III - PROGRESS (cont.)

D. International Program - Mexico

This project has been associated with the international program in Mexico since the program's inception. Dr. George Huebner was named as principal investigator to represent the Naval Oceanographic Office during the planning, overflights, and analysis of the data. Upon completion of the overflights and initial analysis, a more detailed analysis was made by two oceanographers of this project, Mr. Bill Merrell and Mr. Robert Whitaker. Near the end of September, 1969, Dr. Huebner and Bill Merrell met with the Mexican investigators in Mexico City and compared their analysis with our interpretation. The following pages give a review of our work.

AN OCEANOGRAPHIC ANALYSIS OF DATA RECORDED ON SHIPS AND AIRCRAFT-NASA AIRCRAFT MISSION 91, SITE 705, VERACRUZ, MEXICO

INTRODUCTION

This report is limited to an oceanographic analysis of the data received at Texas A & M. Other ship data were taken but have not been received. This report should not be construed to be a complete analysis of the received data. In fact, one section of the report is an attempt to catalog various oceanographic features within the data in the hope that this will assist further analysis, and another section contains recommendations for future work with this data.

The aerial data were obtained by the NASA 927 NP3A Aircraft. Specifications of the aircraft and its sensors can be found in the Mission Plan (1 March 1969), Mission Report (8 May 1969), and Data Review Report (25 June 1969) of Mission 91. Ship data were taken by the BIOS and VIRGILIO URIBE. The last two pages in this section are copies of charts showing the ship coverage and the aircraft flight lines.

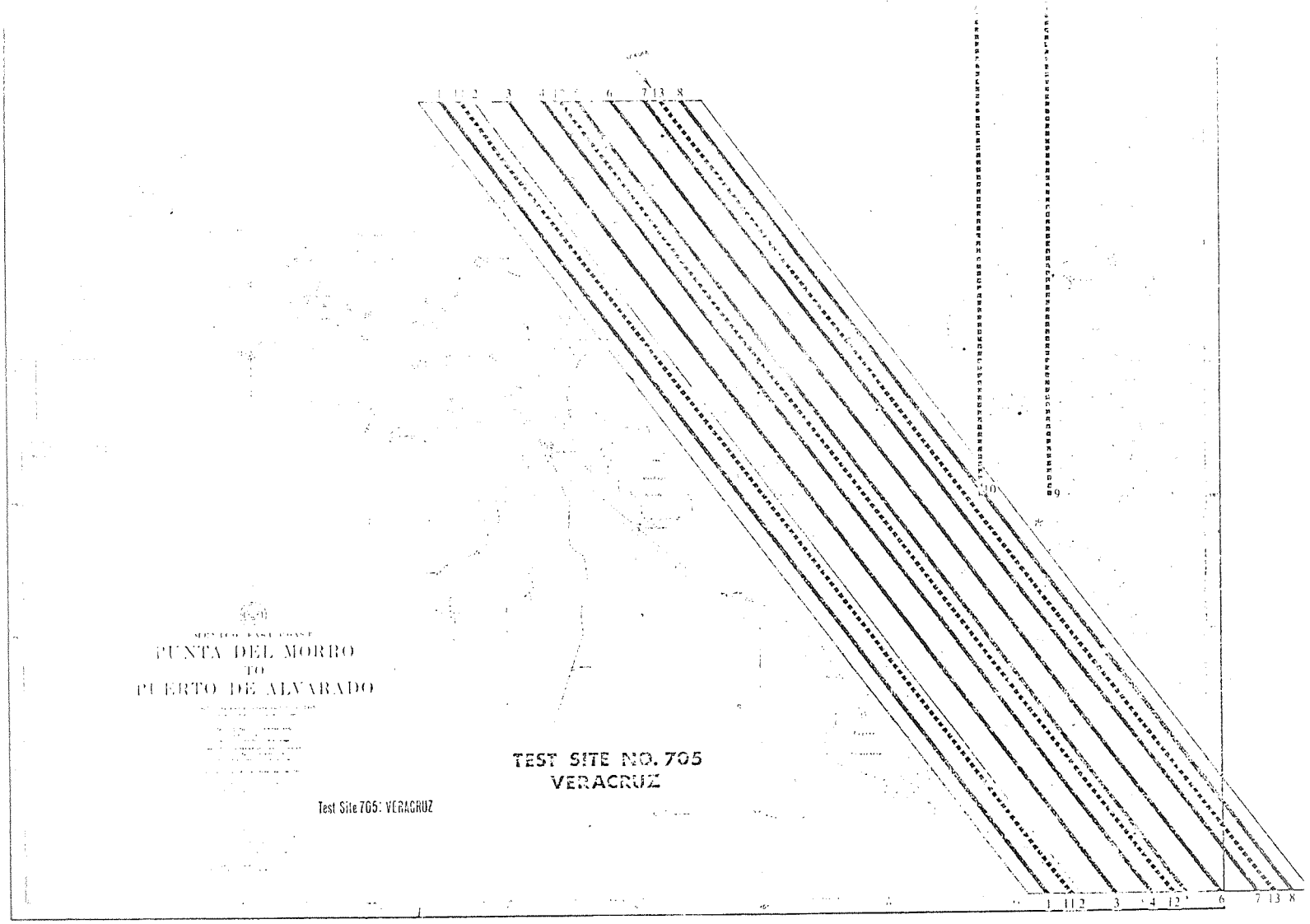

This Map Available From
Earth Resources Data Research Facilities/TF2
NASA - Manned Spacecraft Center
Houston, Texas 77058

VERACRUZ, MEXICO
TEST SITE 705
MISSION 91
NR-01-EM-705-00263

CONTOUR INTERVAL APPROXIMATELY 164 FEET

LEGEND
HIGH ALTITUDE LINES
LOW ALTITUDE LINES

Site 705

10
2
11
12
8
19
22
16
9
3
4
10
20
17
21
13
18
14

SHIP DATA

Types of Data

Data taken on board ship and sent to Texas A & M University included:

- Cruise name and station number
- Date
- Location (Latitude and Longitude)
- Depth of cast
- Wave state
- Wind speed and direction
- Atmospheric pressure
- Air temperature
- Visibility
- Cloud types
- Water transparency
- Water color
- An estimate as to whether an appreciable current existed
- Temperature and salinity at observed depths with sigma-t, delta-a and sound velocity calculated
- From the observed depths, temperature and salinity were interpolated to every three meters and dynamic heights calculated

Quality of Data

The quality of the ship data can only be judged as unknown. Standard oceanographic techniques of judging the consistency of oceanographic data, such as T-S relations or thermometric depth corrections can not be effectively utilized as the water is simply not deep enough. A few observed values seem extremely doubtful and some obvious mistakes exist.

Analysis of the Data

Contour charts of surface salinity, surface temperature, salinity at 10 meters, and temperature at 10 meters were made. Thermal boundaries recorded by the RS-14 were also recorded on the temperature charts.

No contour lines are present on the surface temperature chart, as the effect of the diurnal variation of temperature is large enough at the surface to obscure any indication of the flow patterns. From observations of the temperature at the surface and at 10 meters at each station, it is evident that two different types of thermal structures exist. In the region near Veracruz, the surface temperatures are higher than the area off of Pta. Coyal, but the temperature at 10 meters is about 3°C less. Salinity contour charts also seem to indicate two different water masses in these areas, and the thermal boundary off of Pta. Coyal (which is also a color boundary) may be an indication of the boundary between these two types of sea water.

The charts are contoured to reflect the general flow pattern the authors believe to be in this area; it is consistent with river outflows, etc. However, because of the low density of data in some areas, other interpretations are certainly possible.

AIRCRAFT DATA

NASA Aircraft Mission 91 utilized the following instruments to gather data in the Veracruz vicinity: dual channel infrared imager, side-looking imaging radar, color and color IR mapping cameras, and the multiband camera system. The infrared imager operated on the 3-5.5μ and 8-14μ channels, while the multiband camera system employed the following bandpass filters: 477mμ (blue), 530mμ (green), 617mμ (red), and 750mμ (IR).

The color and color IR, as well as the multi-spectral exposures, were of high quality. Due to noise, the IR imagery was of an inferior grade and nothing intelligent could be gained from the side-looking imaging radar images. Where applicable, forward and side overlap of the imagery was excellent.

The catalog of oceanographic features observed in the color and color IR photography lists the features chronologically, with the box to the left under each feature pertaining to the color frame number and the box to the right pertaining to the color IR frame number. Bottom vegetation is visible in the shallow water over the reefs and the lagoons, while near-shore currents are delineated by distinct color changes caused by sediment transport of river outflow. The land-sea boundary is clearly defined in the color IR photography, and bottom topography in shallow areas is visible in both sets of photographs.

A pollutant can be observed flowing near shore from the area north of the Veracruz port facilities. Several slicks are to be seen off the coast near Veracruz. Sediment transport in the lagoons and in river outflows, as well as sedimentation in river inlets, is discernible.

Long-term temporal studies of sedimentation patterns, in addition to studies of wave diffraction, refraction, and interference as observed in color and color IR photography could aid coastal engineers in jetty construction and dredging. Increased safety for small boat operators could also be realized from such studies.

Since sea water exhibits selective absorption of the incident radiation, the spectrum becomes a function of depth. In general, the greater depth of penetration is achieved by the shorter wave lengths in oceanic and clear coastal water, while the longer wave length radiation exhibits the best transmission in average and turbid coastal waters. Comparison, then, of the four images obtained from the multiband camera system, can yield information concerning relative depths of observed phenomenon.

The IR filter allows us to see only the top few millimeters of the ocean and is, thus, especially efficient in defining land-sea boundaries. In observing the outlying reefs and islands, it is quite clear which portions are dry. Comparison of the red and green photography revealed similar features along the coast. These features are probably either offshore sand bars and turbid water due to wave action on the deposits or turbid water due to a longshore current. Sediment transport in Laguna Alvarado and Laguna Camaronera with subsequent sedimentation at the mouth of Rio Papolaapan was marked. Multi-band studies of this particular area could determine sedimentation rates and patterns.

Both the blue and the green filters yielded good definition of bottom topography and vegetation of all the reefs. This photography could be used in an updating of the available charts of this region and could very well provide the basis for a quantitative survey of marine vegetation in this area.

The thermal imagery obtained by the dual channel infrared scanner was successful in delineating ships' wakes and wave shoaling. Ships themselves were quite readily identifiable. In the other photography, several instances of distinct color changes were noticed. Each color change, except the pollutant flowing northwest near the beach from the vicinity of the port of Veracruz, exhibited a corresponding thermal boundary. Qualitatively then, the sea surface color and thermal configuration were the same. Even the one exception is useful since it is seen that the pollutant's temperature is approximately the same as its environment. This might be of some assistance in determining its source.

NOTE: Under Oceanographic Features, the box to the left is for color and the box to the right is for color IR.

CATALOG OF OCEANOGRAPHIC FEATURES OBSERVED
IN COLOR AND COLOR IR PHOTOGRAPHY
NASA MISSION 91, SITE 705 - 25 APRIL 1969

OCEANOGRAPHIC FEATURES

COLOR FRAME	COLOR IR FRAME	TIME (GMT)	Glitter Pattern		Swells		Wave Refraction		Wave Diffraction		Interference Pattern		Local Topography		Current		Bottom Vegetation		Breakers		COMMENTS
4116	8962	21:07	X	X	X	X	X	X			X	X	X	X					X	X	
4117	8963	21:07					X	X			X	X	X	X	X	X			X	X	Wave Refraction due to topography of Pta. Gorda and Majagua. Turbid coastal waters.
4118	8964	21:07						X					X	X	X	X			X	X	Effluent from port area indicates westward coastal flow.
4119	8965	21:08											X	X	X	X			X	X	Effluent from port area indicates westward coastal flow.
4120	8966	21:08											X	X			X	X			Harbor facilities, shark guard; topography off Pta. Hornos and Pta. Mocambo.
4121	8967	21:08											X	X			X	X	X	X	Topography off Pta. Hornos and Mocambo, Isla Sacrificios.

OCEANOGRAPHIC FEATURES

COLOR FRAME	COLOR IR FRAME	TIME (GMT)	Glitter Pattern		Swells		Wave Refraction		Wave Diffraction		Interference Pattern		Local Topography		Current		Bottom Vegetation		Breakers		COMMENTS
4122	8968	21:09			X	X	X	X			X	X	X	X			X	X	X	X	Topography and wave refraction off Pta. Mocambo.
4123	8969	21:09	X	X	X	X	X	X	X	X	X	X	X	X	X	X	X	X	X	X	Wave diffraction at mouth of Rio Jamapa, river outflow, turbid coastal waters, northward longshore current.
4124	8970	21:09	X	X	X	X			X	X					X	X			X	X	Wave diffraction at mouth of Rio Jamapa, river outflow, turbid coastal waters, northward longshore current.
4125	8971	21:10	X	X	X	X								X	X	X			X	X	Nearshore topography or turbidity pattern due to northward longshore current.
4126	8972	21:10			X	X							X	X	X	X			X	X	Nearshore topography or turbidity pattern due to northward longshore current.
4127	8973	21:10											X	X	X						Nearshore topography or turbidity pattern due to northward longshore current.
4128	8974	21:11											X	X					X	X	Turbid coastal waters.

OCEANOGRAPHIC FEATURES

COLOR FRAME	COLOR IR FRAME	TIME (GMT)	Glitter Pattern		Swells		Wave Refraction		Wave Diffraction		Interference Pattern		Local Topography		Current		Bottom Vegetation		Breakers		COMMENTS
4129	8975	21:11												X					X	X	Turbid coastal waters.
4130	8976	21:11	X	X	X	X							X	X					X	X	Turbid coastal waters.
4131	8977	21:12			X	X							X	X					X	X	Turbid coastal waters.
4132	8978	21:12	X	X	X	X							X	X					X	X	Turbid coastal waters.
4133	8979	21:12	X	X	X	X							X	X					X	X	Turbid coastal waters.
4134	8980	21:12	X	X	X	X							X	X					X	X	Offshore sand bar or turbidity pattern, circulation and sediment transport Laguna Camronera. Possibly local topography of Laguna Camronera in color IR.
4135	8981	21:13	X	X	X	X							X	X				X	X	X	Offshore sand bar or turbidity pattern, circulation and sediment transport Laguna Camronera. Possibly local topography of Laguna Camronera in color IR.
4136	8982	21:13	X	X	X	X							X	X				X	X	X	Offshore sand bar or turbidity pattern, circulation and sediment transport Laguna Camronera and de Alvarado.

OCEANOGRAPHIC FEATURES

COLOR FRAME	COLOR IR FRAME	TIME (GMT)	Glitter Pattern		Swells		Wave Refraction		Wave Diffraction		Interference Pattern		Local Topography		Current			Bottom Vegetation	Breakers		COMMENTS
4137	8983	21:13	X	X	X	X							X	X				X	X	X	Offshore sand bar or turbidity pattern, circulation and sediment transport Laguna Camronera and de Alvarado.
4138	8984	21:14	X	X	X	X							X	X				X	X	X	Offshore sand bar or turbidity pattern, circulation and sediment transport Laguna de Alvarado.
4139	8985	21:14	X	X	X	X							X	X				X	X	X	Offshore sand bar or turbidity pattern, circulation and sediment transport Laguna de Alvarado.
4140	8986	21:14											X	X				X			Circulation and sediment transport in Laguna de Alvarado.
4141	8987	21:14											X	X				X			Circulation and sediment transport in Laguna de Alvarado, river flow pattern, outflow of Rio Papolaapan.
4142	8988	21:15											X	X				X			Circulation and sediment transport in Laguna de Alvarado, river flow pattern, outflow of Rio Papolaapan.
4143	8989	21:18			X	X							X	X					X	X	Offshore sand bar or turbidity pattern.

OCEANOGRAPHIC FEATURES

COLOR FRAME	COLOR IR FRAME	TIME (GMT)	Glitter Pattern		Swells		Wave Refraction		Wave Diffraction		Interference Pattern		Local Topography		Current		Bottom Vegetation		Breakers		COMMENTS
4144	8990	21:19			X	X							X	X					X	X	Offshore sand bar or turbidity pattern.
4145	8991	21:19			X	X			X	X	X	X	X	X	X	X			X	X	River outflow along coast northwest.
4146	8992	21:19	X	X	X	X			X	X				X	X	X		X	X	X	Circulation, sedimentation, and local topography Laguna de Alvarado.
4147	8993	21:20	X	X	X	X					X	X	X	X	X	X		X	X	X	Circulation, sedimentation, and local topography Laguna de Alvarado. Distinct linear color change in Laguna de Alvarado.
4148	8994	21:20	X	X	X	X							X	X				X	X	X	Circulation, sedimentation, and local topography Laguna de Alvarado. Distinct linear color change in Laguna de Alvarado.
4149	8995	21:20	X	X	X	X							X	X					X	X	Nearshore topography or turbidity pattern.
4150	8996	21:20	X	X	X	X															
4151	8997	21:21	X	X	X	X															
4152	8998	21:21	X	X	X	X															

OCEANOGRAPHIC FEATURES

COLOR FRAME	COLOR IR FRAME	TIME (GMT)	Glitter Pattern		Swells		Wave Refraction		Wave Diffraction		Interference Pattern		Local Topography		Current		Bottom Vegetation		Breakers		COMMENTS
4153	8999	21:22	X	X	X	X															
4154	9000	21:22	X	X	X	X															
4155	9001	21:22	X	X	X	X													X	X	
4156	9002	21:22	X	X	X	X													X	X	
4157	9003	21:23	X	X	X	X							X	X					X	X	Nearshore topography or turbidity pattern.
4158	9004	21:23	X	X	X	X	X	X					X	X				X	X	X	Nearshore topography or turbidity pattern.
4159	9005	21:23	X	X	X		X		X	X			X	X			X	X	X	X	Topography off Anton Lizardo, to Arr. Chopas and Blancas, wave diffraction in Anton Lizardo Anch.
4160	9006	21:24	X	X	X				X	X			X	X			X	X	X	X	Wave refraction due to Arr. Blanca.
4161	9007	21:24	X		X	X			X	X		X	X	X			X	X			Topography of Arr. Chopas and Blanca.
4162	9008	21:25	X	X	X	X															
4163	9009	21:25	X	X	X	X															

OCEANOGRAPHIC FEATURES

COLOR FRAME	COLOR IR FRAME	TIME (GMT)	Glitter Pattern		Swells		Wave Refraction		Wave Diffraction		Interference Pattern		Local Topography		Current		Bottom Vegetation		Breakers		COMMENTS
4164	9010	21:26	X	X	X	X			X	X			X	X				X	X	X	Topography Isla Sacrificios and Arr. Pajaros.
4165	9011	21:26	X	X	X	X			X	X	X	X	X	X				X	X	X	Large-scale interference pattern caused by Isla Sacrificios and Arr. Pajaros. Wave diffraction around Isla Verde.
4166	9012	21:26	X	X	X	X	X	X	X	X	X	X	X	X				X	X	X	Large-scale interference pattern caused by Isla Sacrificios and Arr. Pajaros. Diffraction by Veracruz jetty system, wave reflection by inside jetty and inside of south jetty.
4167	9013	21:26	X	X	X	X			X	X	X	X	X	X		X	X	X		X	Diffraction by Veracruz jetty system, wave reflection by inside jetty and inside of south jetty. Diffraction by Arr. Blanquilla and Arr. Galleguilla. Slick north of Arr. Galleguilla. Possible pollutant flowing west from north of harbor.

OCEANOGRAPHIC FEATURES

COLOR FRAME	COLOR IR FRAME	TIME (GMT)	Glitter Pattern		Swells		Wave Refraction		Wave Diffraction		Interference Pattern		Local Topography		Current		Bottom Vegetation		Breakers		COMMENTS
4168	9014	21:27	X	X	X	X			X	X	X		X	X		X	X	X	X	X	Diffraction by Veracruz jetty system, wave reflection by inside jetty and inside of south jetty. Diffraction by Arr. Blanquilla and Arr. Gallequilla. Slick north of Arr. Galleguilla. Possible pollutant flowing west from north of harbor.
4169	9015	21:27	X	X	X	X															
4170	9016	21:27	X	X	X	X															
4171	9017	21:32	X	X	X	X															
4172	9018	21:32	X	X	X	X															
4173	9019	21:32	X	X	X	X	X	X					X	X			X	X	X	X	Topography Arr. de Adentro.
4174	9020	21:32	X	X	X	X	X	X				X	X	X			X	X	X	X	Topography Arr. de Adentro.
4175	9021	21:32	X	X	X	X	X	X					X	X			X	X	X	X	Topography Arr. de Adentro.
4176	9022	21:33	X	X	X	X															
4177	9023	21:33	X	X	X	X															
4178	9024	21:34	X	X	X	X															

OCEANOGRAPHIC FEATURES

COLOR FRAME	COLOR IR FRAME	TIME (GMT)	Glitter Pattern		Swells		Wave Refraction		Wave Diffraction		Interference Pattern		Local Topography		Current		Bottom Vegetation		Breakers		COMMENTS
4179	9025	21:34	X	X	X	X	X	X	X	X			X	X			X	X	X	X	Topography Arr. Chopas and Enmedio.
4180	9026	21:34	X	X	X	X	X	X	X	X	X	X	X	X			X	X	X	X	
4181	9027	21:34	X	X	X	X	X	X	X	X	X	X	X	X			X	X	X	X	Color change distinct and extensive east and west of Arr. Rizo.
4182	9028	21:35	X	X	X	X	X	X			X	X	X	X			X	X			Color change distinct and extensive east and west of Arr. Rizo.
4183	9029	21:35	X	X	X	X	X	X			X	X	X	X			X	X			Color change distinct and extensive east and west of Arr. Rizo.
4184	9030	21:35	X	X	X	X															
4185	9031	21:35	X	X	X	X															
4186	9032	21:35	X	X	X	X															
4187	9033	21:36	X	X	X	X															
4188	9034	21:36	X	X	X	X															
4189	9035	21:36	X	X	X	X															

OCEANOGRAPHIC FEATURES

COLOR FRAME	COLOR IR FRAME	TIME (GMT)	Glitter Pattern		Swells		Wave Refraction		Wave Diffraction		Interference Pattern		Local Topography		Current		Bottom Vegetation		Breakers		COMMENTS
4190	9036	21:36	X	X	X	X															
4191	9037	21:37	X	X	X	X															
4192	9038	21:37	X	X	X	X															
4193	9039	21:37	X	X	X	X			X	X					X	X			X	X	Wave diffraction in mouth of Rio Papolaapan, river outflow flowing nearshore northwest.
4194	9040	21:38	X	X	X	X			X	X	X	X		X	X	X			X	X	Wave diffraction in mouth of Rio Papolaapan, river outflow flowing nearshore northwest.
4195	9041	21:38	X	X	X	X			X	X			X	X	X	X			X	X	Wave diffraction in mouth of Rio Papolaapan, river outflow flowing nearshore northwest.
4196	9042	21:38	X	X	X	X							X	X	X	X			X	X	Wave diffraction in mouth of Rio Papolaapan, river outflow flowing nearshore northwest. Offshore sand bars or turbidity pattern due to longshore current.
4197	9043	21:39	X	X	X	X							X	X	X	X		X	X	X	Wave diffraction in mouth of Rio Papolaapan, river outflow flowing nearshore northwest. Offshore sand bars or turbidity pattern due to longshore current.

OCEANOGRAPHIC FEATURES

COLOR FRAME	COLOR IR FRAME	TIME (GMT)	Glitter Pattern		Swells		Wave Refraction		Wave Diffraction		Interference Pattern		Local Topography		Current		Bottom Vegetation		Breakers		COMMENTS
4198	9044	21:39	X	X	X	X							X	X	X	X		X	X	X	Wave diffraction in mouth of Rio Papolaapan, river outflow flowing nearshore northwest. Offshore sand bars or turbidity pattern due to longshore current. Sediment transport in Laguna de Alvarado.
4199	9045	21:44	X	X	X	X															
4200	9046	21:45	X	X	X	X															
4201	9047	21:45	X	X	X	X															
4202	9048	21:46	X	X	X	X			X	X			X	X			X	X	X	X	Topography Arr. Cabeza.
4203	9049	21:46	X	X	X	X			X	X			X	X			X	X	X	X	Topography Arr. Cabeza.
4204	9050	21:46	X	X	X	X			X	X			X	X			X	X	X	X	Topography Arr. Cabeza.
4205	9051	21:46	X	X	X	X		X	X	X	X	X	X	X			X	X	X	X	Topography Arr. Cabeza.
4206	9052	21:47	X	X	X	X		X	X	X	X	X	X	X			X	X	X	X	Topography Arr. Cabeza.
4207	9053	21:47	X	X	X	X		X	X		X	X	X	X			X	X	X	X	Topography Arr. Cabeza.
4208	9054	21:47	X	X	X	X															

OCEANOGRAPHIC FEATURES

COLOR FRAME	COLOR IR FRAME	TIME (GMT)	Glitter Pattern		Swells		Wave Refraction		Wave Diffraction		Interference Pattern		Local Topography		Current		Bottom Vegetation		Breakers		COMMENTS
4209	9055	21:47	X	X	X	X															
4210	9056	21:47	X	X	X	X															
4211	9057	21:48	X	X	X	X															
4212	9058	21:48	X	X	X	X															
4213	9059	21:48	X	X	X	X															
4214	9060	21:48	X	X	X	X															
4215	9061	21:53	X	X	X	X															
4216	9062	21:53	X	X	X	X															
4217	9063	21:53	X	X	X	X															
4218	9064	21:54	X	X	X	X															
4219	9065	21:54	X	X	X	X															
4220	9066	21:54	X	X	X	X															
4221	9067	21:54	X	X	X	X															
4222	9068	21:55	X	X	X	X	X	X					X	X			X	X	X	X	Topography Arr. Afuerra.

OCEANOGRAPHIC FEATURES

COLOR FRAME	COLOR IR FRAME	TIME (GMT)	Glitter Pattern		Swells		Wave Refraction		Wave Diffraction		Interference Pattern		Local Topography		Current		Bottom Vegetation		Breakers		COMMENTS
4223	9069	21:55	X	X	X	X	X	X					X	X			X	X	X	X	Topography Arr. Afuerra.
4224	9070	21:55	X	X	X	X	X	X	X	X			X	X			X	X	X	X	Topography Arr. Afuerra.
4225	9071	21:56	X	X	X	X	X	X					X	X			X	X	X	X	Topography Arr. Cabeza.
4226	9072	21:56	X	X	X	X	X	X			X	X	X	X			X	X	X	X	Topography Arr. Cabeza.
4227	9073	21:56	X	X	X	X	X	X					X	X			X	X	X	X	Topography Arr. Cabeza. Distinct color changes of reef.
4228	9074	21:57	X	X	X	X							X	X			X	X	X	X	Topography Arr. Cabeza. Distinct color changes of reef.
4229	9075	21:57	X	X	X	X															
4230	9076	21:57	X	X	X	X															
4231	9077	21:57	X	X	X	X															
4232	9078	21:58											X	X				X	X	X	Offshore sand bar or turbid streaks. Circulation and sediment transport Laguna Mandingo Grande.

RESULTS AND RECOMMENDATIONS

Results - Fulfillment of Objectives

In view of the data received at Texas A & M, the present evaluations of the fulfillment of the test objectives are as follows:

A. Correlation of chlorophyll distribution to concentration. No ship data reporting chlorophyll concentration has been received. Recent work by Clarke and Ewing at Woods Hole Oceanographic Institute indicates that some idea of the chlorophyll distribution might possibly be achieved by a careful aerial analysis. However, none of this extremely sensitive and experimental equipment is yet available for general remote sensing work. No data was taken by the aircraft from which the chlorophyll distribution might be inferred. This objective was, therefore, not achieved.

B. Distinguish extent of bottom vegetation. This objective was met in all areas which were sufficiently shallow to permit light penetration to the bottom. Grass distribution is clearly delineated on these photographs; and, moreover, with some ground truth, the distributions of different types of vegetation could be mapped.

C. Define distribution of the sea-surface thermal patterns. PRT-5 (infrared thermometer) data has not been received at Texas A & M, but the RS-14 (infrared imager) effectively mapped the thermal fronts in the area and even delineated the ship wakes.

D. Characterize the nearshore currents. A longshore current to the north was clearly delineated along the entire coastal region near Veracruz. River outflow, sediment patterns, and pollution distribution all clearly

indicated the presence of this current.

E. Locate and define possible upwelling in this area. No positive evidence of upwelling exists in either the ship data or the aircraft data. The dynamics of the wind and current systems near Veracruz are not such as to allow intense upwelling. This is not to say that no upwelling exists. Ship data is too sparse for a complete analysis. Aircraft data show some thermal fronts which may or may not be evidence of upwelling.

F. Delineate subsurface topography and water depths (hydrographic mapping). The entire subsurface topography of the various reefs near Veracruz was very clearly defined. Color IR and black and white IR photographs clearly define the portion of land out of water and the land-water interface. Channels through and into the reefs were delineated. A relative estimate of depth can be easily ascertained in the nearshore and reef regions from photography of the bottom and observations of wave refraction patterns. Absolute values of depth are much harder and more expensive to come by and involve some sort of measurement of the change in the wave pattern as it comes ashore. A Fourier transform is usually made of the glitter pattern; and this process is, in general, quite a tedious task. A good update and permanent record of the Veracruz harbor and approaches has been recorded by this mission; and the data are of sufficient quality to delineate any dangerous areas to marine traffic, so this objective has been achieved.

G. Determine sources and distribution of pollution in nearshore areas. This objective was clearly achieved. A pollution source just north of the port of Veracruz was easily detected and its flow along the coast and into the shore determined. Oil slicks were also located. No evidence of thermal pollution flowing into the ocean was found, and the resolution of the RS-14

was sufficient enough to determine any major source.

H. Determine sediment distribution. The nearshore sediment distribution is evident in color, color IR and multiband photography. River outflow is clearly defined, and sediment patterns in the inshore bays are also delineated.

Recommendations for Future Analysis

More information can be obtained from some of this aircraft data.

Swell patterns can be related to strong winds or storms elsewhere in the Gulf. (This was going to be done by Texas A & M University, but the monthly weather review for April has not been published yet.)

Color separation techniques could be used on certain frames to better illustrate the sediment loads, bathymetry, and distribution of bottom grasses.

Fourier Analysis of wave and swell patterns would give a quantative estimate of the water depths.

Recommendations for Future Missions

The following quantities should be measured or estimated at each ship station if the mission objectives remain as general as those for Mission 91:

Time of day
Continuous record of sea surface temperatures
Wave period
Wave direction
Ship drift (direction and velocity)
Oxygen
Nutrients
Chlorophyll

The time of day and continuous sea surface temperature would be helpful in averaging out diurnal effects on the surface temperature which can be as large as 1°C. The wave period and direction would be helpful for a more

quantitative estimate of depth due to wave refraction. Ships drift (in the absence of strong winds) is often an excellent indication of the strength and direction of the nearshore currents. Some sort of direct measurement of nearshore currents is usually necessary as the depth is not sufficient to apply geostrophic techniques and tidal influence is usually of major importance. The measurement of oxygen and nutrients (nitrogen, phosphate, etc.) is most helpful in measuring areas of upwelling or high biological productivity as is the chlorophyll distribution. Better ship coverage could have been achieved through the use of a bathythermograph and/or surface samples between hydrographic stations.

The general nature of this mission necessitated the use of all the various aircraft sensors. Future oceanographic missions would be more successful if aimed more at certain oceanographic features and all aircraft and ship sensors geared to the oceanographic features requirements. The SLAR was of such poor quality that it presently is of no scientific value. The thermal imagery in the 3-5.5μ region would probably be improved by night flights.

This mission was successful in determining the oceanographic features found in the coastal area near Veracruz. However, Veracruz is not a particularly dynamic oceanographic area. Future aircraft missions in Mexico should include the regions of strong currents and known upwelling near the Yucatan Coast. A mission should also be planned for the Pacific Coast of Mexico, where better dynamic conditions for upwelling exist. Future aircraft missions over the ocean and coastal areas should be planned toward more specific objectives, as the scientific value of data from the various airborne sensors has been well defined by this mission.

E. International Program - Brazil

On September 8, Dr. Huebner, Bill Merrell, and Robert Whitaker traveled to NASA/MSC in Houston to meet with the Brazilians and to assist in their analysis of the multisensor data taken with the NASA Aircraft. This first flight was considered successful by all the participants due to the availability of excellent ground truth and color photography. The data were reviewed and an outline of a preliminary data report prepared.

A "Quick-Look" report of the data taken over Cabo Frio, Brazil (Test Site 805 - Mission 96) under the Earth Resources Program on July 7, 1969, was prepared for use during the Brazilian Data Review in Rio de Janeiro, Brazil, January 12-14, 1970. This report was prepared by Bill Merrell and Robert Whitaker and submitted 31 December 1969.

This report is a preliminary analysis of data taken aboard NASA Aircraft on July 7, 1969, over the Brazilian Coast. The data reviewed in this report consisted of color photography, false color IR photography, multiband photography in four spectral regions, and infrared imagery. The photographic data were taken on five flight lines at 15,000 feet, and infrared data were taken on four flight lines at 3,000 feet. Excellent "surface truth" was obtained by Brazilian vessels in the area. However, no ship data were used in this report, and this analysis is further limited to the aircraft data received by Texas A & M University.

A "QUICK-LOOK ANALYSIS OF AIRCRAFT DATA-NASA AIRCRAFT MISSION 96, SITE 805; CABO FRIO, BRAZIL

INTRODUCTION

This report is a preliminary analysis of data taken aboard NASA aircraft on July 7, 1969, over the Brazilian Coast. The data reviewed in this report consisted of color photography, false color IR photography, multiband photography in four spectral regions, and infrared imagery. The photographic data were taken on five flight lines at 15,000 ft., and infrared data were taken on four flight lines at 3,000 ft. Excellent "surface truth" was obtained by Brazilian vessels in the area. However, no ship data were used in this report, and this analysis is further limited to the aircraft data received at Texas A & M.

Overall, the quality of the data was excellent. The resolution of the photography was good, and the mission was flown on a very clear day, so atmospheric attenuation is minimal. The overlap of individual frames was beneficial to the analysis.

The color, as well as the multi-spectral exposures, of Site 805 were of high quality. The false color IR photography was not of the same quality due to low exposure. Noise impaired the IR imagery obtained from the 3.0-5.5μ channel, but the signal to noise ratio on the 8-14μ channel was larger and the data gathered in this region of the spectrum were of good quality.

AIRCRAFT DATA

The catalog of oceanographic features observed in the color and false color IR photography lists the features chronologically, with the box to the left under each feature pertaining to the color frame number and the box to the right pertaining to the false color IR frame number. Nearshore currents are clearly delineated by distinct color changes caused by sediment transport of river outflow. The land-sea boundary is clearly defined in the false color IR photography, and bottom topography in shallow areas is visible in both sets of photographs.

Studies of sedimentation patterns, in addition to studies of wave diffraction, refraction, and interference as observed in color and false color IR photography could aid coastal engineers in jetty construction and dredging. Increased safety for small boat operators could also be realized from such studies.

Several slicks are seen in the glitter patterns off the Brazilian Coast. When out of the glitter pattern on other photographs, the regions in which the slicks appeared often have foam or seaweed lines or a pronounced color boundary indicating these slicks are formed in areas of convergence as would be expected. These convergence zones are often good fishing areas.

An interesting oceanographic phenomenon is depicted in the predominantly northward flow of the sediment-laden outflow from the rivers and lagoons. This northward flow may be indicative of a nearshore counter-current associated with the Brazil current which flows to the south fairly near the coast in this region. A nearshore counter-current is often associated with western boundary currents.

NOTE: Under Oceanographic Features, the box to the left is for color and the box to the right is for false color IR.

CATALOG OF OCEANOGRAPHIC FEATURES OBSERVED
IN COLOR AND FALSE COLOR IR PHOTOGRAPHY
NASA MISSION 96, SITE 805 - 7 JULY 1969

COLOR FRAME	FALSE COLOR IR FRAME	TIME	OCEANOGRAPHIC FEATURES																				COMMENTS
			Color Boundary		Convergence Lines		Slicks in Glitter Patterns		Wave Refraction		Wave Diffraction		Interference Pattern		Local Topography		Current		Bottom Vegetation		Breakers		
7370	1301	13:15					X																Ship generated bow wave.
7371	1302	13:15	X		X		X	X	X	X													Ship generated bow wave.
7372	1303	13:16	X		X		X	X	X	X			X	X	X	X			X				Diffuse color boundary.
7373	1304	13:16	X		X		X	X	X	X	X	X	X	X	X	X			X				Diffuse color boundary
7374	1305	13:16	X		X						X				X	X					X	X	Diffuse color boundary---Note: Convergence lines were indicated as slicks in the glitter pattern in 7374. This pattern is predominant throughout the entire series of photographs.
7375	1306	13:17			X	X									X	X					X	X	Nearshore turbulence.
7376	1307	13:17					X		X	X					X	X					X	X	Nearshore turbulence.

COLOR FRAME	FALSE COLOR IR FRAME	TIME	Color Boundary		Convergence Lines		Slicks in Glitter Patterns		Wave Refraction		Wave Diffraction		Interference Pattern		Local Topography		Current		Bottom Vegetation		Breakers		COMMENTS
7377	1308	13:18													X	X			X		X	X	Nearshore shore turbulence, shrimp nets.
7378	1309	13:18													X	X			X				Shrimp nets.
7379	1310	13:25													X	X					X	X	Swells.
7380	1311	13:26			X				X	X					X	X					X	X	Swells.
7381	1312	13:26			X				X						X	X	X				X	X	Swells.
7382	1313	13:27					X	X	X	X					X	X	X				X	X	
7383	1314	13:27					X	X	X	X					X	X					X	X	Color streaks.
7384	1315	13:27	X				X	X	X						X	X	X				X	X	Color streaks.
7385	1316	13:28	X				X	X	X	X							X				X	X	Color streaks.
7386	1317	13:28	X				X	X	X	X							X				X	X	
7387	1318	13:28	X	X	X		X		X								X				X	X	Nearshore turbulence.
7388	1319	13:28			X		X		X	X			X		X		X				X	X	Color streaks.
7389	1320	13:29			X				X	X			X	X	X				X		X	X	Color streaks.

COLOR FRAME	FALSE COLOR IR FRAME	TIME	Color Boundary		Convergence Lines		Slicks in Glitter Patterns		Wave Refraction		Wave Diffraction		Interference Pattern		Local Topography		Current		Bottom Vegetation		Breakers		COMMENTS
7390	1321	13:29	X		X		X	X	X						X				X		X	X	
7391	1322	13:29	X				X									X							
7392	1323	13:34			X		X	X	X	X					X		X				X	X	Color streaks, nearshore turbulence.
7393	1324	13:34			X				X	X			X		X		X		X		X	X	Nearshore turbulence.
7394	1325	13:35			X		X	X							X		X				X	X	Nearshore turbulence.
7395	1326	13:35			X		X		X						X		X				X	X	Nearshore turbulence.
7396	1327	13:35							X						X		X				X	X	Nearshore turbulence.
7397	1328	13:36					X								X		X				X	X	Nearshore turbulence.
7398	1329	13:36					X										X				X	X	Nearshore turbulence.
7399	1330	13:43			X	X	X	X	X	X			X	X			X				X	X	Nearshore turbulence.
7400	1331	13:43			X				X				X				X				X	X	Nearshore turbulence.
7401	1332	13:43					X										X				X	X	Nearshore turbulence, color streaks.

COLOR FRAME	FALSE COLOR IR FRAME	TIME	Color Boundary		Convergence Lines		Slicks in Glitter Patterns		Wave Refraction		Wave Diffraction		Interference Pattern		Local Topography		Current		Bottom Vegetation		Breakers		COMMENTS
7402	1333	13:44																			X	X	Nearshore turbulence, color streaks.
7403	1334	13:45	X	X	X	X	X	X									X	X			X	X	Nearshore turbulence, color streaks, river outflow.
7404	1335	13:45	X	X	X	X	X	X									X	X			X	X	River outflow, long convergence line along color boundary.
7405	1336	13:45	X	X	X		X	X	X	X							X	X			X	X	River outflow.
7406	1337	13:45	X	X													X						Color streaks.
7407, 7408	1338, 1339	13:56																					Double exposure.
7409	1340	13:57	X	X													X.						Nearshore turbulence.
7410	1341	13:57	X	X													X						Nearshore turbulence.
7411	1342	13:58	X	X													X	X					Nearshore turbulence.
7412	1342	13:58	X	X													X	X					Nearshore turbulence.
7413	1344	13:58	X	X			X	X									X	X					Nearshore turbulence.
7414	1345	13:59	X	X													X						Nearshore turbulence.

COLOR FRAME	FALSE COLOR IR FRAME	TIME	Color Boundary		Convergence Lines		Slicks in Glitter Patterns		Wave Refraction		Wave Diffraction		Interference Pattern		Local Topography		Current		Bottom Vegetation		Breakers		COMMENTS
7415	1346	13:59			X	X	X	X									X						Color streaks, river outflow.
7416	1347	13:59	X	X	X	X	X	X	X	X							X	X			X	X	Nearshore turbulence, river outflow.
7417	1348	14:00	X	X	X	X	X	X	X	X	X	X	X				X	X			X	X	Nearshore turbulence, river outflow.
7418	1349	14:00	X	X	X		X	X	X	X	X	X	X	X	X	X	X	X			X	X	Nearshore turbulence.
7419	1350	14:00	X	X			X	X	X	X					X		X				X	X	Eddy formation, old river channel.
7420	1351	14:01	X	X	X	X			X	X							X				X	X	Eddy formation, nearshore turbulence.
7421	1352	14:01	X	X	X	X	X	X	X	X			X	X			X				X	X	Nearshore turbulence.
7422	1353	14:01	X	X	X	X			X	X	X	X	X	X			X				X	X	Color streaks.
7423	1354	14:02	X		X	X	X	X	X				X				X				X	X	Nearshore turbulence.
7424	1355	14:02	X	X	X	X	X	X									X				X	X	River outflow, nearshore turbulence.
7425	1356	14:03	X		X		X		X								X				X	X	River outflow, nearshore turbulence.

COLOR FRAME	FALSE COLOR IR FRAME	TIME	Color Boundary		Convergence Lines		Slicks in Glitter Patterns		Wave Refraction		Wave Diffraction		Interference Pattern		Local Topography		Current		Bottom Vegetation		Breakers		COMMENTS
7426	1357	14:03	X	X			X	X	X	X	X	X	X	X							X	X	Color streaks.
7427	1358	14:03	X	X	X	X	X	X	X	X							X	X			X	X	Boat's wake, river outflow.
7428	1359	14:04	X	X	X	X	X	X	X	X							X	X			X	X	Boat's wake, river outflow, nearshore turbulence.
7429	1360	14:04	X	X	X	X			X	X	X		X	X			X	X			X	X	Boat's wake, river outflow, nearshore turbulence.

MULTIBAND CAMERA SYSTEM

The K-62 multiband camera system employed the following bandpass filters: 477mμ (blue, Wr 47), 530mμ (green, Wr 57), 617mμ (red, Wr 25A), and 750mμ (IR, Wr 89B). Since sea water exhibits selective absorption of the incident radiation, the spectrum becomes a function of depth. In general, the greater depth of penetration is achieved by the shorter wavelengths (470mμ) in oceanic and clear coastal waters, while longer wavelength radiation (550mμ) exhibits the better transmission characteristics in average and turbid coastal waters due to selective absorption.

A comparison of the four images obtained from the K-62 multiband camera system can yield information concerning relative depths of observed phenomenon. For example, in the multiband photography utilizing the blue bandpass filter, the river effluent (Frames 0064-0066) can be delineated some distance offshore and downstream while the green bandpass filter enables us to trace this flow even farther (Frames 0064-0077). Exposures of the same region using the red bandpass filter exhibit the surface features quite well due to low atmospheric attenuation (Frames 0535-0537). The IR bandpass filter illustrates no near-shore features but readily defines the land-sea boundaries (Frames 4781-4783). A time-series of such photography could be useful in determining the variability and relative depth of the river's sediment load.

In Frames 0010 and 0011 (Wr 47 filter), the bottom topography in the inlet and along the beach can be seen but not with the clarity and detail one finds on Frames 0010 and 0011 (Wr 57 filter). No details of the bottom topography in Frames 0470 and 0471 (Wr 25A) can be observed although the bottom can be seen. As expected, IR exposures employing the Wr 89B filter (Frames 4728 and 4729) exhibit no bottom topography.

INFRARED IMAGER

The RS-14 infrared imager was flown on flight lines 5, 6, 7, and 8 at an altitude of 3,000 ft. Imaged data are available in both the 8-14μ and 3.0-5.5μ regions. The 8-14μ data are of better definition.

The IR imagery employing the 8-14μ channel delineates numerous thermal boundaries. These boundaries can sometimes be associated with color boundaries and/or convergence lines evident in the color and false color IR photography. However, without better spatial confirmation, this association can not be made with certainty. A few thermal boundaries, most of which are nearshore, could be found in the imagery utilizing the 3.0-5.5μ channel.

CHAPTER III - PROGRESS (cont.)

F. Apollo IX - Oceanography (Note: Reproduction of actual photography as called for in figure numbers has not been done for this report).

INTRODUCTION

The photography of the oceanic and coastal regions of earth taken from Apollo IX is far superior to that of previous manned missions. The handheld photography is of very high quality with a minimum of unfocused and poorly exposed frames. Many oceanographic sites were photographed, and most of these were from the vertical or near-vertical. Overall, the men aboard Apollo IX did a good job of photographing interesting oceanographic phenomena although some specifically requested sites were not photographed and few frames were taken over the central oceans.

The SO-65 experiment was also conducted on the flight of Apollo IX. Four cameras were mounted in the spacecraft window and simultaneously recorded photographs, one on color IR film and the other three on black and white film with different filter combinations. Too few photographs of ocean phenomena were recorded, but some of the photographs of coastal areas illustrate the benefits of the multispectral approach. Indeed, the SO-65 experiment is the start of a new dimension in orbital photography which should eventually lead to more quantitative measurements of ocean parameters from space.

OCEAN FEATURES OBSERVED

The oceanographic features observed in Apollo IX photographs are, in general, similar to those recorded in previous photography from space. However, many of these features are most vividly displayed in the Apollo IX series.

This section is a general discussion of the types of oceanic features observed. In the next section, specific examples of these phenomena are illustrated and discussed in more detail.

Apollo IX photography includes many outstanding photographs of river plumes and coastal turbidity patterns. Estimates of the sediment load, types of sediments and strength of flow of these rivers can be determined from these patterns. The direction of longshore currents is often evident in the coastal turbidity patterns, and the effects of jetties and coastal topography are recorded. The additional information obtained by using different filter combinations on the SO-65 experiment can be used to establish the true cause of some doubtful photographic features seen in this region. In regular color photographs, it is often impossible to determine whether color streaks in coastal regions were due to bottom reflection, turbidity, surface contaminants or light cloud cover. The SO-65 experiment photographs, when viewed together, give conclusive evidence as to whether the color feature is above or below the sea surface and even provide an estimate as to its depth.

As in previous space flights, some excellent photographs of the Bahama Banks were obtained. The ocean water is very clear in this area and the bathymetry is clearly defined in the photographs as well as the different types of grasses and ocean bottom. Color IR photographs of the Georgia coast clearly delineate underwater channels and the land-sea boundaries.

Ocean wave swell is very clearly recorded as are "bow" waves associated with the flow around islands.

Some oceanic phenomena not often seen in space photography are also evident in the Apollo IX series. An upwelling region on the north coast of Jamaica is clearly defined. Moreover, a single photograph taken in the deep ocean shows an eddy formation, long white streaks apparently on the surface

of the ocean, and a surface roughness boundary probably associated with a convergence zone or a wind shear pattern.

SELECTED APOLLO IX FRAMES

Ocean Waves Near Morocco. Figure 1 (Apollo IX Frame 3617) shows a portion of the Mediterranean Sea near Agadir, Morocco. In the glitter pattern, one can see a very regular pattern of swell traveling toward the coast. This pattern is the clearest photography of ocean swell yet made from space in the manned program of the NASA.

Atmospheric Waves and the St. Johns River. Figure 2 shows Apollo IX Frame 3049. One should note the black plume of the St. Johns River located in the center of the photograph. The river water is dark due to its high content of brownish humic acids from decaying vegetation in the swamps and marshes of Florida (Joyce, 1969). Tidal effects on this river are large and at the time of this photograph, it is likely that the tide is out or moving out. During high tides, the blackish plume would probably be cut off by the salt wedge. Also, one may see elongated patterns extending from the lower left of Figure 2 to the upper right. The cloud patterns appear to be a continuation of the hazy patterns. Thus, it seems that internal waves in the atmosphere are causing a concentration of sub-cloud particles on the lower left.

Great Bahama Banks. Apollo IX Frames 3343 and 3344 (Figure 3) are the clearest space photographs of this well-studied area made to date. The dark area is the Old Bahama Channel, and the islands are Cayo Romano and Cayo Coco, Cuba. Intricate patterns of grass on the sandy, shallow bottom of the banks can be seen.

Boundaries of Gulf Stream. The edge of the Gulf Stream is often marked by a large change in temperature. In Frames 3047 and 3552 (Figure 4), it appears

Insert Frame 3617

Figure 1, Apollo IX Frame 3617, Ocean Waves Near Morocco

Insert Frame 3049

Figure 2, Apollo IX Frame 3049,
Atmospheric Waves and the St. Johns River

Insert Frame 3343

Figure 3a, Apollo IX Frame 3343

Insert Frame 3344

Figure 3b, Apollo IX Frame 3344
Figure 3, Apollo IX Frames 3343 and 3344, Great Bahama Banks

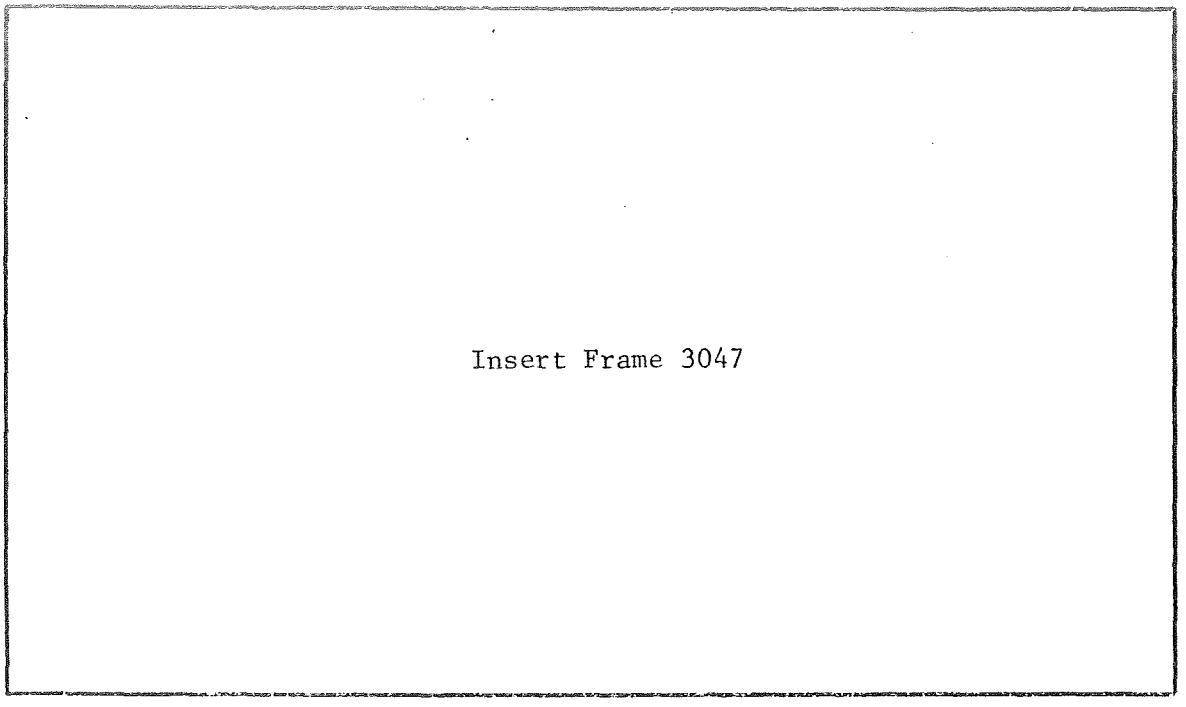

Figure 4a, Apollo IX Frame 3047

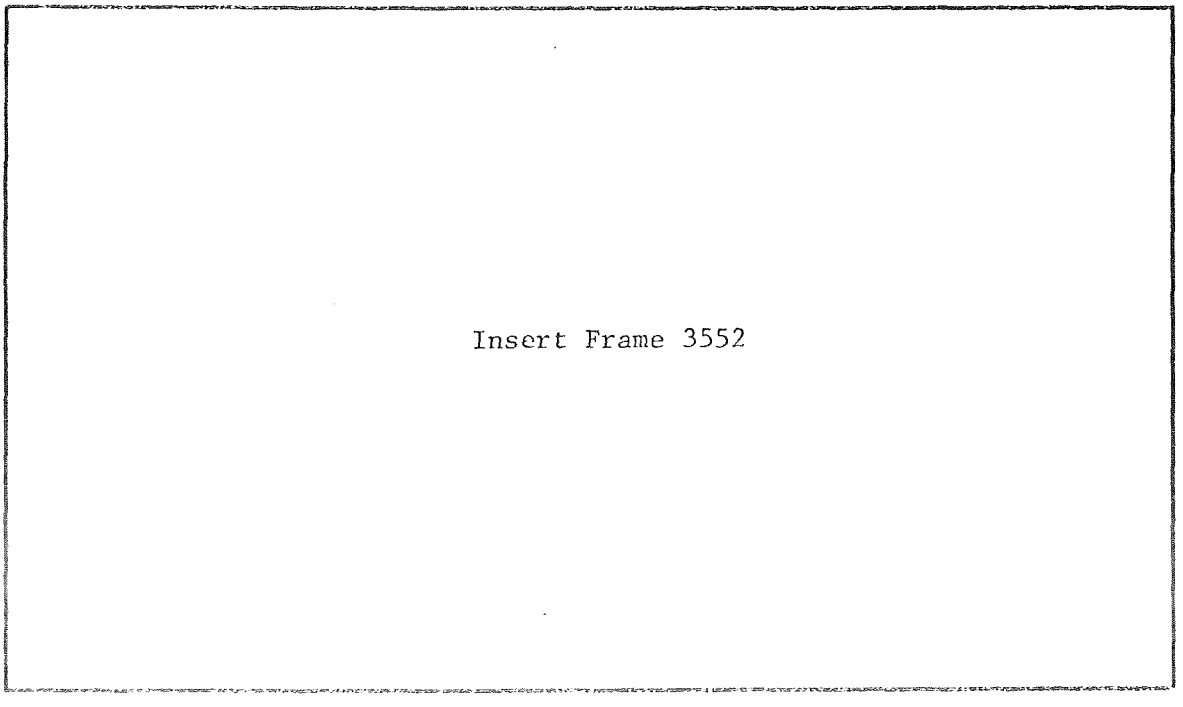

Figure 4b, Apollo IX Frame 3552
Figure 4, Apollo IX Frames 3047 and 3552,
Boundaries of the Gulf Stream

that the Gulf Stream's eastern boundary is marked by a change in low level cloud development in the former case and by a change in color in the latter case. Note that this boundary appears to be about 15 nautical miles off Cape Kennedy. This corresponds approximately to the edge of the continental shelf.

Upwelling and Bow Waves Around Jamaica. Figure 5a, Apollo IX Frame 3315, is of Jamaica. The sharp color change which extends northwest from the west end of the island is probably the result of upwelling off the island's north coast. Apollo IX Frame 3316, Figure 5b, indicates that no such color change is present on the eastern side of Jamaica. From H. O. Pub. 106, it is apparent that the ocean currents and winds are predominantly from the east during March in this region. The dynamics then satisfy the conditions necessary for upwelling to occur on the north coast. Bow waves formed by the westward flow around the island are visible in the glitter pattern. Many doubtful hydrographic features are present in this photograph, and they illustrate the need for multispectral photography. For example, what appears to be thin clouds just to the north of the island in Figure 5a, Apollo IX Frame 3315, appears to be a feature on the sea surface in Figure 5b, Apollo IX Frame 3316.

An Eddy at 12°N, 50°W. Figure 6 is Apollo IX Frame 3588 which was taken from an altitude of 107 N.M. and the position of 12°N, 50°W. This photograph illustrates a convergence or wind shear zone which is delineated by the change in the glitter pattern in the upper left center. In the lower left, one can easily discern a large anticyclonic eddy. The cause of the color changes which define the eddy is unknown. The color pattern to the left of the eddy could be related to horizontal motion of the eddy or to horizontal diffusion.

The large white streak in the lower center and the smaller streak in the upper left-hand corner are thought to be due to film processing. However, the

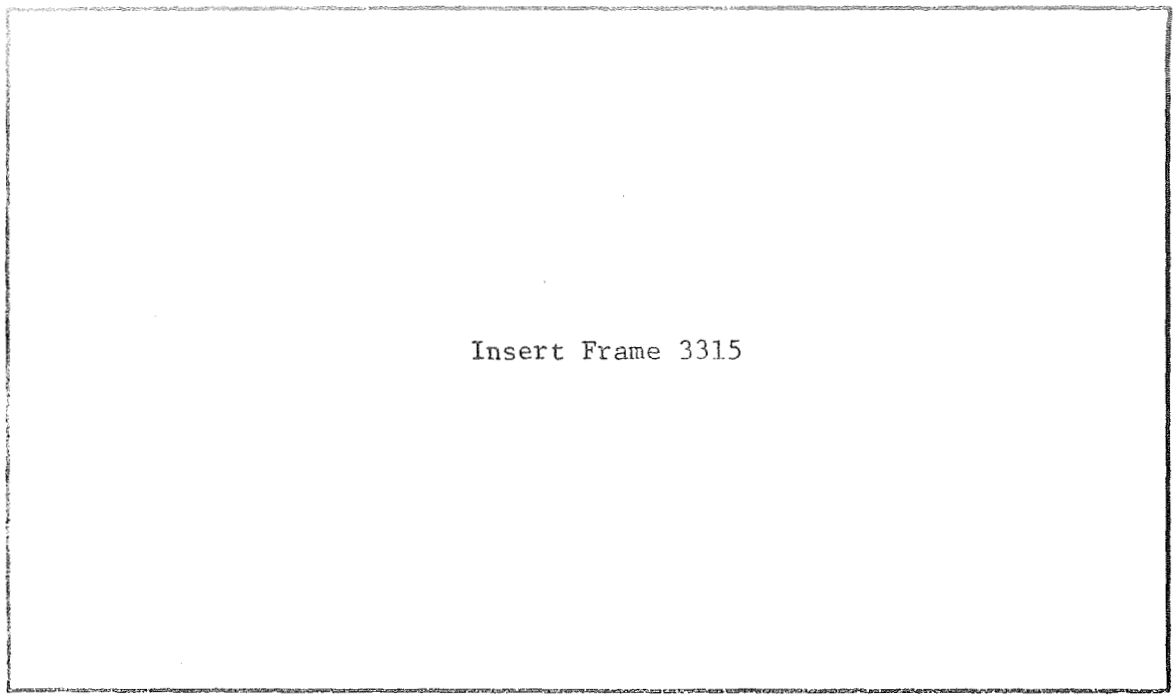

Figure 5a, Apollo IX Frame 3315

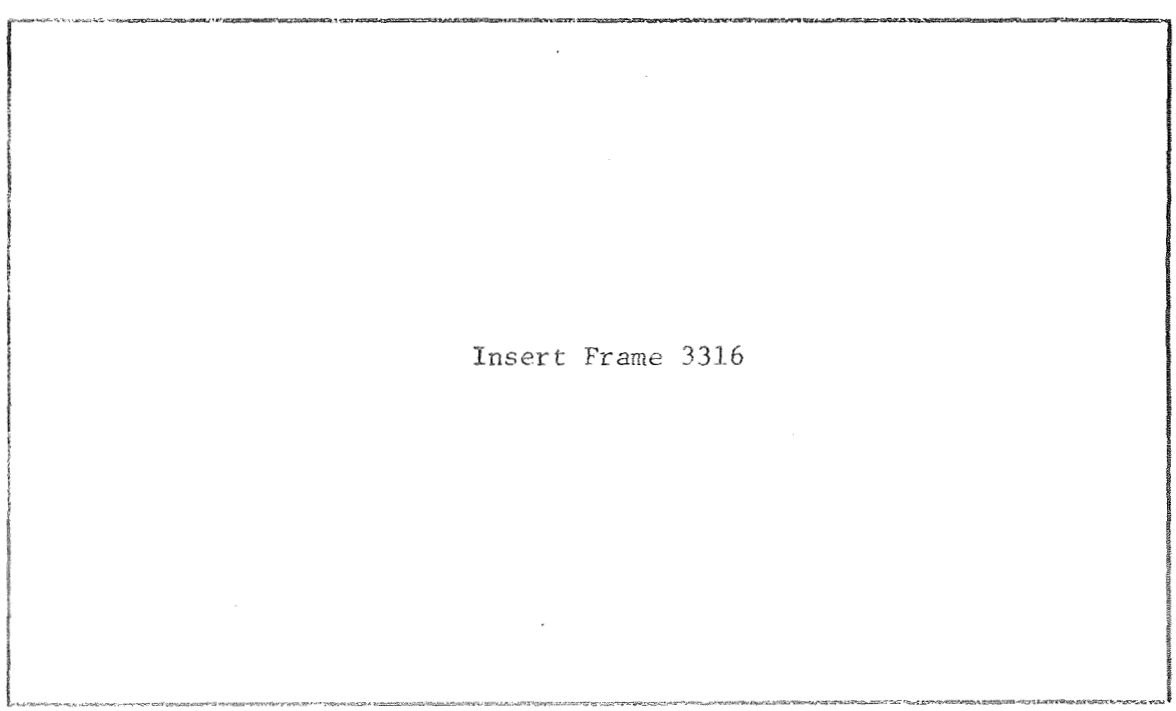

Figure 5b, Apollo IX Frame 3316
Figure 5, Apollo IX Frames 3315 and 3316,
Upwelling and Bow Waves Around Jamaica

Insert Frame 3588

Figure 6, Apollo IX Frame 3588, An Eddy at 12°N, 50°W

white filamentary features to the near right and far left of the central streak appear to be real and on the sea surface. Exactly what these are manifestations of is unknown.

This photograph is unique in the Apollo IX series. Color differences of the type illustrated in this photograph were thought to occur only in coastal regions. Few photographs have been taken over the central oceans, so it is impossible to say how indicative of the total world ocean Figure 6 is. Multispectral photographs of features similar to those illustrated by Figure 6 would be most helpful in the accurate identification of this type of ocean phenomena.

Longshore Current and Deltaic Deposits Along the Texas Coast. If we scan Apollo IX Frames 3465 (Figure 7a), 3728A (Figure 9), 3342 (Figure 7b), and 2989 (Figure 8), respectively, it is apparent that the south longshore current revealed by the color pattern comes nearer to the coast as it travels south. It should be noted that Frame 3728A is a color IR photograph taken in the SO-65 experiment. In Frame 3465, the Sabine River plume in the left center has intruded some distance into the Gulf before being turned slightly south. Proceeding to Frame 3728 (Figure 9), the effluents from Galveston Bay (lower left and the Freeport Channel (center) tend southward close to the coast. The same can be said for the outflow of the Colorado River (lower center) and Pass Cavallo (left center) as viewed in Frame 3342 (Figure 7b). The panoramic view afforded by Frame 2989 (Figure 8) illustrates how close to the shoreline this south longshore current approaches as it nears the mouth of the Rio Grande. From this frame, the width of the longshore current can be deducted.

Deltaic deposits are visible in Frames 3728A, 3342, and 2989. The Brazos River deposits are seen in the center of Frame 3728A, while the Colorado River Delta (left side of Frame 3728A) is seen in all three frames. Shoals can be seen in Pass Cavallo shown in Frame 3342.

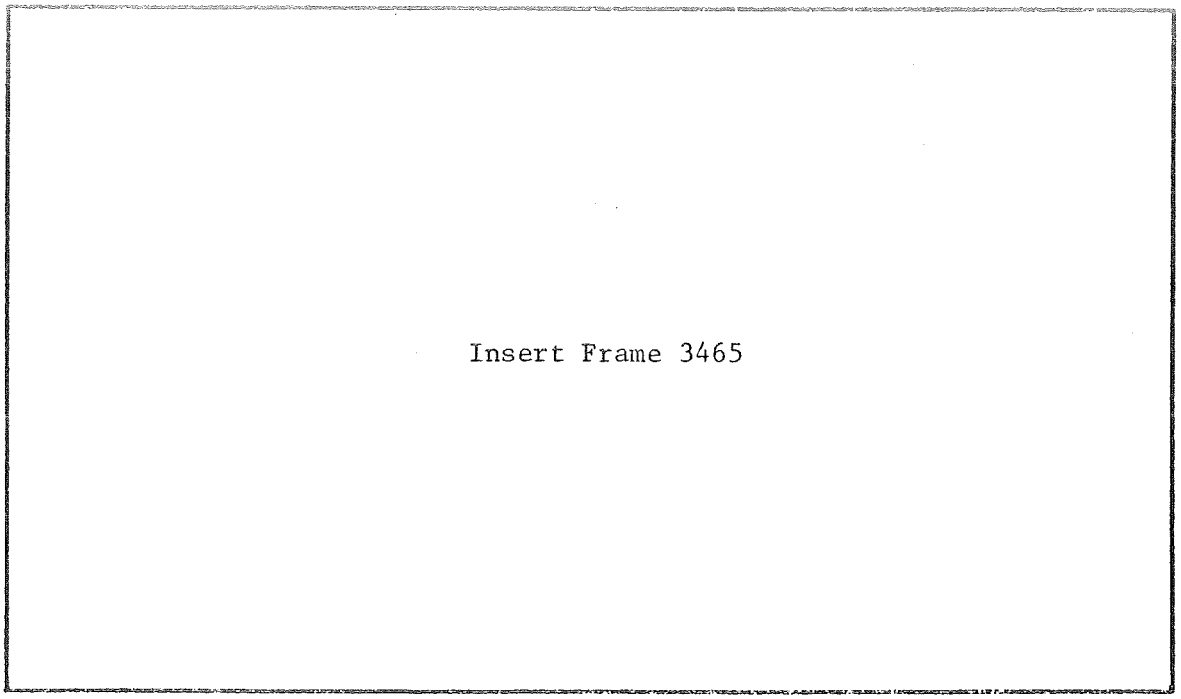

Figure 7a, Apollo IX Frame 3465

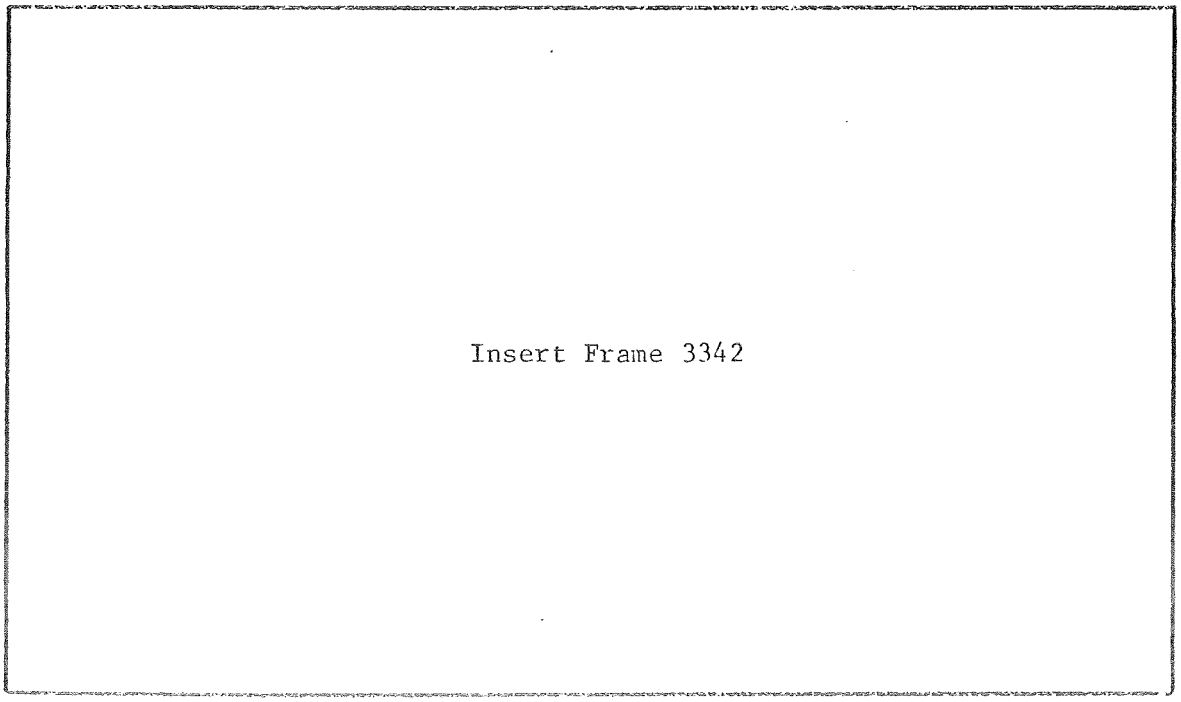

Figure 7b, Apollo IX Frame 3342
Figure 7, Apollo IX Frames 3465 and 3342,
Longshore Current and Deltaic Deposits Along the Texas Coast

Insert Frame 2989

Figure 8, Apollo IX Frame 2989,
Longshore Current and Deltaic Deposits Along the Texas Coast

Insert Frame 3728A

THIS FRAME SHOULD BE IN COLOR

Figure 9, Apollo IX Frame 3728A,
Longshore Current and Deltaic Deposits Along the Texas Coast,
Beach Development and Erosion Along the Upper Texas Coast,
Color IR and Multispectral Photography of the Coastal Zone

Beach Development and Erosion Along the Upper Texas Coast. Apollo IX Frame 3728A (Figure 9) enables us to grasp quite readily what might otherwise take us some time to realize concerning beach building and retention. The effect of the jetty system at Galveston on the longshore current is evident. The near closing of San Luis Pass (southwest end of Galveston Island) and offshore bars can be seen at the mouths of the San Bernard River (first outflow south of Brazos River) and Brown Cedar Cut (first outlet from east Matagorda Bay north of Colorado River Delta).

A considerable sum of money has been spent by a number of sportsmen and state agencies since 1961 in maintaining Brown Cedar Cut. Possibly by noting the effects of man-made structures on beach retention, desirable links between estuaries and the open ocean could be made with longer longevity.

Color IR and Multispectral Photography of the Coastal Zone. Apollo IX Frames 3728A (Figure 9) and 3816A (Figure 11), false-color IR photographs of the SO-65 experiment, illustrate the advantages of using color IR film in photographs of the coastal regions. The land-water boundary is clearly defined and a good representation of the sediment load is obtained.

Figure 10 is composed of three black and white photographs taken simultaneously with Frame 3728A (Figure 9). Each of the three black and white frames utilized a different filter; and although none of these individual black and white frames contains as much total information as the color IR photograph, each brings out certain features to the best advantage. Therefore, when all three of these black and white photographs are viewed together, they contain more information than the color IR frame.

Frame 3728B (Figure 10a) was taken with a Wr58 filter. This filter allows light in the green region to pass; and in the turbid, yellow-green

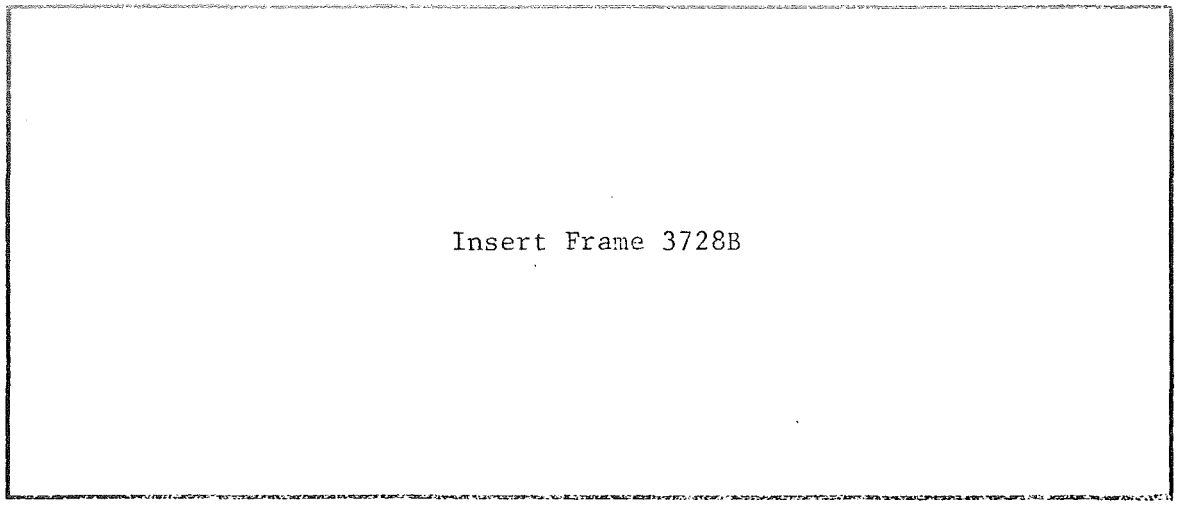

Figure 10a, Apollo IX Frame 3728B

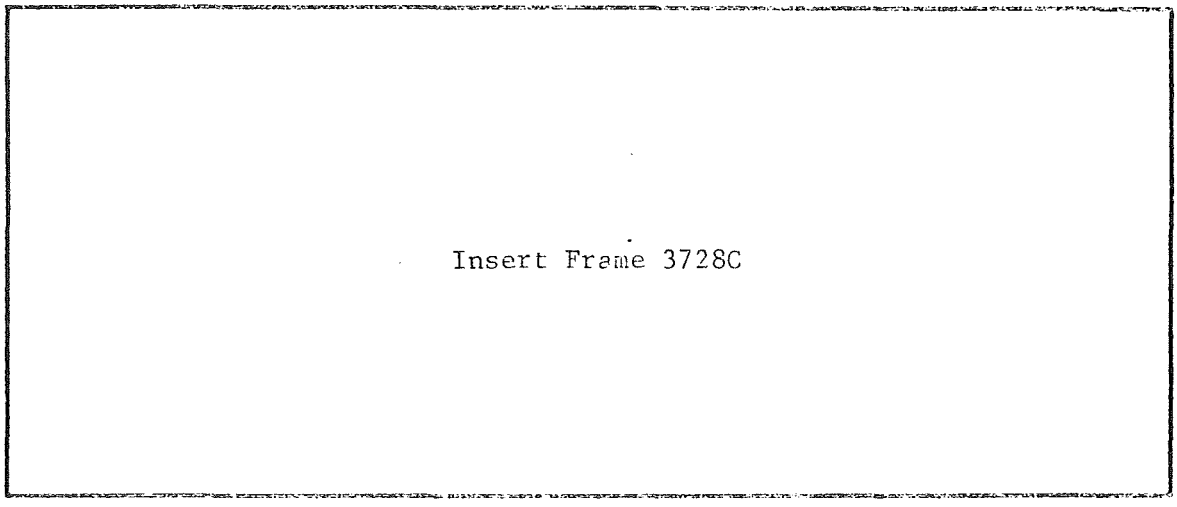

Figure 10b, Apollo IX Frame 3728C

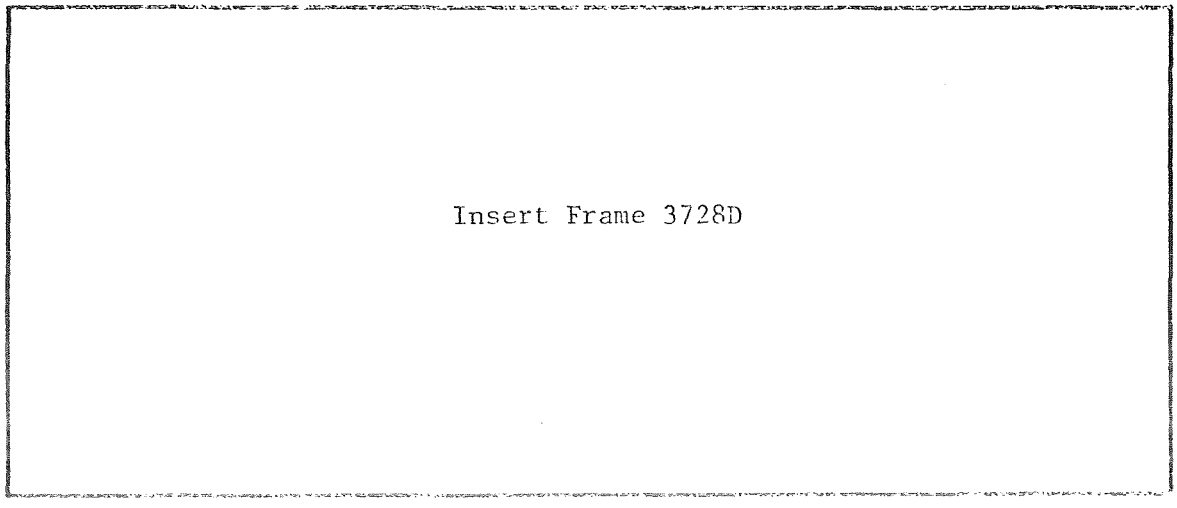

Figure 10c, Apollo IX Frame 3728D

Figure 10, Apollo IX Frames 3728B, 3728C, 3728D,
Color IR and Multispectral Photography of the Coastal Zone

Insert Frame 3816A

THIS FRAME SHOULD BE IN COLOR

Figure 11, Apollo Frame 3816A,
Color IR and Multispectral Photography of the Coastal Zone

coastal waters, maximum depth penetration is obtained. Frame 3728B (Figure 10a) better depicts the total sediment load than the color IR photograph of the other two black and white IR photographs. However, the poorest resolution of the land-water interface is obtained, and atmospheric haze effects are the greatest.

Frame 3728D (Figure 10c) was taken with a Wr25 filter which allows the maximum passage of light at a longer wavelength than the filter used with Frame 3728B (Figure 10z). The water penetration with this is not as great, so the sediment load portrayed is not over as great a depth as that in Figure 10a. A comparison between Figure 10a and Figure 10c gives an indication of the relative depth of the sediments. This concept could be extended further with more photographs of the same region utilizing still different filters. Moreover, although Figure 10c does not have the depth penetration Figure 10a does, the details of the flow around the Galveston jetties and from the river mouths are much more apparent.

Frame 3728C (Figure 10b) was taken with an 89A filter which limits the light recorded to still longer wavelengths. This filter passes radiation in the infrared region so practically no depth penetration is recorded. However, the land-water interface is the most clearly defined.

Figure 11 shows Frame 3816A of the SO-65 experiment. This false-color, infrared photograph is especially useful in delineating the land-sea boundary and the deeper river channels in this section of the Georgia Coast. As with the other false-color IR photographs, a good indication of the sediment outflow is also obtained.

RECOMMENDATIONS

The data from future manned missions should include more photographs over the central oceans. Preferably, this photography should be near-vertical and include photographs with different filters similar to those in the SO-65 experiment. Any deep ocean color boundaries observed from space should be photographed as often as possible so that any changes in the structure of this ocean feature could be determined. Some photographs of an area of the deep ocean free from cloud cover and surface features should also be taken to see if the different filters or laboratory techniques such as color separation can bring out any ocean or atmospheric phenomenon.

Offshore areas such as the Texas Bays, Colorado River Delta, and the Bahama Banks, which have been photographed often in the past, should continue to be photographed on every mission. A time sequence of these areas will be valuable to the scientist studying geological changes in these regions. Changes in the sea grass distributions, river delta development, beach development and erosion, and changes in the amount of pollution could all be observed. On a smaller time scale, areas which undergo large tidal variations should be photographed as often as possible on a single mission to better understand the effects tidal currents have on river outflow, longshore currents, and nearshore turbidity.

Better ideas of the surface circulation patterns of an area could be obtained if several photographs are taken of the area on a single pass. The different photographic angles show different areas of sun glitter from which more complete circulation patterns can be observed.

Multispectral experiments, such as the SO-65 experiment, should be continued and expanded in both the number of photographs and the number of spectral bands

available. A multispectral approach to ocean photography is not only desirable but necessary if any truly new and different oceanographic information is to be obtained from satellite photography.

References for Apollo IX

Anonymous, Atlas of Pilot Charts, Central American Waters and South Atlantic Ocean, U. S. Navy Hydrographic Office, H. O. Pub. No. 106, 1958.

Joyce, E. A., Jr., "St. Johns River," Oceans 1(3):19--22, March, 1969.

CHAPTER III - PROGRESS (cont.)

G. Newsletter

On December 3, 1969, the project issued its first Newsletter to a rather limited distribution list of approximately 150 persons and organizations.

As indicated in the "Purpose" of the Newsletter, ". . . *it is an attempt to provide a medium for oceanographers to become better acquainted with the research and development of remote sensors and their oceanographic applications. To accomplish this end, the format was designed to emphasize current developments of oceanographic applications of remote sensors, publish selected abstracts and a limited bibliography, and list scheduled conferences, symposia, and so forth . . .*" Attached to the Newsletter is a form requesting comments concerning the publication or items which the readers felt should be included. Also attached to each issue is a request form for names and addresses of persons who might like to receive the Newsletter.

After three issues, the response to the requests has resulted in the addition of 180 names to the distribution list. The new subscription requests range from high schools and junior college to industry, university and government agencies.

Foreign requests now stand at 31, with subscriptions concentrated in Argentina, Canada, and Brazil.

Comments received have been extremely favorable and the suggestions have been informative. Several examples of such comments and suggestions are shown on the following page.

". . . the Newsletter will fill a gap in the field of oceanographic information, especially for professionals interested in air-sea interaction. . ." Jose Alvarez, Capitan de Navio, Buenos Aires, Argentina.

" . . . it is excellent and should be continued. . ." Dr. R. A. Geyer, Chairman, Department of Oceanography, Texas A & M University.

". . . this is of interest for a more comprehensive knowledge of current activities and progress." Maynard M. Nichols, Associate Professor, Virginia Institute of Marine Science, Gloucester Point, Virginia.

"Please include methods and research results on the detection of fish, fisheries, algae, etc., and their signature analysis. . ." Dr. Lou Castiglione, Department of Biology, New York University, Bronx, New York.

"I am happy to inform you that our Committee has selected your publication, REMOTE SENSING OCEANOGRAPHY NEWSLETTER, for display on the Reprint Table to be exhibited during our state meeting, American Chemical Society Florida Sub-sections Meeting, May 7, 8, 9." Dr. Louis J. Polskin, Chairman, Scientific Program Committee, American Chemical Society of Florida.

Plans are being made to invite recognized authorities in the diverse oceanographic applications of remote sensors to write short expositions of pertinent studies for inclusion in the Newsletter. Several well-known investigators have been contacted and all have indicated willingness to participate in contributing articles to the Newsletter.

The correspondence received indicates that a genuine need exists for such a publication. As the Newsletter evolves, many of the suggestions given to us are expected to be utilized. All suggestions with a low time-cost-effectiveness ratio are examined and the more promising ones are undergoing feasibility studies.

This occurs off the west coasts of continents where the winds have a persistant equatorward component. An Ekman type transport can also be induced by bottom friction on the ocean floor. In either case, the integrated mass transport is normal to the direction of flow.

A third cause of upwelling is presented by inertial forces which generate positive or negative horizontal divergences in conserving potential vorticity (Arthur, 1965). These are the three basic mechanisms by which upwelling is induced.

There are several regions where upwelling is well documented and may have been photographed from spacecraft. It would be worthwhile to examine these photographs.

Photography of Regions of Upwelling

From the Gemini VII Mission, color frames 66-24903 and 66-24904 of India and the Bay of Bengal, wind induced upwelling might be inferred from the existing cloud pattern. This pattern is partly associated with offshore winds.

Cloud patterns as seen in color frames 66-38290 and 66-38307 taken during Gemini IX of the Peruvian Coast, might be associated with upwelling, again wind induced.

Prior to certifying the above photographs as being indicative of upwelling, the regional meteorological conditions which existed would have to be known and the photographs interpreted in view of those conditions.

During the Apollo IX Mission, two color exposures were taken of Jamaica. Wind data from climatological charts indicate a steady

(approximately 4 m/sec) wind from the east with a small southward component existed in this region during March, 1969, the time of the Apollo IX Mission. Such winds would transport water to the north and cause upwelling off the north coast of Jamaica.

Color frame AS9-21-3315 depicts a color boundary off the north coast of Jamaica. Note portions of the darker and lighter colors lie in the sunglint pattern. The import of this will be discussed later. In the second frame, AS9-21-3316, a definite streak appears in the sunglint pattern which seems to indicate a boundary between the different water types.

Taiwan, as shown in color frame 66-45868 (Gemini X) is a well known photograph. Since the area of interest is cloud free, this photograph has become somewhat of a standard in pressing the case for visible region sensors applicability to detect regions of upwelling. In discussions of this photograph, color differences have been utilized to identify regions of upwelled water, these regions being of darker color. Assuming that this is upwelling, a brief digression will illustrate how inertial forces could cause such a phenomenon.

Charney (1955) has shown that the western boundary currents can be predicted by inertial theory in which the conservation of potential vorticity is valid. Therefore, the equation below should hold for the Kuroshio Current, particularly in the southern part of sub-tropical gyre off of Taiwan Island.

$$\frac{D\xi}{Dt} + \beta v = - \nabla_n \cdot \tilde{V} (\xi + f)$$

Assume that the Kuroshio can be approximated by a single streamline, which lies in the core of the current. Give this streamline a constant velocity. Assume that the streamline follows the coastal irregularities approximately and that these irregularities are larger than the width of the stream.

Then;

$$\xi = K V$$

Where K is the curvature of the coastal irregularity.

Consider the Taiwan Island case where;

$$V \sim 50 \text{ cm/sec}$$

$$K = \frac{1}{R} \sim 10^{-7} \text{ cm}$$

In a schematic drawing, three zones appear around the island depending upon the sign of K.

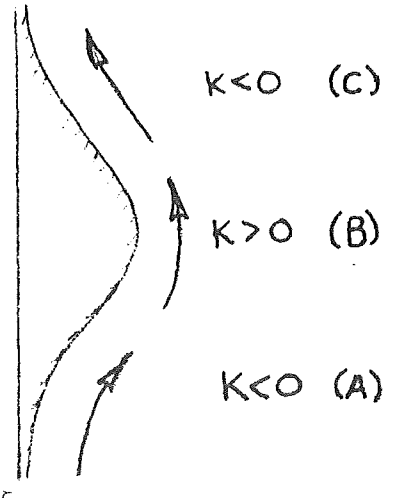

	$\frac{D\xi}{Dt}$	βv	ω
(A)	-3.1×10^{-11}	$+1 \times 10^{-11}$	2.1×10^{-3} cm/sec
(B)	$+3.1 \times 10^{-11}$	$+1 \times 10^{-11}$	-4.1×10^{-3} cm/sec
(C)	-3.1×10^{-11}	$+1 \times 10^{-11}$	2.1×10^{-3} cm/sec

The details of these calculations are given by Arthur (1965). Therefore, upwelling occurs in zones (A) and (C) with downwelling existing in zone (B). In this case, the relative vorticity changes more extensively than the Coriolis parameter. It should be noted that the theories involving upwelling in Western Boundary Currents are practically non-existent; and this approach, while valid for Eastern Boundary Currents, needs modification before being extended to Western Boundary Currents.

This pattern of upwelling appears to fit the Taiwan Island case very well. In addition, examination of H. O. charts shows the east side of Taiwan has a broad shelf while the west has none. Yoshida's (1967) explanation of the shelf effect upon upwelling with this type of topography would again agree very well.

So far, we have seen examples of photography recording zones of possible upwelling. In most cases, however, knowledge of the meteorological conditions of the region photographed must be known before one can state with any confidence that upwelling has been recorded. For other examples, we relied on past experience for interpretation; that is, past experience tells us that during a certain period of time, upwelling may be expected in the region photographed.

So, we still have the basic question before us--can photography from remote platforms be utilized to detect upwelling? Some promise seems to be offered in the sunglint patterns one occasionally sees in existing photographs of Earth from space.

Bowley, Greaves, and Spiegel (1969) in a recent article in SCIENCE, suggest that unusual dark patches occasionally seen in the glitter patterns

in the full disc ATS picture sequences may be related to upwelling. The anomalous patches, first reported by Strong and McClain (1969), appear dark while on the edge of a sunglint pattern but appear bright when near the center of the pattern. The following sequence of photographs of the Galapagos Island region illustrates this point:

ATS-III	IDCS	27 March 1968	1757Z
ATS-III	IDCS	27 March 1968	1843Z
ATS-III	IDCS	27 March 1968	1945Z

As the sunglint pattern "passed" over this region, an area near the Galapagos Island is alternately dark, bright, then dark again. These observations seem readily explained by a model where the isolated dark areas represent areas of relatively calm surface conditions against a background of higher sea states.

A surface film or slick over an area due to biological activity generated by upwelling will inhibit the generation of capillary waves on the sea surface (Deacon and Webb, 1962). Accordingly, the turbulent transfer of energy from the atmosphere to the ocean will be reduced. The overall result is that due to the reduction in the number of short wavelengths which cause high sloping waves in such an area, the ordinary diffuse sunglint pattern will be absent.

The mean monthly sea surface temperature analysis, based on ship data for March 1968, does indicate upwelling to the west of the Galapagos Islands (Bowley, et al., 1969). But it appears to be upwelling under somewhat special conditions--it is the surfacing or near surfacing of the Pacific equatorial undercurrent (Cromwell Current). Data taken in March, 1967, illustrates the same occurrences; light westward winds, the

Cromwell Current surfacing near the Galapagos Islands, then dividing into a northward and southward current and diving again (EASTROPAC, 1967). It is also possible that what we are seeing in these ATS-III imagery sequences are runoff effects and/or sea surface roughness effects associated with the downwind side of the islands. So, this appears to be a special case, upwelling possibly, but also a complicated process.

Referring back to the Taiwan photography, we note on the east side of the island a southward flowing counter-current brought about by the low salinity runoff, which appears dark out of the sunglint and bright in it. Also, the sequential frames of Jamaica, referred to earlier, illustrate regions of the north side of the island with the same anomalous dark patches.

The central problem associated with this type of analysis is not that the glitter patches are caused by some type of surface films but what causes these films. Certainly, on a small scale (see data taken off the coast of Brazil) slicks and patches occur in regions of convergence not divergence. Strong and McClain (1969) indicate that the large sunglint patches they found are all caused by convergence. On the other hand, Bowley, Greaves, and Spiegel (1969) believe these large patches are indicative of the increased biological activity associated with upwelling.

So, the possibility of correlating the anomalous dark areas with regions of surface divergence remains. Work needs to be done in a "ship documented" upwelling zone with photographs of the region taken in and out of the sunglint pattern. This is what Project 658, Texas A&M University, via the Research Triangle Institute, proposes to accomplish in the Virgin Islands.

References

1965 Arthur, Robert S., *On the calculation of vertical motion in eastern boundary currents from determinations of horizontal motion*, Journal of Geophysical Research, Vol. 70, no. 12, June 15, 1965.

1969 Bowley, C. J., Greaves, J. R., and Spiegel, S. L., *Sunglint patterns--unusual dark patches*, Science, Vol. 165, 26 September 1969.

1955 Charney, J. G., *The Gulf Stream as an inertial boundary layer*, Proceedings National Academy of Science, Vol. 41, 1955.

1962 Deacon, E., and Webb, E., *The Sea*, New York: Interscience, 1962.

1905 Ekman, V. W., *On the influence of the Earth's rotation on ocean currents*, Ark. Mat. Ast. Fysik, Vol. 2, no. 11, 52 pp., 1 pl., 1905.

1969 Strong, Alan E., and McClain, E. Paul, *Sea state measurements from satellites*, reprinted from Mariners Weather Log, Vol. 13, no. 5, September, 1969, p. 205.

1967 Yoshida, K., *Circulation in the eastern tropical oceans with special references to upwelling and undercurrents*, Japanese Journal of Geophysics, Vol. IV, no. 2, March 1967.

1967 _____, EASTROPAC, Data from Texas A & M Cruise 67-A-1, On File, Dept. of Oceanography, Texas A & M University, 1967.

CHAPTER III - PROGRESS (cont.)

I. Staff Travels - June, 1969 through March, 1970

June 3, 1969 - Bill Merrell and Jack Paris visited with Dr. James Zaitzeff, Rebecca Kinard, and Jay Harnage at NASA/MSC in Houston, Texas, and reviewed data from the Mexican Program.

June 9, 1969 - Dr. Huebner and Bill Merrell made a second trip to NASA/MSC to consult with representatives from the Mexican government regarding the above data.

June 10-12, 1969 - Jack Paris attended the SPOC Microwave Meeting in Washington, D. C., where he presented a paper, "Microwave Studies in the Gulf of Mexico."

June 11-22, 1969 - Bill Merrell participated in a departmental cruise of the R/V ALAMINOS, which surveyed the area of upwelling in the Yucatan Straits.

June 23-24, 1969 - Dr. Huebner visited the NASA facilities at Langley, Virginia, where he discussed applications of spectrometry to fish detection with Mr. McIvers of Airborne Instruments Laboratory. Mr. McIvers has begun some work with the Bureau of Commercial Fisheries and will work with Kirby Drennan of the BCF office in Pascagoula, Mississippi. They are planning to adapt one of their units for this work. The data previously obtained with the TRW unit while it was in Pascagoula, Mississippi, was reviewed. While there, Dr. Huebner gave a three-hour seminar on remote sensing of the oceans to a group of scientists who had the task of looking at remote sensing satellites from several aspects, not only the technical

aspects but also the economic and political aspects as well.

June 29 - July 1, 1969 - Jack Paris conferred with members of NASA Electronic Research Center (NASA-ERC) and Radiation Tech., Inc., regarding mutual coordination work in general and passive microwave work in particular.

July 1, 1969 - A staff meeting was held with only personnel of the A&M Project in attendance. Dr. James Zaitzeff was unable to attend. Such business as the existing budget, future travel plans, past trips by our staff, and various managerial forms to be used by the project's planned activities.

July 15-18, 1969 - Dr. Huebner, Jack Paris, and Bill Merrell visited with G. F. Williams and Dr. K. Rooth of the University of Miami; C. S. Yentsch of Nova University; and Dr. K. Warsh of Florida State University. Microwave studies were discussed at the University of Miami. A tour of the Nova University facilities was made and a discussion held of their oceanographic activities. Brief meetings were also held with ESSA personnel, including Dr. William McLeish, Mr. Saul Broida, and Mr. Bernard Zetler. Dr. Warsh of Florida State was contacted by telephone regarding their ship schedules.

August 5-6, 1969 - Both Dr. Huebner and Bill Merrell attended the Color of the Ocean Workshop at Woods Hole Oceanographic Institution.

August 23-27, 1969 - Dr. Huebner and Jack Paris traveled to Boulder, Colorado, to confer with scientists at the National Bureau of Standards (NBS), ESSA Research Labs, and National Center for Atmospheric Research (NCAR). From there, they went to Lubbock, Texas, to make further visits at Texas Tech University. The major portions of the discussions dealt with microwave studies.

September 1-13 - Dr. Capurro attended the SCOR meeting in Göteburg, Sweden, and the Upper Mantle meeting in Madrid, Spain, since he is a member of the bureau of both international organizations. He informed European oceanographers of our program in remote sensing and made an informal agreement to use the research vessels engaged in international cooperative expeditions as instrument platforms to provide ground truth should the NASA aircraft or any satellite fly over the region. Also, he was charged with the convening of a symposium of "Remote Sensing of Ocean Variables" to be held in Tokyo in September, 1970, during the Joint Oceanographic Assembly.

September 8, 1969 - Dr. Huebner, Robert Whitaker, and Bill Merrell traveled to NASA/MSC in Houston to meet with the Brazilians and to assist in their analysis of the multisensor data taken with the NASA Aircraft.

September 24-28, 1969 - Dr. Huebner and Bill Merrell met with the Mexican investigators to review the report prepared by the project staff of Texas A&M University.

October 13-17, 1969 - Dr. Capurro was invited to attend a seminar held at the University of La Plata, Argentina, on the Evaluation of Earth Resources from Aircraft and Spacecraft. He delivered two papers dealing mainly with the sampling program in the ocean. These papers will be published by the Argentine Center for Space Research.

October 15-16, 1969 - Dr. Huebner and Robert Whitaker attended the Sixth Symposium on Remote Sensing of Environment held at the University of Michigan in Ann Arbor. They attended the Sessions regarding

Oceanographic Applications of Remote Sensing, Parts I, II, and one regarding Extraterrestrial Applications of Remote Sensing.

November 28, 1969 - Bill Merrell and Robert Whitaker conferred with Dr. Robert Stevenson, BCF, Galveston, concerning the paper on upwelling which was to be presented in Washington, D. C., December 18, at the Workshop.

December 5, 1969 - Dr. Huebner and Bill Merrell conferred with Dr. James Zaitzeff, Dale Browne, and other individuals at NASA/MSC to obtain additional data and slides for the upwelling paper.

February 2, 1970 - Bill Merrell traveled to NASA/MSC to meet with Dr. James Zaitzeff and discuss cooperative efforts with Dr. T. Ichiye, Physical Oceanographer with the Oceanography Department, in his study of coastal processes. The direction of the Newsletter and the possibilities of getting NASA aircraft to overfly the northern Gulf when research vessels are available were included in the discussion.

February 5, 1970 - Bill Merrell returned to NASA/MSC to attend the planning meeting on Sea Ice. He was joined the following day by Dr. Huebner who also attended the meeting. While there, they conferred with Mr. John Sherman and Dr. Zaitzeff regarding project activities.

February 13, 1970 - Bill Merrell went to NASA/MSC to confer with Dr. Zaitzeff on the possibility of participating in a NASA aircraft experiment near the Virgin Islands. Mr. Merrell is particularly interested in an area of man-induced upwelling in this area.

March 18-22, 1970 - Dr. Huebner, Bill Merrell, and Mrs. June Hagler from this project participated in Cruse 70-A-5 of the R/V ALAMINOS. Dr. T. Ichiye (a co-investigator for the proposed project, FY70-71) was the chief scientist of the cruise which covered the outflow from the Galveston Bay area. The shipboard data was taken by computer and processed synoptically. Efforts were made to improve techniques for better comparisons between shipboard and remotely sensed data, thereby resulting in better coordination of aircraft and ship surveys. It is presently proposed for Dr. Ichiye's cruises in this series to have accompanying overflights.

CHAPTER IV

CONTRIBUTIONS - May, 1969 - March, 1970

1. Paris, J. F., and William J. Merrell, Jr., Scientific Value (of Apollo 7 photography) for Oceanography, Chapter 9, NASA Report on the Scientific Value of Apollo 7 Photography for Earth Sciences, (in press), 4 March 1969.

2. Huebner, George L., Advances in Remote Sensing of the Ocean's Parameters, IEEE Symposium on Remote Sensing, Washington, D. C., 15 pages, 16 April 1969, (unpublished).

3. Huebner, George L., Methods of Sensing of the Ocean's Parameters, ASEE-NASA Engineering Systems Design Program, NASA Langley Research Center Symposium, 45 pages, 24 June 1969, (unpublished).

4. Merrell, William J., Jr., et al., Scientific Value (of Apollo 9 photography) for Oceanography, Chapter 9, NASA Report on the Scientific Value of Apollo 9 Photography for Earth Sciences, (in press), 28 August 1969.

5. Merrell, William J., Jr., and Robert E. Whitaker, An Oceanographic Analysis of Data Recorded on Ships and Aircraft-NASA, Aircraft Mission 91, Site 705, Veracruz, Mexico, 13 pages, 22 September 1969.

6. Capurro, Luis R. A., Studying the Oceans from Space, Presented at the University of La Plata, Buenos Aires, Argentina, October 1969.

7. Walsh, CMDR Don, Remote Sensor Oceanography in the Mississippi Delta Region, The Texas Journal of Science, Vol. XXI, No. 1, pages 29-35, October 1969.

8. Merrell, William J., Jr., and George L. Huebner, Jr., The Use of Aerial Photography in Offshore Operations, Offshore Magazine, March 1970.

9. Paris, Jack F., Microwave Studies at Texas A&M University, Submitted on January 5, 1970, for inclusion in the Proceedings of the "NASA-Navy Review of Recent Microwave Studies of the Ocean Surface" held at NASA Headquarters on 11-12 June 1969.

CHAPTER V

REPORTS

A. Progress Reports

1. Quarterly Progress, A&M Project 658, May-July 1969.

2. Quarterly Progress, A&M Project 658, August 1-November 1, 1969.

3. Quarterly Progress, A&M Project 658, November 1-February 1, 1970.

B. Technical Reports

1. Walsh, CMDR Don, Characteristic Patterns of River Outflow in the Mississippi Delta, Ref. 69-8-T, Department of Oceanography, Texas A&M University, 222 pages, June 1969.

CHAPTER IV

OFFICE FACILITIES AND PERSONNEL

Office facilities have been located in the Olin E. Teague Research Center since 1967; however, during the month of May, they will be moved to the west wing of Cushing Library on the campus.

Professional staff for the existing project consists of:

Dr. Luis R. A. Capurro, Project Supervisor, who is a professional physical oceanographer, has been with the Department of Oceanography a number of years, and is primarily interested in environmental studies.

Dr. George L. Huebner, a professional electrical engineer, also with the Department a number of years, is considered a specialist in remote sensing instrumentation.

Mr. Jack F. Paris, graduate student currently working toward a Ph.D. in meteorology, is specializing in remote sensing.

Mr. William J. Merrell, Jr., graduate student, is currently working toward a Ph.D. in physical oceanography.

Mr. Robert Whitaker, graduate student, currently working toward a Ph.D. in physical oceanography.

Dr. Guy Franceschini, professional meteorologist, is acting as a consultant on air-sea interaction and radiation.

In addition to the above, there is a full-time secretary and full-time office manager.

CHAPTER VII

FILM DATA ACQUIRED FROM MAY, 1969 - MARCH, 1970

Earth Resources Aircraft Mission 91 - Veracruz, Mexico:

Instrument	Site	Type Data	Rolls
RC-8	705	Dup. Pos. Transp.	2
KA-62 (4 cameras)	705	Dup. Pos. Transp.	1
SLAR	705	Dup. Pos. Transp.	1
RS-14	705	Dup. Pos. Transp.	1

Earth Resources Aircraft Mission 96 - Cabo Frio, Brazil:

Instrument	Site	Type Data	Rolls
RS-14	805	Dup. Pos. Transp.	1
KA-62 (4 cameras)	805	Dup. Pos. Transp.	4
RC-8	805	Dup. Pos. Transp.	2